STATE OF CALIFORNIA• DEPARTMENT OF TRANSPORTATION

TECHNICAL REPORT DOCUMENTATION PAGE

TR0003 (REV 10/98)

ADA Notice
For individuals with sensory disabilities, this document is available in alternate formats. For information call (916) 654-641o or TDD (916) 654-3880 or write Records and Forms Management, 1120 N Street, MS-89, Sacramento, CA 95814.

1. REPORT NUMBER	2. GOVERNMENT ASSOCIATION NUMBER	3. RECIPIENT'S CATALOG NUMBER
CA-22-3712	*NIA*	*NIA*

4. TITLE AND SUBTITLE
System impact of connected and automated vehicles: An application to the 1-210 Connected Corridors pilot

5. REPORT DATE
06110/2022

6. PERFORMING ORGANIZATION CODE
NIA

7. AUTHOR(S)
Dr. Qiiian Gan

8. PERFORMING ORGANIZATION REPORT NO.
CA-22-3713

9. PERFORMING ORGANIZATION NAME AND ADDRESS
University of California, BERKELEY
409A McLaughlin Hall
MC 1720 Berkeley,
CA 94720-1720

10. WORK UNIT NUMBER
NIA

11. CONTRACT OR GRANT NUMBER
Caltrans Grant 65A0757

12. SPONSORING AGENCY AND ADDRESS
Caltrans DRISI
1120 N Street
Sacramento, CA 95814

13. TYPE OF REPORT AND PERIOD COVERED
Final Report (Jan 2020 - Dec 2021)

14. SPONSORING AGENCY CODE
Caltrans

15. SUPPLEMENTARY NOTES
NIA

16. ABSTRACT
In current Integrated Corridor Management (ICM), the control targets are ordinary objects of vehicles, buses, pedestrians, and etc. However, in recent years, a great amount of efforts has been devoted to the field of connected and automated vehicles (CAVs), which may be implemented in the near future and become one of the dominated travel modes. Given this important piece is missing from current ICM systems, it will become a serious problem for public agencies like Caltrans and local Traffic Management Centers (TMCs) to manage traffic properly and efficiently once CAVs are deployed in the field. In this project, we are going to solve this problem by developing an integrated platfoRM in microsimulations that allows the modeling of CAVs in current ICM systems.

In this task, we are particularly interested in the following two topics: (i) improve current microsimulation PLATFORMS to enable the tests of different CAV's control and communication strategies; (ii) understand the system impact of CAVs on the development of ICM strategies. For demonstration purposes, we use the 1-210 Connected Corridors pilot as an application example.

17. KEYWORDS	18. DISTRIBUTION STATEMENT
Integrated Corridor Management, ICM, Connected Corridor, CAV, TMC, travel modes, microsimulation, ICM stratergies	No restrictions.

19. SECURITY CLASSIFICATION *(of this report)*	20. NUMBER OF PAGES	21. COST OF REPORT CHARGED
Unclassified	144	

DISCLAIMER STATEMENT

This document is disseminated in the interest of information exchange. The contents of this report reflect the views of the authors who are responsible for the facts and accuracy of the data presented herein. The contents do not necessarily reflect the official views or policies of the State of California or the Federal Highway Administration. This publication does not constitute a standard, specification or regulation. This report does not constitute an endorsement by the Department of any product described herein.

For individuals with sensory disabilities, this document is available in alternate formats. For information, call (916) 654-8899, TTY 711, or write to California Department of Transportation, Division of Research, Innovation and System Information, MS-83, P.O. Box 942873, Sacramento, CA 94273-0001.

PARTNERS FOR ADVANCED TRANSPORTATION TECHNOLOGY
INSTITUTE OF TRANSPORTATION STUDIES
UNIVERSITY OF CALIFORNIA, BERKELEY

System impact of connected and automated vehicles

Task 3712 (65A0757)

Final Report

June 10th, 2022

Partners for Advanced Transportation Technology works with researchers, practitioners, and industry to implement transportation research and innovation, including products and services that improve the efficiency, safety, and security of the transportation system.

This page left blank intentionally

Primary Author

Dr. Qijian Gan

Computational Data Science Research Specialist

California PATH

University of California, Berkeley

qgan@berkeley.edu

This page left blank intentionally

REVISION HISTORY

Date	Sections	Change Description
12/31/2021	All	Initial document by Qijian Gan
01/24/2022	All	Reviewed by Supanpreet Kaur
06/10/2022	All	Final revision by Qijian Gan

This page left blank intentionally

Table of Contents

List of Figures

List of Tables

Executive Summary

With rapid development in sensing and communications technologies, algorithms, and computing capabilities, tremendous efforts have been devoted to the research, development, and testing of connected and autonomous vehicles (CAVs). Many studies projected that a significant portion (30%~50%) of vehicle fleets will be Level 4 Automated Vehicles (AVs) in the 2040s. Despite the significant advancement in AVs, the latest released report "*AV 4.0"* by the U.S. Department of Transportation pointed out the need of a consistent United States (U.S.) Government approach to AV technologies. It also stated that the U.S. government will focus on opportunities in improving transportation system-level performance, efficiency, and effectiveness while avoiding negative transportation system-level effects from AV technologies. Even though many automakers and high-tech companies have been conducting a lot of field tests to evaluate their autonomous driving systems, their tests are not systematic and comprehensive enough to inform government agencies about potential impacts of the deployment of AVs/CAVs at the network scale. Therefore, it is of great importance to develop tools to understand system-level impacts of CAVs to help government agencies make better decisions and policies.

In this project, we successfully developed an integrated microsimulation platform for mixed traffic with CAVs using the Adaptive Cruise Control/ Cooperative Adaptive Cruise Control (ACC/CACC) and the Vehicle to Everything (V2X) modules in the microsimulation software, Aimsun. Different from the state-of-the-practice approach which connects microsimulation software (e.g., Vissim) with a network simulator (e.g., Network Simulator-2 (NS-2)), this integrated microsimulation platform, to the best of our knowledge, is the first "All-in-One" microsimulation platform that can replicate the mixed traffic environment in the real world and has great potential for network-level analysis of CAV applications. This integrated microsimulation platform has two levels of functionalities. At the vehicle control level, it uses the ACC/CACC module to regulate CAV's longitudinal movements. At the communications level, it uses the V2X module to enable Vehicle to Infrastructure/ Infrastructure to Vehicle (V2I/I2V) communications between Roadside Units (RSUs) and CAVs and Vehicle to Vehicle (V2V) communications between CAVs.

To demonstrate how to apply this integrated microsimulation platform to evaluate the network-level impacts of CAV applications, we implemented the following three CAV applications in this project: (i) freeway speed harmonization with CAVs, (ii) route guidance with CAVs for traffic incident management, and (iii) traffic light optimal speed advisory with CAVs. We also generated three different subnetworks from the original I-210 network for testing purposes: (i) a Freeway-Only subnetwork for the application of freeway speed harmonization with CAVs, (ii) a Freeway-and-Arterial Combined subnetwork for the application of route guidance with CAVs for traffic incident management, and (iii) an Arterial-Only subnetwork for the application of traffic light optimal speed advisory with CAVs.

For the application of freeway speed harmonization with CAVs, we implemented the required workflow to enable the V2I/I2V communications between RSUs and CAVs as well as the V2V communications between CAVs. We also selected three speed harmonization algorithms for demonstration purposes: (i) a rule-based speed harmonization algorithm; (ii) a variable speed limit (VSL) and variable speed advisory (VSA) algorithm; and (iii) a cooperative variable speed limit system (C-VSLS). We conducted various simulations under different traffic demand levels and percentages of CAVs in the Freeway-Only subnetwork. Simulation results showed that the selected speed harmonization algorithms can only perform well under certain conditions. The rule-based and the VSL-VSA algorithms tend to perform well under

high percentages of CAVs, e.g., 80% or higher, while the C-VSLS tends to perform well under relatively low percentages of CAVs, e.g., about 40%, and light traffic congestion. In terms of performance improvement, the rule-based algorithm and the C-VSLS can only achieve a relatively small delay reduction between 1% to 2%, while the VSL-VSL algorithm can achieve a relatively large delay reduction between 2% to 6%. Through conducting various simulations, we found that many factors can impact the performance of the speed harmonization algorithms, for example, road geometries, existing detector placement and control settings, traffic demand and Origin-Destination (OD) patterns, settings of speed harmonization zones, settings in the RSUs and the V2I/I2V communications, and parameter settings in the speed harmonization algorithms.

For the application of route guidance with CAVs for traffic incident management, we implemented two separated workflows: (i) an incident management workflow to manage different stages of a traffic incident and the activation and termination of response plans, and (ii) a communications workflow to manage the information exchange between RSUs and their connected CAVs. We also implemented a route choice algorithm to mimic CAV's route choice decisions with considerations of potential impacts from lane index (e.g., inner lanes vs. shoulder lanes), vehicle types (e.g., car vs. truck), and number of detoured vehicles. We tested this application with two traffic accidents occurring at the same place but with different levels of severity under 30% and 50% CAVs in the Freeway-and-Arterial Combined subnetwork. Simulation results demonstrated that with timely sharing of detour route information with CAVs, traffic performance can be significantly improved with delay reduction of over 3% when traffic accidents occur. However, we want to emphasize that this information sharing should not be limited to CAVs but should include road users who have the capability to receive real-time traffic information, e.g., navigation app users. This is important because when traffic incidents occur, uncoordinated decisions of navigation app users may significantly degrade the performance of the response plans recommended by the TMCs or may even make them invalid.

For the application of traffic light optimal speed advisory with CAVs, we implemented the communications workflow to allow RSUs to send real-time SPaT and MAP messages to nearby CAVs. We also implemented the Green Light Optimal Speed Advisory (GLOSA) application with some minor revisions to allow CAVs to adjust their approaching speeds at signalized intersections. We tested this GLOSA algorithm at the Arterial-Only subnetwork under different time periods, demand levels, and percentages of CAVs. Simulation results showed that the GLOSA algorithm generally performs better than the baseline model. However, the performance improvement is minor with delay reduction less than 1% for most of the scenarios. This reveals that it is hard to reduce vehicle delay by solely adjusting CAV's approaching speeds. Through various simulation scenarios, we also found that many factors, for example, signal coordination settings, permitted left-turn settings, and existence of vehicle queues and lane blockages, need to be considered if we want to develop new optimal vehicle and signal control strategies.

Furthermore, we activated the ACC/CACC module in the I-210 corridor network and the subnetworks and conducted various simulation scenarios under different time periods, demand levels, and percentages of CAVs. Simulation results showed that ACC/CACC can significantly improve network performance. For freeway networks, the improvement is more obvious with delay reduction over 40% and speed improvement over 22% for 100% CAVs. However, the improvement is lower for arterial networks, with about 15% delay reduction and 6.25% speed improvement for 100% CAVs. This difference makes sense since vehicle delay in arterial networks is mostly caused by traffic signals. Without V2I/I2V communications between signalized intersections/RSUs and CAVs, it is hard to further reduce vehicle's

travel delay. In addition, we found that there exists an optimal threshold of CAV percentages, above which the performance improvement becomes marginal. Through various simulation scenarios in our study networks, it seems this threshold is about 50%. When the percentage of CAVs is between 0% and 50%, we do see significant performance improvement. However, when the percentage of CAVs is above 50%, the performance improvement is not obvious.

In the future, with the integrated microsimulation platform developed in this project and the well-calibrated I-210 corridor network, we would like to continue our studies in the following directions: (i) developing a guideline on RSU placement so as to achieve desired performance for CAV applications with particular interest while staying within the budget; (ii) creating a microsimulation model for the California Connected Vehicle (CV) Testbed and connecting it to the Multi-Modal Intelligent Traffic Signal System (MMITSS) to test and evaluate various CV applications; (iii) enhancing the features in the integrated microsimulation platform with more V2X applications for multi-modal traffic; (iv) developing information sharing policies and strategies with navigation app users for more effective and efficient traffic incident management; (v) developing optimal signal control strategies with CAVs to improve intersection performance.

This page left blank intentionally

Acronyms

ACC	Adaptive Cruise Control
API	Application Programming Interface
AV	Automated Vehicle
BPR	Bureau of Public Roads
CACC	Cooperative Adaptive Cruise Control
CAM	Cooperative Awareness Message
CAMP	Crash Avoidance Metrics Partnership
CAV	Connected and Automated Vehicle
CMS	Changeable Message Sign
CV	Connected Vehicle
DENM	Decentralized Environmental Notification Message
I2V	Infrastructure to Vehicle
ICM	Integrated Corridor Management
MAP	Map Message
MIXIC	MICroscopic model for Simulation of Intelligent Cruise control
MPR	Market Penetration Rate
NS-2	Network Simulator-2
OBU	On-Board Unit
OD	Origin-Destination
RSU	Roadside Unit
SPaT	Signal Phase and Timing Message
TMC	Traffic Management Center
WT	Wavelet Transform
V2I	Vehicle to Infrastructure
V2V	Vehicle to Vehicle
V2X	Vehicle to Everything

This page left blank intentionally

1. Introduction

With rapid development in sensing and communications technologies, algorithms, and computing capabilities, tremendous efforts have been devoted to the research, development, and testing of connected and autonomous vehicles (CAVs). Automakers are expected to increasingly bundle connected services and/or autonomous features at the point of sale over the next five years (Aiello et al., 2017). Many studies (Bansal and Kockelman, 2017; Litman, 2020) projected that a significant portion (30%~50%) of vehicle fleets will be Level 4 AV in the 2040s. In terms of CAV-related research, the following five major areas have been advanced significantly in recent years (Elliott et al., 2019): (i) inter-CAV communications, (ii) security, (iii) intersection control, (iv) collision-free navigation, and (v) pedestrian detection and protection.

Despite the above-mentioned significant advancement in CAVs, better guidance is needed for the future deployment of CAVs. As mentioned in (Aiello et al., 2017; Perkins Coie LLP and AUVSI, 2019), a comprehensive and coherent regulatory framework is expected in order to help companies broadly deploy new technologies. In the latest released report "*AV 4.0*" (USDOT, 2019) by the U.S. Department of Transportation, it pointed out the need of a consistent United States (U.S.) Government approach to AV technologies. It also stated that the U.S. government will focus on opportunities in improving transportation system-level performance, efficiency, and effectiveness while avoiding negative transportation system-level effects from AV technologies. Even though many automakers and high-tech companies (Waymo, 2018; Tesla, 2019; Cruise, 2020; Huawei, 2021) have been conducting a lot of field tests to evaluate their autonomous driving systems, their tests are not systematic and comprehensive enough to inform government agencies about potential impacts of the deployment of AVs/CAVs at the network scale. Therefore, it is of great importance to develop tools to understand system-level impacts of CAVs to help government agencies make better decisions and policies.

In this project, we aim to develop an integrated microsimulation platform to evaluate the impact of different CAV applications on large-scale transportation networks. In particular, we will leverage the ACC/CACC and the V2X modules in the microsimulation software, Aimsun, to develop such a platform. Although other prevailing microsimulation software like Vissim (PTV Vissim, 2017; PTV Vissim, 2021) and TransModeler (TransModeler, 2021) provide modules/APIs to model the vehicle-level control of AVs/CAVs, the components to enable communications among Intelligent Transportation Systems (ITS) elements such as RSUs and CVs/CAVs with OBUs are missing. To bridge this gap, the state-of-the-practice approach is to develop external APIs to connect to some network simulators, e.g., Vissim+NS-2 in (Sun et al., 2016). However, this approach is hard to scale up to large networks as frequent external communications between the two simulators will significantly reduce the overall simulation speed. To the best of our knowledge, Aimsun (Aimsun Next, 2020b; Aimsun Next, 2020c, Aimsun Next, 2020d; Aimsun Next, 2020e) is the only microsimulation software that enables the V2X communications among ITS elements. That means the integrated microsimulation platform developed in this project, to the best of our knowledge, is one of the first "All-in-One" platforms in microsimulation for mixed traffic with CAVs.

In terms of study networks, we use the I-210 corridor network shown in Figure 1, which contains about 1000 lane miles of road links, 5000 traffic detectors, 459 signalized intersections, 45 freeway ramp meters, Metro gold line and all bus routes. It has been well calibrated for 24-hr simulations of Weekday, Saturday, and Sunday traffic. Complete sets of response plans and detour routes have been developed and approved

by stakeholders for freeway incidents. Using this corridor network, we should be able to assess the network-level impacts of various CAV applications.

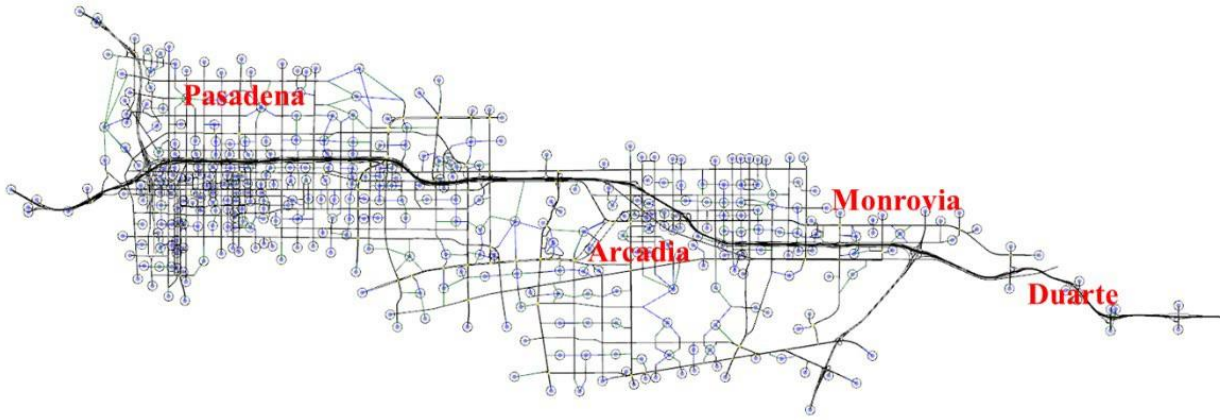

Figure 1. The I-210 network.

As a first step, we conduct a comprehensive review on recent development of CAVs, which includes vehicle-level control models as well as V2X applications. Since our goal is to evaluate system-level impacts of CAV applications on large-scale transportation networks, we focus on the review of the following applications given their importance and high potential for field deployment: (i) Co-operative adaptive cruise control (CACC) and Platooning, (ii) Freeway speed harmonization, (iii) Traffic light optimal speed advisory, and (iv) Route guidance. Besides that, we also provide a brief review of the car-following model implemented in Aimsun to help better understand how it controls regular vehicle's longitudinal movements.

Next, we provide a detailed tutorial on how to build the integrated microsimulation platform in Aimsun using the ACC/CACC and the V2X modules. We first introduce the steps to install all required software components, which include Aimsun Next 20, V2X SDK, V2X Framework, Visual Studio, and Qt. Then we list the available control modes in the ACC/CACC module and explain the decision chart on how these modes switch between each other. Furthermore, we introduce the key components and their properties in the V2X module, which include Messages, Channels, OBUs, RSUs, and TMCs. However, the ACC/CACC and the V2X modules were developed separately and thus could not be activated at the same time under Aimsun's current software design if the percentage of CAVs is less than 100%. Therefore, we provide a practical solution to bridge the gap between these two modules so as to build the integrated microsimulation platform for mixed traffic with any percentages of CAVs.

Furthermore, we demonstrate how to apply this integrated microsimulation platform to evaluate the network-level impacts of CAV applications. In particular, we implement the following three applications with CAVs for demonstration purposes: (i) freeway speed harmonization with CAVs, (ii) route guidance with CAVs for traffic incident management, and (iii) traffic light optimal speed advisory with CAVs. For each application, we implement the required workflows to enable the communications between RSUs and CAVs as well as algorithms to regulate CAV's driving behaviors and route choice decisions. We also generate different subnetworks from the original I-210 network for each of these applications: (i) a Freeway-Only subnetwork for the application of freeway speed harmonization with CAVs; (ii) a Freeway-

and-Arterial Combined subnetwork for the application of route guidance with CAVs for traffic incident management; and (iii) an Arterial-Only subnetwork for the application of traffic light optimal speed advisory with CAVs. With the above settings, we conduct various simulation scenarios under different time periods, demand levels, and percentages of CAVs to assess the performance of these three applications.

Ideally, it would be great to apply this integrated microsimulation platform to the I-210 network. However, we find that Aimsun becomes extremely slow and drains physical memory quickly for each simulation replication in the I-210 network when the V2X module is enabled. Therefore, we only enable the ACC/CACC module in the I-210 network to see how ACC/CACC can help improve transportation network performance, e.g., reducing vehicle delay and improving vehicle travel speed. In our scenario design, we do consider various factors that may impact the simulation results, for example, road geometries, vehicle routing and travel patterns, traffic demand, percentages of CAVs, and random seeds in microsimulation. Therefore, the network-level performance of ACC/CACC is concluded based on the averaged simulation results under various settings of network sizes, time periods, demand levels, and CAV percentages.

The rest of this report is organized as follows. In Section 2, we provide a review on recent development of CAVs. In Section 3, we provide a tutorial to set up an integrated microsimulation platform in Aimsun for mixed traffic with CAVs. In Section 4, we demonstrate three CAV applications in small networks. In Section 5, we show the impact of ACC/CACC on large-scale networks. In Section 6, we discuss some future research plans. In Section 7, we conclude our research findings in this project.

This page left blank intentionally

2. Literature review

Before developing Aimsun APIs and running simulations with CAVs, in this section, we would like to provide a comprehensive review on recent development of CAVs, which includes vehicle-level control models as well as V2X applications. Specifically, in (ETSI, 2009; ETSI, 2010), a basic set of V2X applications are listed for cooperative traffic efficiency, which are summarized below:

- **Speed Management**: Regulatory/contextual speed limit notification; Traffic light optimal speed advisory.
- **Cooperative Navigation**: Traffic information and recommended itinerary; Enhanced route guidance and navigation; Limited access warning; Detour notification.
- **Cooperative Vehicle Control:** Cooperative adaptive cruise control (CACC); Cooperative vehicle-highway automation system (Platoon); Cooperative flexible lane change; Intersection management.

Since our goal is to evaluate system-level impacts of CAVs on large-scale transportation networks, we decided to incorporate the following applications into our study given their importance and high potential for field deployment:

- **Co-operative adaptive cruise control (CACC) and Platooning**
  With V2X communications, CAVs are able to obtain leading vehicle's dynamics and general traffic information ahead and use this information as inputs to enhance the performance of ACC models. In addition, to maximize road capacities, they can form platoons with smaller gaps whenever possible. Therefore, better road efficiency is expected with the deployment of CAVs in the field, even with a small market penetration rate (MPR).

  Like car-following models for regular automobiles, a number of car-control algorithms have been proposed to model CAV's (or AV's) longitudinal movements. The most influential ones, to list a few, are the CACC control algorithm in (Van Arem et al., 2006), the family of the Intelligent Driver Model in (Treiber et al., 2000; Kesting et al., 2010; Schakel et al., 2010), the control framework in mixed traffic in (Talebpour and Hahmassani, 2016), and the PATH ACC/CACC model in (Shladover et al., 2012; Milanés et al., 2013; Milanés and Shladover, 2014; Lu et al., 2017; Liu et al., 2018a; Liu et al., 2018b; Liu et al., 2019). In particular, the PATH ACC/CACC model has been tested with field experiments and implemented in Aimsun (Version 8.4.3 or newer).

- **Freeway speed harmonization**
  Freeway speed harmonization is used to smooth traffic, reduce delays, or even eliminate the formation of freeway bottlenecks. With the presence of CAVs and the installation of Roadside Units (RSUs), speed harmonization will become more effective and efficient due to more accurate information inputs and a 100% compliance rate. Specifically, with V2I/I2V communications, an RSU can receive information (e.g., speed) from CAVs to help better estimate traffic conditions. Meanwhile, it can broadcast local speed limits generated by speed harmonization algorithms to the CAVs. For individual CAVs, once the recommended speed limit is received, they can use it as the reference speed input into the ACC/CACC model to regulate their longitudinal movements.

In the literature, a number of speed harmonization algorithms have been proposed with the consideration of CVs/CAVs, for example, the rule-based algorithm in (Talebpour et al., 2013), the cooperative variable speed limit system (C-VSLS) in (Grumert et al., 2015), the variable speed limit and advisory (VSL-VSA) algorithm in (Lu et al., 2015; Hale et al., 2016), and the speed recommendation strategy in (Learn et al., 2017). Note that, both the aforementioned VSL-VSA algorithm and the speed recommendation strategy have been tested with field experiments. Simulation and field test results have demonstrated that the presence of CAVs can help speed harmonization application achieve better performance to further reduce traffic oscillations and delay the formation of freeway bottlenecks.

- **Traffic light optimal speed advisory**

  This application aims to provide CAVs with real-time traffic light information (e.g., timing plans and phases) to help them make better decisions when crossing arterial intersections. Specifically, an RSU will periodically broadcast SPaT and MAP messages that contain real-time signal and road geometry information to incoming CAVs. A CAV, in particular the leader if a platoon is formed, will use this real-time signal and map information together with its current status (e.g., position and speed) to determine its best action. For example, it will maintain its current speed when the traffic light is expected to be green when it reaches the stopbar. However, it will start to decelerate and stop if a red light is expected.

  In the literature, many algorithms have been proposed for this application, to list a few, the green light optimal speed advisory (GLOSA) application in (Katsaros et al., 2011; Bodenheimer et al., 2014), the eco-approach and departure (EAD) application in (Hao et al., 2015; Hao et al., 2018), the GuidePath prototype system in (Xia et al., 2013; Wu et al., 2014; Altan et al., 2017), and the model predictive control (MPC) approach in (Smith et al., 2020). All the aforementioned algorithms/approaches have been tested with field experiments. However, for the deployment in large-scale networks, the GLOSA application will be more appropriate due to its simplicity.

- **Route guidance**

  When heavy traffic congestion occurs, it is important to inform incoming traffic about better routing options to avoid the impacted areas. Under recurrent traffic congestion, various algorithms have been proposed to incorporate CAVs into the development of optimal routing options for transportation networks. Examples can be found in (Davis, 2017; Houshmand et al., 2019; Chu et al., 2017; Chu et al, 2019; Djavadian and Farooq, 2018; Alfaseeh et al., 2018). However, solving such an optimal network routing problem is not easy. Many of these methods end up either to be too complicated or with a lot of unpractical assumptions. Furthermore, this situation is not as critical as when we have severe traffic incidents.

  When traffic incidents occur, traffic management centers (TMCs) will propose a series of detour routes to divert upstream traffic from the impacted areas. Along the detour routes, traffic signals at associated intersections will be changed with more green times allocated to preferred directions. However, only partial information is shown on dynamic message signs (DMSs) and/or wayfinding signs. As a result, very few drivers are able to follow the recommended routes, which makes the incident management very ineffective. With V2I/I2V communications, CAVs can get most up-to-

date detour information and help divert traffic to the recommended routes, which in return makes incident management more controllable and efficient.

In the literature, there have been some studies on how to incorporate CAVs into incident management, for example, dynamic routing behaviors for CAVs in (He, 2018), contraflow operations with CAVs in (Ekram and Rahman, 2018), and En-Route diversions with CAVs in (Li and Khattak, 2018). Furthermore, when a CAV receives the routing information, it can determine whether to take the new route or not. To model CAV's willingness to change routes, Samimi Abianeh et al. (2020) proposed a normal distribution function and introduced the number of rerouted vehicles and their lane distribution as parameter inputs to adjust the probability.

In the rest of this section, we will provide a detailed review on the above applications. Since there are many studies in each application, we have a higher priority to select the ones that have been tested with field experiments and have high potential for large-scale network deployment. In Section 2.1, we review the most influential car-control algorithms for AVs/CAVs. In Section 2.2, we review different algorithms on freeway speed harmonization for CAVs. In Section 2.3, we review some field applications on traffic light optimal speed advisory. In Section 2.4, we review studies on route guidance with CAVs under recurrent congestion and non-recurrent traffic incidents. In Section 2.5, we review the car-following model in Aimsun to help better understand how it controls regular automobile's longitudinal movements. Finally, we summarize our literature review in Section 2.6.

2.1 Control algorithms for CAVs

With advanced sensing techniques, a CAV can better detect movements of its surrounding vehicles and react quicker to unexpected changes, e.g., sudden braking and vehicle cut-in. Meanwhile, with information exchanged via V2V and V2I/I2V communications, it can better anticipate traffic states ahead, e.g., traffic jams or stop-and-go waves. Therefore, CAVs are expected to provide safer, smoother, and faster responses. Since many control algorithms have been proposed to model CAV's longitudinal movements, in the following subsections we only select those either widely used in simulations or have been tested with field experiments.

2.1.1 Van Arem's CACC control algorithms

In (Van Arem et al., 2006), a CACC model was incorporated into the simulation model, MIXIC (MICroscopic model for Simulation of Intelligent Cruise control), to simulate the impact of CAVs on road capacity and traffic stability. In MIXIC, the control of a CACC-equipped vehicle is divided into two steps: the CACC controller first determines a reference acceleration, and then the vehicle model will transform this reference value into actual realized values to control vehicle movements. For a subject vehicle ii (CACC-equipped), its reference acceleration $aa_{rrrrr,ii}$ is computed as follows:

$$\begin{aligned} aa_{rrrrr,ii} &= \min\{aa^{vv}_{rrrr,ii}, aa^{dd}_{rrrr,ii}\} \\ aa^{vv}_{rrrr,ii} &= kk \times (vv_{iiiii} - vv_{ii}) \\ aa^{dd}_{rrrr,ii} &= kk_{aa} \times aa_{ii-1} + kk_{vv} \times (vv_{ii-1} - vv_{ii}) + kk_{dd} \times (rr_{ii} - rr_{rrrr}) \end{aligned} \quad (1)$$

where

kk: a constant speed error factor;

kk_{aa}, kk_{vv}, kk_{dd}: constant factors;
aa_{ii-1}: acceleration of the leading vehicle $(ii-1)$;
vv_{ii-1}, vv_{ii}: speed of the leading $(ii-1)$ and subject (ii) vehicles, respectively;
vv_{iiiiii}: intended speed of the subject vehicle;
rr_{rrrrrr}, rr_{ii}: reference and current clearances between the leading and the subject vehicle, respectively.

The above calculation shows the reference acceleration $aa_{rrrrrr,ii}$ is taken as the minimum between the proposed acceleration $aa_{mmmm,ii}^{vv}$ based on its speed difference to the intended speed and the other proposed acceleration $aa_{mmmm,ii}^{dd}$ based on its speed and distance differences to its leader. Also, this reference acceleration is bounded by the maximum acceleration of $2 mm/ss^2$ and the maximum deceleration of $-3 mm/ss^2$.

In addition, the reference clearance rr_{rrrrrr} is defined as the maximum among the following three parameters: (i) safe following distance $rr_{ssaarrrr}$, (ii) following distance restricted by the system time setting $rr_{sssssssssrrss}$, and (iii) minimum allowed distance rr_{ssiiii}. Detailed calculation is provided below:

$$\begin{aligned} rr_{rrrr} &= \max\{rr_{ssaarrrr}, rr_{sssssssssrrss}, rr_{ssiiii}\} \\ rr_{ssaarrrr} &= \frac{vv_{ii}^2}{2}\left(\frac{1}{dd_{ii}} - \frac{1}{dd_{ii-1}}\right) \\ rr_{sssssssssrrss} &= tt_{sssssssssrrss} \times vv_{ii} \\ rr_{ssiiii} &= 2 \, mmmmtmmss \end{aligned} \tag{2}$$

where
dd_{ii-1}, dd_{ii}: deceleration capabilities (i.e., rates) of the leading and the subject vehicles, respectively;
$tt_{sssssssssrrss}$: system target time gap, e.g., 0.5s for CACC vehicles and 1.4s for regular automobiles.

In the Integrated full-Range Speed Assistant (IRSA) controller (Van Arem et al., 2007), the above CACC model was used. Besides that, additional CACC models were proposed to consider more vehicles (e.g., nn vehicles) in front. In particular, the following model (Van Arem et al., 2007; Schakel et al., 2010), CACC2, can function properly even under mixed traffic.

$$\begin{aligned} aa_{rrrrr,ii} &= \min\{kk(vv_{iiiiii} - vv_{ii}), kk_{vv} mm_{vv,ii} + kk_{dd} mm_{dd,ii} + \frac{kk_{v\_v}}{nn-2}\left(\sum_{kk=2}^{ii-1} mm_{kk,kk}\right)\} \\ mm_{vv,ii} &= vv_{ii-1} - vv_{ii} \\ mm_{dd,ii} &= rr_{ii} - rr_{rrrr} \end{aligned} \tag{3}$$

With information from the leading vehicle as well as vehicles further ahead, simulation results (Van Arem et al., 2007; Schakel et al., 2010) have demonstrated that the CACC2 model provides significantly better performance with respect to safety, string stability, and comfort.

2.1.2 The family of Intelligent Driver Model

2.1.2.1 Original IDM

The initial Intelligent Driver Model (IDM) was proposed in (Treiber et al., 2000), in which the acceleration $aa_{IIIIII,ii}$ of a subject vehicle ii is a continuous function of its speed vv_{ii}, its distance gap ss_{ii} and speed difference Δvv_{ii} to the leading vehicle. Therefore, the acceleration $aa_{IIIIII,ii}(ss_{ii}, vv_{ii}, \Delta vv_{ii})$ can be computed as

$$aa_{IIIIII,ii}(ss_{ii}, vv_{ii}, \Delta vv_{ii}) = aa_{ssaamm,ii}\left[1 - \left(\frac{vv_{ii}}{vv_{0,ii}}\right)^{\delta} - \left(\frac{ss^*(vv_{ii}, \Delta vv_{ii})}{ss_{ii}}\right)^2\right] \quad (4)$$

$$ss^*(vv_{ii}, \Delta vv_{ii}) = ss_{jjaass,ii} + vv_{ii}TT_{ii} + \frac{vv_{ii}\Delta vv_{ii}}{2\sqrt{aa_{ssaamm,ii}\, bb_{ii}}}$$

where

$aa_{ssaamm,ii}$: maximum acceleration of vehicle ii;

$vv_{0,ii}$: desired speed of vehicle ii;

$\delta\delta$: free acceleration exponent;

$ss_{jjaass,ii}$: jam distance/spacing of vehicle ii;

TT_{ii}: desired time gap of vehicle ii;

bb_{ii}: desired deceleration of vehicle ii.

The above IDM model can be divided into two components: a free-road acceleration strategy $aa_{ssaamm,ii}\left[1 - \left(\frac{vv_{ii}}{vv_{0,ii}}\right)^{\delta}\right]$ and a deceleration strategy $-aa_{ssaamm,ii}\left(\frac{ss^*(vv_{ii},\Delta vv_{ii})}{ss_{ii}}\right)^2$. When the vehicle gap ss_{ii} is not significantly larger than the effective "desired gap" $ss^*(vv_{ii}, \Delta vv_{ii})$, these two components become relevant. Also, in the effective "desired gap" $ss^*(vv_{ii}, \Delta vv_{ii})$, the term $\frac{vv_{ii}\Delta vv_{ii}}{2\sqrt{aa_{ssaamm,ii}\, bb_{ii}}}$ is a dynamic contribution that only activates in non-stationary traffic conditions with $\Delta vv_{ii} \neq 0$ and implements an "intelligent" driver behavior to limit the deceleration to a "comfortable deceleration" bb_{ii} under normal traffic conditions.

2.1.2.2 IDM with constant-acceleration heuristic

The original IDM model is designed to be "collision-free" since it can avoid collision even when the leading vehicle suddenly breaks with the maximum possible deceleration to a complete stand still. However, (Kesting et al., 2010) pointed out that it also leads to over-reactions in situations with comparatively low-speed differences and gaps significantly smaller than the desired ones. To overcome this issue, they proposed a so-called Constant-Acceleration Heuristic (CAH) to provide a more relaxed driving behavior with an assumption that both the subject and leading vehicles maintain constant accelerations in the next few seconds. Detailed calculation is provided below:

$$aa_{CCCCCC,ii}(ss_{ii}, vv_{ii}, vv_{ii-1}, aa_{ii-1}) = \begin{cases} \dfrac{vv_{ii}^2\, aa_{ii-1}}{vv_{ii-1}^2 - 2ss_{ii}aa_{ii-1}} & vv_{ii-1}(vv_{ii} - vv_{ii-1}) \leq -2\, ss_{ii}\, aa_{ii-1} \\ aa_{ii-1} - \dfrac{(vv_{ii} - vv_{ii-1})^2\,\Theta(vv_{ii} - vv_{ii-1})}{2ss_{ii}} & otherwise \end{cases} \quad (5)$$

where $aa_{ii-1} = \min\{aa_{ii-1}, aa_{ssaamm,ii-1}\}$ is the effective acceleration and $\Theta(vv_{ii} - vv_{ii-1})$ is the Heaviside step function to avoid negative approaching rates.

To model the behavior of ACC equipped vehicles, the following control logit is used in (Kesting et al., 2010):

$$a_{CACC,i}(t+\Delta t) = \begin{cases} (1-c)a_{IIDM,i}(t) + c\left[a_{CACC,i}(t) + b_i \tanh\left(\frac{a_{IIDM,i}(t) - a_{CACC,i}(t)}{b_i}\right)\right] & a_{IIDM,i}(t) \geq a_{CACC,i}(t) \\ a_{IIDM,i}(t) & \text{otherwise} \end{cases} \quad (6)$$

where c is a cooling factor. When $c = 0$, it converges to the original IDM model. However, it is inappropriate to set $c = 1$ because the ACC acceleration model has low sensitivity to the changes in gaps under situations of small gaps and no speed difference. Therefore, in (Kesting et al, 2010), c is set to be 0.99.

In the proposed ACC model, the acceleration of a subject ACC vehicle not only depends on its speed and spacing, but also the speed and acceleration of the leading vehicle. It works better than the original IDM model especially in situations of approaching congested traffic and vehicle cut-in from adjacent lanes. Regarding the ACC driving strategy, Kesting et al. (2010) divided traffic conditions into the following categories and assigned different multiplication factors (e.g., λ_{TT}, λ_{aa}, and λ_{bb}) to the IDM parameters of Safety Time Gap T_i, Maximum Acceleration $a_{max,i}$, and Comfortable Deceleration b_i. Details are provided below:

- Free traffic: default/comfort driving behavior with $\lambda_{TT} = 1$, $\lambda_{aa} = 1$, and $\lambda_{bb} = 1$;
- Upstream jam front: increased safety driving behavior with $\lambda_{TT} = 1$, $\lambda_{aa} = 1$, and $\lambda_{bb} = 0.7$;
- Congested traffic: default/comfort driving behavior with $\lambda_{TT} = 1$, $\lambda_{aa} = 1$, and $\lambda_{bb} = 1$;
- Downstream jam front: high dynamic capacity driving behavior with $\lambda_{TT} = 0.5$, $\lambda_{aa} = 2$, and $\lambda_{bb} = 1$
- Bottleneck sections: breakdown prevention driving behavior with $\lambda_{TT} = 0.7$, $\lambda_{aa} = 1.5$, and $\lambda_{bb} = 1$.

2.1.2.3 IDM+ with triangular fundamental diagrams

As mentioned in (Schakel et al., 2010), even though the original IDM generates realistic shockwave patterns, it has to use unreasonable values of desired time headways in order to reach reasonable capacity values. To address this problem, Schakel et al. (2010) made some adjustments by explicitly separating the free-flow and interaction terms in the original IDM. As a result, the IDM changes from a smooth topped-off shape to a triangular shape in the equilibrium fundamental diagram. Detailed formulation is provided below:

$$\begin{aligned} a_{IIDM+,i}(s_i, v_i, \Delta v_i) &= a_{max,i} \min\left\{1 - \left(\frac{v_i}{v_{0,i}}\right)^{\delta}, 1 - \left(\frac{s^*(v_i, \Delta v_i)}{s_i}\right)^2\right\} \\ s^*(v_i, \Delta v_i) &= s_{jam,i} + T_i v_i + \frac{v_i \Delta v_i}{2\sqrt{a_{max,i} b_i}} \end{aligned} \quad (7)$$

2.1.3 Control framework in mixed traffic

In (Talebpour and Hahmassani, 2016), a comprehensive acceleration framework was proposed to model driving environment in mixed traffic: different acceleration models are used for regular, connected, and autonomous vehicles under different assumptions.

When V2V communications is available, drivers can have information about other drivers' behaviors as well as the surrounding environment. In this case, the original IDM model (Treiber et al., 2000) is used, which is provided in Equation (4). For V2I/I2V communications, it will provide vehicles real-time

information about TMC's decisions to improve safety and mobility. But from driver's standpoint, it won't influence driver's acceleration choice. Therefore, the acceleration model in this case depends on whether active V2V communications is available or not: if yes, the IDM model is used; or else, the model for regular drivers is used.

To model autonomous vehicles, the acceleration model proposed by (Van Arem et al., 2006) is used to model vehicle's movement, which is provided in Equation (1). Besides that, for safety consideration, the maximum speed of autonomous vehicles is limited by the sensor's detection range and is formulated as below:

$$\begin{aligned} vv_{ssaamm} &= \sqrt{\cdot - 2aa_{ii}^{ddmmiiii}\Delta xx} \\ \Delta xx &= \min\{SSmmssoorr\ DDmmttmmaattiioomm\ RRaannRRmm, \Delta xx_{ii}\} \\ \Delta xx_{ii} &= (xx_{ii-1} - xx_{ii} - ll_{ii-1}) + vv_{ii}\tau\tau + \frac{vv_{ii-1}^{2}}{2aa_{ii-1}^{ddmmddll}} \end{aligned} \tag{8}$$

where

ll_{ii-1}: the length of vehicle $ii-1$;

$aa_{ii}^{ddrrddddd}$ and $aa_{ii-1}^{ddrrddddd}$: maximum deceleration rates of vehicle ii and $ii-1$, respectively;

$\tau\tau$: vehicle's reaction time.

2.1.4 The PATH's ACC/CACC models

The California Partners for Advanced Transportation Technology (PATH) program has been involved in the research, development, and testing of CAVs for more than three decades, since its inception in 1986. As in (Shladover et al., 2012), depending on the distance to leading vehicles, two control strategies were proposed for ACC and CACC equipped vehicles:

- When the spacing is larger than 120m: Speed control is activated, and it tries to keep vehicles close to the speed limit $vv_{0,ii}$.

$$\begin{aligned} vv_{rrrr,ii} &= vv_{ii} - vv_{0,ii} \\ aa_{ii} &= aa_{ssdd,ii} = bbooddmmdd(-0.4 \times vv_{rrrr,ii}, 2, -2) \end{aligned} \tag{9}$$

  Here $bboobbmmdd()$ is used to bound the acceleration inside the region $[-2, 2]$ mm/ss^2. 2 mm/ss^2 and -2 $mm/ss^2$are the maximum acceleration and deceleration for the ACC/CACC equipped vehicles.

- When the spacing is smaller than 100m: Gap control is activated, and it tries to maintain the desired gap between the subject vehicle and the leading vehicle.

$$\begin{aligned} ss_{dd,ii} &= TT_{ii} \times vv_{ii} \\ ss_{rr,ii} &= ss_{ii} - ss_{dd,ii} \\ aa_{ii} &= bboobbmmdd(ss_{ii} + 0.25 \times ss_{rr,ii}, aa_{ssdd,ii}, -2) \end{aligned} \tag{10}$$

  where

  $ss_{dd,ii}$: desired spacing for vehicle ii;

$ss_{rr,ii}$: error between current and desired spacings for vehicle ii.

- When the spacing is between 100m and 120m: the subject vehicle remains in the speed control if its spacing decreases from 120m, while it remains in the gap control if its spacing increases from 100m.

For the selection of desired time gaps of ACC and CACC vehicles, the following values are used: (i) 31.1% at 2.2s, 18.5% at 1.6s, and 50.4% at 1.1s for ACC vehicles; (ii) 12% at 1.1s, 7% at 0.9s, 24% at 0.7s, and 57% at 0.6s for CACC vehicles.

The ACC/CACC control algorithms have improved a lot based on simulation studies and fields tests. To list a few, refer to the studies in (Milanés et al., 2013; Milanés and Shladover, 2014; Lu et al., 2017; Liu et al., 2018a; Liu et al., 2018b; Liu et al., 2019). In particular, a more comprehensive description of the latest ACC and CACC models was provided in (Liu et al., 2018b), which are also used as the CAV models in the latest release of Aimsun (e.g., Version 8.4.3 or newer).

In (Liu et al., 2018b), the CACC controller consists of three driving modes: ACC mode, speed regulation mode, and (leader & follower) gap regulation mode. When the distance to a manually driven vehicle in front is longer than 120m or when the time gap to a CACC leader is more than twice of the desired value, the following speed regulation mode is used:

$$aa_{ii} = kk_3(vv_{mmmm} - vv_{ii}) \tag{11}$$

where kk_3 is the gain in the speed difference between the free-flow speed vv_{mmmmm} and the current speed of the subject vehicle ii.

When the subject vehicle is following a manually driven vehicle, the following ACC mode is used:

$$aa_{ii} = kk_1(dd - TT_{ii}vv_{ii} - ll_{ii-1}) + kk_2(vv_{ii-1} - vv_{ii}) \tag{12}$$

where
kk_1 : gain in position difference between the leading vehicle $ii-1$ and the subject vehicle ii;
kk_2 : gain in speed difference between the leading vehicle $ii-1$ and the subject vehicle ii;
dd: distance between the subject vehicle's front bumper and the leading vehicle's front bumper;
ll_{ii-1} : the length of the leading vehicle $ii-1$;
vv_{ii-1} : current speed of the leading vehicle $ii-1$;
TT_{ii}: desired time gap of the subject vehicle ii. Its value is drawn from the following distribution provided in (Nowakowski et al. 2010): 31.1% at 2.2 s, 18.5% at 1.6 s; and 50.4% at 1.1 s.

When the subject vehicle is in the car-following status and the leading vehicle is a CACC vehicle, the following gap regulation mode is used:

$$\begin{aligned} aa_{ii}(tt) &= \frac{vv_{ii}(tt) - vv_{ii}(tt - \Delta tt)}{\Delta tt} \\ vv_{ii}(tt) &= vv_{ii}(tt - \Delta tt) + kk_{pp}mm_{kk}(tt) + kk_{dd}\dot{mm}_{kk}(tt) \\ mm_{kk}(tt) &= dd(tt - \Delta tt) - TT_{aaaaaaa}vv_{ii}(tt - \Delta tt) - ll_{ii-1} \end{aligned} \tag{13}$$

$$mm_{ik}(tt) = vv_{i-1}(tt - \Delta tt) - vv_{ii}(tt - \Delta tt) - TT_{cccccccc} aa_{ii}(tt - \Delta tt)$$

where

kk_{pp} and kk_{dd}: gains for adjusting the time gap between the subject vehicle ii and the leading vehicle $ii - 1$;

$mm_{ik}(tt)$: time gap error;

$\dot{m}_{ik}(tt)$: speed error;

Δtt: updating time step;

$TT_{cccccccc}$: constant time gap adopted by the CACC controller.

When the leading vehicle's CACC string reaches its maximum length, the subject vehicle is operated in the string leader gap regulation mode and the constant time gap $TT_{cccccccc}$ is selected to be 2s. Otherwise, the subject vehicle is operated in the string follower gap regulation mode. Its constant time gap is drawn from the following distribution (Nowakowski et al. 2010): 57% at 0.6s, 24% at 0.7s, 7% at 0.9s, and 12% at 1.1s.

2.2 Freeway Speed Harmonization with CAVs

When recurrent traffic congestion occurs on freeways, many studies and field experiments have demonstrated Speed Harmonization is an effective strategy to smooth traffic, reduce delays, or even eliminate the formation of traffic bottlenecks. But as mentioned in (Ma et al., 2016), traditional speed harmonization control approaches, e.g., Variable Speed Limits (VSLs), usually demand a high compliance rate to be effective. However, with the existence of Connected Vehicles (CVs), many studies showed that a relatively low compliance rate (e.g., 5-10%) can assure improvements on system performance. This may be because CVs are in fact Lagrangian sensors, and thus a small number can yield accurate information. Considering the deployment of CAVs, it is expected that Speed Harmonization will be more effective due to better vehicle control and a 100% compliance rate.

In (Talebpour et al., 2013), a rule-based speed harmonization algorithm was used to control, reduce delays, or even eliminate the formation of traffic breakdowns. The Wavelet Transform (WT) method proposed by (Zheng et al., 2011) was used to detect initial points of traffic breakdown, e.g., traffic shock wave, from vehicle trajectories. Once detected, the rule-based method similar to (Allaby et al., 2007) was used to generate recommended speeds for vehicles in the upstream. The detailed decision tree in the method is provided in Figure 2. Simulation results demonstrated that this speed harmonization algorithm can effectively manage and even eliminate the formation of traffic breakdowns. It indicated that there is an optimal location in the upstream to display the recommended speeds, which can result in the most effective congestion control. It showed that a 10% compliance rate is sufficient for the system to attain its objectives, which can be easily adapted by CVs/CAVs in the near future.

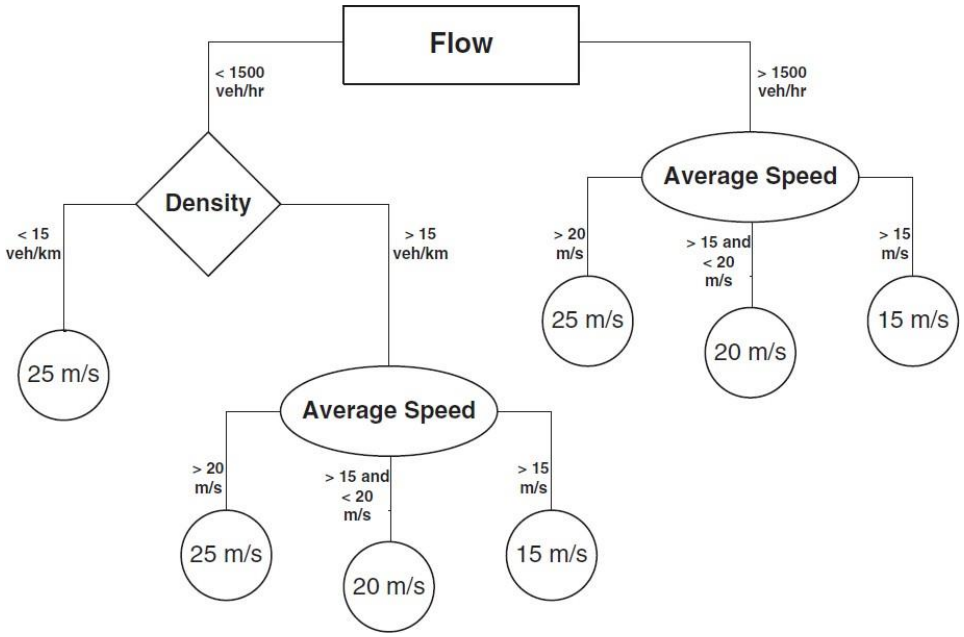

Figure 2. Speed harmonization decision tree in (Talebpour et al., 2013).

As an extension to the existing variable speed limit system (VSLS) (van Toorenburg and de Kok, 1999), Grumert et al., (2015) proposed a cooperative variable speed limit system (C-VSLS) for CAVs to harmonize traffic flow and reduce exhaust vehicle emissions. With the C-VSLS, information about the variable speed limit can be received at an earlier point in time via V2I/I2V communications. CAVs are fed with individual speed limits that are determined by the speed limits recommended by the existing VSLS, the current speeds and positions of CAVs. For the existing VSLS, the mean speed $vv_{dd,ssrraaii}$ at detector dd is calculated as the following smoothed harmonic mean speed:

$$\frac{1}{vv_{dd,ssrraaii}(tt+1)} = \alpha\alpha \frac{1}{vv_{dd,ssrraassmmnnrrrrdd}} + (1-\alpha\alpha)\frac{1}{vv_{dd,ssrraaii}(tt)} \tag{14}$$

where $vv_{dd,ssrraassmmnnrrrrdd}$ is the measured speed at detector dd and $\alpha\alpha$ is a smoothing parameter between 0 and 1. If the mean speed $vv_{dd,ssrraaii}$ goes below 45km/h, the closest variable speed limit sign near the detection point is set to be 60 km/h, while the upstream two variable speed limit signs are set to 80km/h and 100 km/h, respectively. In contrast, if the mean speed $vv_{dd,ssrraaii}$ increases back to 55km/h, all related variable speed limit signs are updated to 120km/h. Then for an individual CAV ii, the recommend individual speed limit $vv_{ii,VVVVV}$ is calculated as follows.

$$\begin{aligned} aa_{ii} &= \frac{vv_{jj,WWW}^2 - vv_{ii}^2}{2LL_{iijj}} \\ vv_{ii,WWW} &= vv_{ii} + aa_{ii}TT \\ vv_{ii,WWW} &= \max\{vv_{jj,WWW}, \min\{VV_{ssaamm}, vv_{ii,WWW}\}\} \end{aligned} \tag{15}$$

where

LL_{iijj}: distance to the speed limit sign jj when vehicle ii receives the message;

$vv_{jj,VVVVV}$: speed limit recommended by the variable speed limit sign jj;

VV_{ssaamm}: maximum speed on the road;

TT: time interval to update the speed limits;

vv_{ii} : vehicle's current speed.

Once $vv_{ii,VVVVVV}$ is received, the CAV ii can use it as reference inputs to adjust its speeds with information from surrounding environments.

With the aim to improve traffic performance at a freeway corridor with multiple bottlenecks, a Variable Speed Limit (VSL) and Advisory (VSA) algorithm was proposed in (Lu et al., 2015; Hale et al., 2016). The proposed algorithm aims to delay traffic breakdown and improve throughputs for heavy traffic by: (i) reducing the in-flow from the upstream of a bottleneck with lower recommended speeds, and (ii) increasing the recommended speeds at the bottleneck. For a given bottleneck location mm, the proposed algorithm can be described as below:

- At the bottleneck section, the following speed advisory $bb_{ss}(tt)$ is recommended.

$$bb_{ss}(tt) = \alpha\alpha_{ss}\, \bar{v}_{ss}(tt)$$
$$\alpha\alpha_{ss} \in [1.1, 1.5]; \text{ default value: } \alpha\alpha_{ss} = 1.3 \quad (16)$$

  where $vv_s\,(tt)$ is the measured speed, $\alpha\alpha_{ss}$ is a scaling factor at the freeway section mm.
- At the immediate upstream section relative to the bottleneck, the following speed limit $bb_{ss+1}(tt)$ is used.

$$bb_{ss+1}(tt) = \begin{cases} vv_{mmmmm} & \text{iii } \bar{O}_{ss}(tt) \le OOcccc_{ssss} \\ \beta\beta_{ss}\, v_{ss}(tt) & \text{iiii } \bar{O}_{ss}(tt) > OOcccc_{ssss} \end{cases} \quad (17)$$
$$\beta\beta_{ss} \in [0.7, 0.9]; \text{ default value: } \beta\beta_{ss} = 0.8$$

  where $O\bar{O}cc\bar{O}cc\bar{O}_{ss}$ is the measured occupancy at the bottleneck location mm, $OOccccc_{ssss}$ is the switch occupancy threshold close to capacity flow, and $\beta\beta_{ss}$ is a scaling factor.

This algorithm can be applied to CAVs with V2I/I2V communications by directly using the recommended speeds as reference speeds in the ACC and CACC control algorithms. Such a framework has been demonstrated with a field test in (Lu et al., 2015). Simulation results also demonstrated that: (i) the proposed algorithm can produce reasonable recommended speeds; and (ii) system performance improves moderately in the following aspects: Total Travel Time, Total Delay, Total Travel Distance, Speed Variation, Total Number of Stops, and Downstream Bottleneck Throughput.

Similarly, in (Learn et al., 2017), a field experiment was carried out to demonstrate how to incorporate CAVs into speed harmonization to regulate traffic upstream of a bottleneck so as to provide better traffic performance. In the experiment design, CAVs are used to control the flow of traffic and the system performance is analyzed at the microscopic level. V2I/I2V communications is used to provide CAVs with recommended speeds which are determined by the speed recommendation strategies based on downstream traffic conditions. The CAVs receive speed recommendations every 2 seconds and adjust their speeds accordingly via the ACC control. Two trailers were placed at the beginning and the end of a speed harmonization segment to measure average vehicle speeds, i.e., $vv_{mmpp}(tt)$ and $vv_{ddddssii}(tt)$, respectively. The recommended speed $vv_{rrrrdd}(xx, tt)$ is a linear interpolation function between these two speed measurements, which is provided below.

$$vv_{rrrdd}(xx, tt) = \frac{vv_{ddddssii}(tt) - vv_{mmpp}(tt)}{L_s}\, xx + vv_{ddddssii}(tt) \quad (18)$$

where LL_{ss} is the length of the speed harmonization segment and xx is the distance to the downstream end of the segment. Experiment results showed that the proposed speed harmonization strategy with CAVs can smooth traffic oscillations at freeway bottlenecks, which will lead to reduced fuel consumption and emissions.

2.3 Traffic light optimal speed advisory with CAVs

According to (Guo et al., 2019), advanced traffic control at arterial intersections under connected and/or autonomous vehicles can be divided into the following three categories:

- **C1: Driver guidance control systems based on signal and vehicle data**. Such systems provide instructions to drivers/AVs to properly operate vehicles so as to minimize fuel consumptions, reduce travel delays, etc.
- **C2: Optimization of signal timings and phases based on data from CAVs.** Such a category includes actuated signal control, platoon-based signal control, and planning-based signal control.
- **C3: Signal-vehicle coupled control (SVCC) systems with CAVs.** Such systems aim to optimize both vehicle and signal timings/phases to achieve better performance at intersections.

Considering the readiness of the above control categories as well as the scope of our study, we focus on the studies in the first category **C1**.

In (Katsaros et al., 2011), a so-called Green Light Optimal Speed Advisory (GLOSA) application was evaluated under the V2I/I2V communications environment. In this application, RSUs attached to traffic lights will periodically broadcast CAMs (Cooperative Awareness Messages) that contain information like their positions and signal timings to nearby vehicles. For each vehicle equipped with an OBU, it receives these CAMs and determines its actions based on the predicted traffic light status when it reaches the intersection.

- When the predicted traffic status is green, it should continue with the goal to reach the maximum speed limit.
- When the predicted traffic status is red, it calculates its speed so as to reach the next green phase.
- When the predicted traffic status is yellow, it determines whether it should accelerate or decelerate given the remaining yellow time and the acceleration capability of the vehicle.

In the GLOSA algorithm, an updating interval of 1 second is used to guarantee its robustness against external interference. The projected time to reach the traffic light is determined through the following equation,

$$TT_{TW} = \begin{cases} \dfrac{dd}{vv_0} & eehmmmaaa = 0 \\ -\dfrac{vv_0}{aa} + \sqrt{\dfrac{vv_0^2}{aa^2} + \dfrac{2dd}{aa}} & eehmmmaaa \neq 0 \end{cases} \quad (19)$$

where

d: distance to the intersection stopbar;

vv_0: initial speed when the vehicle receives a CAM;

aa: acceleration of the vehicle.

Meanwhile, when the projected traffic light status is either yellow or red, the target speed $vv_{ssaarrttrrss}$ is calculated as

$$vv_{ssaarrttrrss} = \frac{2 * dd}{tt} - vv_0$$

$$tt = \begin{cases} TT_{TTW} & \text{eehvmaqpprojjrmactrmadlttrcaiiiiicc lliiRRttiissRRrmmmmm} \\ TT_{TTW} + TT_{rrrrdd} & \text{eehvmaqpprojjrmactrmadlttrcaiiiiicc lliiRRttiissrmmadl} \\ TT_{TTW} + TT_{rrrrdd} + TT_{ssrryyyyddss} & \text{eehvmaqpprojjrmactrmadlttrcaiiiiicc lliiRRttiissyyrmlllooee} \end{cases} \quad (20)$$

where TT_{rrrrdd} is the remaining red time, and $TT_{ssrryyyyddss}$ is the remaining yellow time.

The advisory speed is determined as follows.

$$vv_{aaddvviissrr} = \max\{vv_{ssaarrttrrss}, vv_{ssiiii}\} \& \min\{vv_{ssaarrttrrss}, vv_{ssaarrmm}\} \quad (21)$$

where vv_{ssiiii} and $vv_{ssaarrmm}$ are the permitted min and max speed limits. Simulation results showed that the benefit of the GLOSA application starts to be visible when the MPR exceeds 50%. The total benefit can reach a maximum of 80% reduction in stop time and 7% reduction in fuel consumption. Also, there exists an optimal activation distance for the GLOSA application, which is about 300m from the traffic light. Furthermore, studies in (Bodenheimer et al., 2014) developed a method that is able to predict a traffic light change 15s in the future with an accuracy of over 80% in adaptive signal control, which guarantees the proper application of GLOSA to fully or semi-adaptive traffic lights.

To better minimize idling times and avoid unnecessary accelerations and decelerations when vehicles approach an intersection, an Eco-Approach and Departure (EAD) application has been proposed and validated with simulations and field tests. In (Hao et al., 2015; Hao et al., 2018), a generalized framework of EAD application for actuated signal control was proposed. A vehicle trajectory planning algorithm is used to provide speed recommendations based on inputs of the subject and the preceding vehicles' states as well as information from upcoming traffic signals. When the subject vehicle approaches an intersection, depending on the traffic signal status, it can choose to: (i) stop with a prescribed speed profile; (ii) accelerate or keep speed at the speed limit; (iii) accelerate or decelerate to a designed uniform speed; and (iv) keep its current speed. Field test results showed that the proposed EAD system can reduce the idling or near-idling cases by 22% and save 6% energy for the EAD activated trip segments. Results also showed such a system performs better for light traffic conditions when no or few preceding vehicles exist.

Similar to the aforementioned EAD studies, in (Xia et al., 2013; Wu et al., 2014; Altan et al., 2017), four different scenarios are considered when a subject vehicle approaches an intersection:

- Cruise: if the subject vehicle can pass through the intersection easily during a green traffic signal phase without speeding up or slowing down;
- Speed up: if the subject vehicle can pass the intersection on the green phase with its speed increased to a certain safe speed range;
- Coast down with stop: when it is not possible to pass through the intersection;
- Coast down without stop: when it is possible to pass through the intersection with lower speeds.

With the consideration of partial vehicle automation which can better conduct the recommended speed profiles, a so-called GuidePath Prototype system was developed and tested with field experiments. Results

showed that GuidePath can reduce fuel consumption by 17% on average, while manual driving can only save 5% on average. It also pointed out that higher benefits can be expected from the GuidePath Prototype system with a longer communication range, e.g., 300m.

When the MPR of CAVs increases, it is also possible to form platoons in arterial streets. Therefore, in (Smith et al., 2020), a model-predictive-control (MPC) based approach was proposed to allow vehicle platooning on urban streets. V2I/I2V communications is enabled to allow vehicles receive SPaT (signal, phase, and timing) messages from nearby traffic lights, while V2V communications is used to allow vehicles to receive information (e.g., velocity forecasts, GPS coordinates, radar measurements, and signal plan status) from the front and the leading vehicles. Finite State Machine (FSM) with four states, "Ready", "Plan Proposed", "Plan Active", and "Plan cancel", is used as a mechanism for safely forming and maintaining a platoon. Two different MPCs are proposed for the leader and followers: (i) the MPC for the leader aims to generate desired velocities for the followers according to changing traffic conditions; (ii) the other MPC for the followers aims to maintain a desired distance to the leader as well as a minimum safety distance to the front vehicle at all times. Simulation results showed that intersection capacity can be doubled with the proposed platooning architecture, and field tests were conducted to show its readiness for field implementation.

2.4 Route guidance with CAVs

2.4.1 Under recurrent traffic conditions

With the presence of CAVs, routing in transportation network should become more effective and efficient. On the one hand, with V2I/I2V communications, TMCs and RSUs will have better estimates of traffic states through information collected from CAVs. This is a significant improvement from the traditional way of using functions like the US Bureau of Public Roads (US BPR, 1964) to determine travel times from link flows. On the other hand, CAVs will receive and strictly follow up-to-date personalized routing guidance from TMCs and RSUs, which eliminates the uncertainties from human drivers and makes the network traffic more controllable. Therefore, a number of routing schemes/models have been proposed with consideration of the presence of CAVs.

In (Davis, 2017), information from CAVs on a road network was used as inputs to predict the optimal route for a given Origin-Destination pair. Simulations were performed on a homogeneous arterial grid network. Results showed that when potential routes have the same lengths, only the one with the minimum number of vehicles needs to be considered. However, for routes with different lengths, it would be better to use average vehicle velocities to calculate route travel times and then use them to determine the optimal one. In terms of effectiveness, algorithms based on the number of vehicles and on the average vehicle velocity have similar performance since these two attributes are closely related. However, no correlation is observed between the link flows and the number of vehicles or travel time, which indicates the prevailing Bureau of Public Roads (BPR) function is not useful for CAVs in the test network.

Considering the presence of mixed traffic, time-optimal and eco-routing algorithms were proposed in (Houshmand et al., 2019). In the proposed framework, system-centric routing schemes are used for CAVs while for traffic assignment with Wardrop equilibrium is used for non-CAVs. An iterative procedure is used to find an equilibrium for mixed traffic flows of CAVs and non-CAVs. In each iterative step, routes are optimized for CAVs first and non-CAVs next. The whole iteration will stop when the solution is

converged. BPR function is still used for the calculation of travel times according to the flow inputs. Numerical results from the Braess network as well as the Eastern Massachusetts road network demonstrated that the proposed collaborative routing decisions can help reduce travel times as well as energy costs for both CAVs and non-CAVs. Results also showed that even a small penetration rate of CAVs can significantly impact the overall network travel cost. However, it is interesting to observe that with the proposed algorithm, CAVs always have longer travel times (or high energy cost) compared to the non-CAVs under various market penetration rates.

To avoid unnecessary traffic jams and thus improve transportation efficiency, a dynamic lane reversal-traffic schedule management (DLR-TSM) scheme was proposed for CAVs in (Chu et al., 2017; Chu et al, 2019). The proposed DLR-TSM scheme assumes CAVs are able to receive timely information regarding lane direction reversals and thus can run on the reversible roads. Information of vehicle OD and travel time window is taken as inputs, and the objective function is to minimize total travel times while penalizing late arrivals. Linear Integer Programing (LIP) is used to solve the problem and obtain optimal routes for CAVs. To reduce the computational complexity, an asynchronous distributed algorithm of alternating direction method of multipliers (ADMM) (Boyd et al., 2011) is proposed to decompose the optimization problem into sub-problems to achieve a linear computational time. Simulations were performed on a small grid network in Manhattan, NY, with real-world taxi data that contains pick-up and drop-off times and locations. Assumptions of constant speeds and no traffic signal control were made for simplicity. Results showed that the proposed DLR-TSM scheme can significantly improve travel times for CAVs and the distributed algorithm can dramatically reduce the computational time.

When dealing with large-scale traffic networks, distributed routing system outperforms central routing system since quicker control actions can be obtained with local data. Traffic condition, Market Penetration Rate (MPR), and updating time interval are key factors that have significant impacts on the performance of any distributed routing systems. In (Djavadian and Farooq, 2018; Alfaseeh et al., 2018), an End-to-End Distributed Routing System, E2ECAV, was proposed for intelligent intersections and Level 5 CAVs. In E2ECAV, each intersection hosts a routing table, which is updated based on the information from downstream intersections. When a CAV arrives, the intersection routes it to the next intersection according to its destination so as to minimize travel times for both individual CAVs and the network and to maximize intersection capacities. A large-scale urban network of downtown Toronto was used to assess the effectiveness of the proposed distributed routing system under various MPRs and traffic conditions. Analysis results demonstrated that an updating interval of 60 seconds is optimal and realistic considering communication and process delays. Also, with the proposed distributed routing strategy, higher MPRs of CAVs lead to better traffic network performance, e.g., less travel times and higher throughputs. This is profound especially in the case of congested and highly congested traffic networks.

2.4.2 Under traffic incidents

When traffic incidents occur, CAVs will receive latest incident-related information from TMCs and RSUs via V2I/I2V communications. Meanwhile, CAVs on impacted road segments can also perceive some incident information via sensing the speeds of front vehicles. Together with the above information inputs, CAVs can make decisions on whether to divert into alternative routes to avoid congestion. Therefore, many studies have proposed models to provide routing suggestions to CAVs so as to reduce network traffic congestion caused by incidents.

In (He, 2018), a Markov Decision Process (MDP) was proposed to model dynamic routing behaviors for a single CAV under stochastic situations of receiving incident information. The state space in the MDP is formed by the node states that consist of location, information, and incident. The action space for a given state is defined as all possible links that the vehicle may choose to go next. The transition probabilities are the set of probabilities from current states to the next possible states. The cost of travelling along a link is the associated travel time. The objective of the MDP is to find an optimal policy to minimize the sum of expected travel cost for each state, and backward induction is used to find the optimal solution. Analysis results on different networks showed that less travel cost is expected when incident information is available to the CAVs. Furthermore, with readily available incident information, switching to alternative routes can help avoid congested traffic to achieve shorter travel times.

Ekram and Rahman (2018) used microsimulations to analyze the effectiveness of connected and autonomous vehicles on contraflow operations for emergency evaluation. Results showed that CAVs can provide better network performance in terms of average speed, overall delay, travel time, and queueing delay. Li and Khattak (2018) investigated En-Route diversion under traffic incidents through simulations on large-scale networks. In particular, important factors such as existence of CAVs and incident information availability were considered in the process of determining driver's routing options. Results showed that CAVs can help save more travel costs when the En-Route diversion strategy is implemented under heavy congestion caused by severe traffic incidents on freeways. Besides that, the availability of real-time travel information provides positive impacts on (both truck and passenger) driver's selection of En-Routes to reduce its travel delay.

Recently, in (Samimi Abianeh et al., 2020), the impact of connected vehicles on network-level traffic operations and fuel consumptions was investigated under various incident scenarios. In the modeling of routing schemes for connected vehicles, it is assumed that connected vehicles have the ability to send and receive information from other vehicles (i.e., V2V communications) and roadside devices (i.e., V2I/I2V communications), and thus are able to reroute when heavy traffic congestion occurs due to traffic incidents. A new route will be determined with real-time link travel times calculated from information shared by connected vehicles. Drivers of connected vehicles will be informed about the traffic congestion and will determine whether to take the new route or not. To model driver's willingness to change routes, the following normal distribution function is used:

$$PP_{rrrddrrssrr} = \alpha\alpha \times \frac{\exp\left(-\frac{nn^2}{2 \times \sigma\sigma^2}\right)}{\sqrt{2\pi} \times \sigma\sigma} \tag{22}$$

where

$\alpha\alpha$: constant to adjust the probability function;

nn: number of rerouted vehicles on each link;

$\sigma\sigma$: standard deviation of the normal distribution.

Here $\alpha\alpha$ can be used to simulate the behavior of travelers on each lane of the links so that vehicles on the inner lanes will have lower probability to reroute. In addition, the above equation also considers a higher number of rerouted vehicles will result in a lower probability to choose the alternative route. Simulation results showed that for an incident with a duration of 900 seconds, the total fuel consumption and total travel time can be reduced by 10% with a market penetration rate (MPR) of 20% connected vehicles. A total reduction of 20% can be expected when the MPR increases to 80%.

2.5 Car-following models in Aimsun

In practice, various software has been developed to simulate vehicle dynamics in transportation networks. The prevailing commercial microsimulation software includes Aimsun[1], Vissim[2], TransModeler[3], and Paramics[4]. Among them, different car-following models are implemented to control vehicle's longitudinal movements. For example, Aimsun uses the collision-free model developed in (Gipps, 1981), while TransModeler uses the GHR model in (Chandler et al., 1958). The psychophysical model developed in (Wiedemann, 1974; Wiedemann and Reiter, 1992) is used in Vissim, and a similar psychophysical model developed in (Fritzsche, 1994) is used in Paramics. Interested readers can refer to (Brackstone and McDonald, 1999; Olstam and Tapani, 2004; Panwai and Dia, 2005) for more details.

In our study, we choose Aimsun as the simulation software mainly because the current I-210 model is developed in Aimsun. Besides that, Aimsun provides very flexible API functions that enable us to change driver's behaviors if needed. The newly added features like the ACC/CACC and V2X modules provide strong support for the study of CAVs. In this subsection, we provide a review of the car-following model implemented in Aimsun so as to help readers better understand how it controls regular driver's longitudinal movements.

2.5.1 The Gipps' model

In the Gipps' model, bounded acceleration and deceleration are considered, and a vehicle's speed is restricted by two speed limits: one is the desired speed when it can travel freely, while the other is the maximum speed when it follows a lead vehicle under congested conditions. When vehicle ii can travel freely, its desired speed can be formulated as

$$vv_{ii}^{aadddd}(tt+\tau\tau) = vv_{ii}(tt) + 2.5 \times aa_{ii}^{ssaamm} \times \tau\tau \times \left(1 - \frac{vv_{ii}(tt)}{vv_{ii}^{dd}}\right) \times \sqrt{0.025 + \left(\frac{vv_{ii}(tt)}{vv_{ii}^{dd}}\right)} \tag{23}$$

where

$\tau\tau$: reaction time;

aa_{ii}^{ssaamm}: maximum acceleration of vehicle ii;

vv_{ii}^{dd}: desired speed of vehicle ii.

Meanwhile, when vehicle ii has to follow its leader ($ii-1$), its maximum speed can be calculated as

$$vv_{ii}^{ddrrdd}(tt+\tau\tau) = dd_{ii}^{ssaamm} \times \tau\tau + \sqrt{\left(dd_{ii}^{ssaamm} \times \tau\tau\right)^2 - dd_{ii}^{ssaamm} \times \left\{2\left[xx_{ii-1}(tt) - ll_{ii-1} - xx_{ii}(tt)\right] - vv_{ii}(tt) \times \tau\tau - \frac{vv_{ii-1}(tt)^2}{dd_{ii-1}}\right\}} \tag{24}$$

where

dd_{ii}^{ssaamm}: maximum deceleration of vehicle ii;

$\hat{dd}_{ii-1}$: estimate of desired maximum deceleration of vehicle $(ii-1)$;

[1] https://www.aimsun.com/

[2] https://www.ptvgroup.com/en/solutions/products/ptv-vissim/

[3] https://www.caliper.com/transmodeler/default.htm

[4] https://www.paramics.co.uk/en/

ll_{ii-1}: effective vehicle length of vehicle $(ii-1)$.

Then the speed for vehicle ii during the interval $[tt, tt+\tau\tau]$ is the minimum of the above two speeds, which can be formulated as

$$vv_{ii}(tt+\tau\tau) = \min\{vv_{ii}^{acceleration}(tt+\tau\tau), vv_{ii}^{deterministic}(tt+\tau\tau)\} \tag{25}$$

2.5.2 Further development in Aimsun

In Aimsun, there have been some further development based on the Gipps model to make vehicle's behaviors more realistic. In the following subsections, we provide some more details (Aimsun Next, 2020a).

2.5.2.1 Incorporation of influence of local parameters

The Gipps model has been developed by including model parameters which are not global but determined by the influence of local parameters, e.g., the type of driver (speed limit acceptance of the vehicle), the geometry of the section (speed limit of the section, speed limits on turns, etc.), the influence of vehicles on adjacent lanes, etc.

2.5.2.2 Asymmetrical update of vehicle's position

Once vehicle ii's speed $vv_{ii}(tt+\tau\tau)$ at $tt+\tau\tau$ is determined, its position $xx_{ii}(tt+\tau\tau)$ is updated with different methods under acceleration and deceleration phases. In the acceleration phase, the following rectangle method is used to calculate vehicle ii's position,

$$xx_{ii}(tt+\tau\tau) = xx_{ii}(tt) + vv_{ii}(tt+\tau\tau)\times\tau\tau \tag{26}$$

However, in the deceleration phase, the following trapezoid method is used to update vehicle ii's position,

$$xx_{ii}(tt+\tau\tau) = xx_{ii}(tt) + 0.5[vv_{ii}(tt) + vv_{ii}(tt+\tau\tau)]\times\tau\tau \tag{27}$$

2.5.2.3 Sensitivity factor in estimating a leader's deceleration

To estimate the leader's deceleration rate, $\hat{a}_{ii-1}$, a so-called "Sensitivity Factor" parameter α_{VVSS} is introduced per vehicle type. Then $\hat{a}_{ii-1}$ is computed as

$$\hat{a}_{ii-1} = a_{ii-1}\times\alpha_{VVSS} \tag{28}$$

where a_{ii-1} is the actual deceleration rate of the leader $(ii-1)$. Clearly, when $\alpha_{VVSS} > 1$, the follower overestimates the deceleration rate of the leader, and as a result it becomes more careful with a larger gap ahead of it. In contrast, when $\alpha_{VVSS} < 1$, the follower underestimates the deceleration rate of the leader, and as a result it becomes more aggressive with a smaller gap ahead of it.

2.5.2.4 Minimum headway constraint

Before updating the position $xx_{ii}(tt+\tau\tau)$, a restriction of minimum headway between leader and follower is introduced. This restriction can be formulated as:

If $xx_{ii-1}(tt+\tau\tau) - [xx_{ii}(tt) + vv_{ii}(tt+\tau\tau) \times \tau\tau] < vv_{ii}(tt+\tau\tau) \times h_{ii}^{ssiiii}$,

$$vv_{ii}(tt+\tau\tau) = \frac{xx_{ii-1}(tt+\tau\tau) - xx_{ii}(tt)}{h_{ii}^{ssiiii} + \tau\tau} \tag{29}$$

2.5.2.5 Modified model for congested highways

It is noted that in congested conditions the Gipps model fails to predict the speed that is consistent with field observations. Therefore, in Aimsun a modified model is used to adjust the dependency of speed as a function of density, which is achieved by introducing vehicle clearance into the calculation of speed. Before the modification, vehicle clearance can be calculated as

$$ss_{ii}(tt) = xx_{ii-1}(tt) - xx_{ii}(tt) - ll_{ii-1} = \frac{vv_{ii-1}(tt)^2}{2dd_{ii-1}} - \frac{vv_{ii}(tt)^2}{2dd_{ii}^{mmaaxx}} + [0.5vv_{ii}(tt) + vv_{ii}(tt+\tau\tau)]\tau\tau \tag{30}$$

where $ss_{ii}(tt)$ is the clearance between vehicle ii and $(ii-1)$.

After the modification, the clearance and the corresponding speed can be calculated as

$$\begin{aligned} ss_{ii}(tt) = {} & \frac{vv_{ii-1}(tt)^2}{2dd_{ii-1}} - \frac{vv_{ii}(tt)^2}{2dd_{ii}^{mmaaxx}} + (1-\beta\beta)[0.5vv_{ii}(tt) + vv_{ii}(tt+\tau\tau)]\tau\tau \\ & + \beta\beta[0.5vv_{ii}(tt) + vv_{ii}(tt+\tau\tau)]\left(\frac{\overline{vv_{ii}(tt)}}{vv_{ddrrss}}\tau\tau\right) \end{aligned} \tag{31}$$

$$vv_{ii}(tt+\tau\tau) = dd_{ii}^{ssaamm} \times \tau\tau^{*} + \sqrt{dd_{ii}^{ssaamm} \times \tau\tau^{*2} - dd_{ii}^{ssaamm} \times \{2ss_{ii}(tt) - vv_{ii}(tt) \times \tau\tau^{*} - \frac{vv_{ii-1}(tt)^2}{dd_{ii-1}}\}} \tag{32}$$

$$\tau\tau^{*} = \tau\tau[1 + \beta\beta(1 - \frac{vv_{ii}(tt)}{vv_{ddrrss}})] \tag{33}$$

where vv_{ddrrss} is the desired speed, and $\beta\beta$ is a parameter that adjust the calculation of clearance. In Aimsun, there is an option to use $+\beta\beta$ in acceleration and $-\beta\beta$ in deceleration. So, if $\beta\beta$ is positive, the clearance between the leader and the follower will be larger during acceleration than deceleration even for the same speed.

2.5.2.6 Two-lane car-following model

It is normal to see a platoon of vehicles driving slowly on multi-lane highways. As a result, vehicles on adjacent lanes will be impacted and reduce their speeds. Aimsun takes into account this impact and will determine a new maximum desired speed of a vehicle in the corresponding link/section. Below is the logit to address the maximum desired speed based on different link types, e.g., on-ramp and regular links.

- If the adjacent slower lane is an on-ramp,
  MaximumSpeed=MeanSpeedVehicleDown + MaximumSpeedDifferenceOnRamp
- Else,

MaximumSpeed=MeanSpeedVehicleDown + MaximumSpeedDifference

- Then,
  DesiredSpeed=min{$v_{ii,jj}^{ssaamm}$; MaximumSpeed× $\theta\theta_{ii}$}
  where
  MeanSpeedVehicleDown: mean speed of those slowly-moving vehicles;
  MaximumSpeedDifferenceOnRamp: maximum allowable speed difference on on-ramps;
  MaximumSpeedDifference: maximum allowable speed difference on other lanes/links;
  $v_{ii,jj}^{ssaamm}$: maximum speed of vehicle ii on link jj,
  $\theta\theta_{ii}$: tuning parameter.

2.6 Discussion

In this section, we reviewed a number of studies in four CAV applications that include vehicle-level control algorithms, freeway speed harmonization, traffic light optimal speed advisory, and network route guidance. In addition, we reviewed the current car-following model implemented in Aimsun so as to have a better understanding on how it controls longitudinal movements of regular automobiles. Based on the above review, we have selected the following models/applications/algorithms for our project.

- For vehicle-level control algorithms, many models have been proposed in the literature. The most influential ones, to list a few, are the CACC control algorithm in (Van Arem et al., 2006), the family of the Intelligent Driver Model (IDM) in (Treiber et al., 2000; Kesting et al., 2010; Schakel et al., 2010), the control framework in mixed traffic in (Talebpour and Hahmassani, 2016), and the PATH ACC/CACC model in (Milanés et al., 2013; Milanés and Shladover, 2014; Lu et al., 2017; Liu et al., 2018a; Liu et al., 2018b). As mentioned in (Milanés and Shladover, 2014), the IDM controller in (Treiber et al., 2000) is unstable in field tests. Therefore, we decided to choose the PATH ACC/CACC model as the CAV model for our study, which has been tested with field experiments and implemented in Aimsun (Version 8.4.3 or newer).
- For freeway speed harmonization, we aim to control the movements of CAVs with recommended speeds so as to smooth traffic, reduce delay or even eliminate the formation of freeway bottlenecks. Various algorithms have been proposed, for example, the rule-based algorithm in (Talebpour et al., 2013), the cooperative variable speed limit system (C-VSLS) in (Grumert et al., 2015), the variable speed limit and advisory (VSL-VSA) algorithm in (Lu et al., 2015; Hale et al., 2016), and the speed recommendation strategy in (Learn et al., 2017). In our study, we will try to implement the above algorithms and assess their performance under different traffic conditions and percentages of CAVs.
- For traffic light optimal speed advisory, we aim to provide CAVs, especially the leader if a platoon is formed, with real-time signal timing and phase information so as to help them make better decisions when crossing arterial intersections. In the literature, there exist several algorithms/approaches that have been tested with field experiments, for example, the green light optimal speed advisory (GLOSA) application in (Katsaros et al., 2011; Bodenheimer et al., 2014), the eco-approach and departure (EAD) application in (Hao et al., 2015; Hao et al., 2018), the GuidePath prototype system in (Xia et al., 2013; Wu et al., 2014; Altan et al., 2017), and the model predictive control (MPC) approach in (Smith et al., 2020). However, considering model complexity and potential for network-level deployment, we decided to implement the GLOSA application in our study for demonstration purposes.

- For route guidance, many models have been proposed to provide CAVs with optimal routes under traffic congestion. Examples can be found in (Davis, 2017; Houshmand et al., 2019; Chu et al., 2017; Chu et al, 2019; Djavadian and Farooq, 2018; Alfaseeh et al., 2018). Besides that, there also have been studies on how to incorporate CAVs into incident management, for example, dynamic routing behaviors for CAVs in (He, 2018), contraflow operations with CAVs in (Ekram and Rahman, 2018), and En-Route diversions with CAVs in (Li and Khattak, 2018).

  However, in our study, we are more interested in analyzing how CAVs help TMCs better control traffic when incidents occur. More specifically, we consider the scenario that CAVs will receive detour information from TMCs and help divert traffic to the recommended routes. Since the routes are predefined by TMCs, we only need to model CAV's willingness to take the new detour route. One good candidate model we found is the one in (Samimi Abianeh et al., 2020), in which a normal distribution function is proposed and the number of rerouted vehicles and their lane distribution are introduced as parameter inputs to adjust the probability.

In this project, we will develop Aimsun APIs to implement the applications selected above. We will evaluate the performance of these applications using the following scenarios: (i) small subnetworks vs. the I-210 corridor network, (ii) various traffic demand patterns, e.g., AM peak, PM peak, and Off-peak, and (iii) recurrent congestion vs. traffic incidents. Results from this project will provide valuable insights to stakeholders to help them make better decisions and policies for the deployment of CAVs.

This page left blank intentionally

3. Tutorial to set up an integrated microsimulation platform in Aimsun for CAVs

Many prevailing simulation software has implemented the feature to incorporate AVs/CAVs into their core simulation platforms, for example, Vissim (PTV Vissim, 2017; PTV Vissim, 2021), TransModeler (TransModeler, 2021), and Aimsun (Aimsun Next, 2020b; Aimsun Next, 2020c). With this feature, users are able to simulate and evaluate the impacts of different penetration rates of AVs/CAVs on various transportation networks. However, this feature only focuses on the vehicle-level control of AVs/CAVs, which is not sufficient to simulate mixed traffic with CVs/CAVs when V2X communications is involved. To the best of our knowledge, Aimsun (Aimsun Next, 2020d; Aimsun Next, 2020e) is the only commercial traffic simulation software that provides additional features to enable V2X communications. The V2X module implemented in Aimsun enables the communications among ITS stations, for example, V2I/I2V communications between Roadside Units (RSUs) and CAVs equipped with On-Board Units (OBUs), and V2V communications between CAVs equipped with OBUs. However, these two modules, ACC/CACC (Aimsun Next, 2020c) and V2X (Aimsun Next, 2020d; Aimsun Next, 2020e), are developed separately in Aimsun, and thus simulation results may not be as expected if they are used at the same time to simulate the mixed traffic environment.

In this section, we aim to bridge the gap between the ACC/CACC and the V2X modules in Aimsun and provide a practical solution to build a microsimulation environment for mixed traffic with these two modules. In particular, with functions provided by these two modules, we aim to build an integrated microsimulation platform that can mimic the following features in mixed traffic with CAVs:

- At the vehicle control level, a CAV will be controlled by the ACC/CACC module while a human-driven vehicle will be controlled by the default mode in Aimsun. More specifically, a CAV will follow the ACC control modes if there is no leader or the leader is a human-driven vehicle. However, it will form platoons with other consecutive CAVs and follow the CACC control modes.
- At the communications level, a CAV will be able to send various message types to nearby CAVs via V2V communications and to RSUs via V2I communications. Similarly, an RSU can send various message types to nearby CAVs via I2V communications. It also can connect to local intersection controllers and Traffic Management Centers (TMCs) to exchange traffic data and transportation management actions.

In the rest of this section, we will provide a detailed tutorial on how to build such an integrated microsimulation platform. In Section 3.1, we provide detailed installation instructions for the required software components. In Section 3.2, we describe the properties of available control modes in the ACC/CACC module and explain the decision chart of these modes. In Section 3.3, we provide detailed descriptions of key components in the V2X module and show how to create and set them up in Aimsun. In Section 3.4, we provide a practical solution to bridge the gap between the ACC/CACC and the V2X modules to build the integrated microsimulation platform for mixed traffic. In Section 3.5, we summarize the properties of this integrated platform with some potential applications in this project.

3.1 Installation Guidance

3.1.1 Required installation files

In order to build an integrated microsimulation platform in Aimsun for mixed traffic, especially for CAVs, we need to use the following modules:

(i) The ACC/CACC module for longitudinal control of individual AVs/CAVs;
(ii) The V2X communications module to exchange information among CVs/CAVs, RSUs and TMCs.

Since the ACC/CACC module has been embedded into the core Aimsun simulation platform, what we need to install will be the following:

(i) Aimsun Next 20 (Python 2)
https://aimsun-releases.s3.amazonaws.com/Next_20/Pre-20_0_4/Python_2/Aimsun_Next_20_0_4_Windows_Python2_2021_08_12_14774095625.html (Last Visited: 12/26/2021)
(ii) V2X SDK
https://aimsun-releases.s3.amazonaws.com/Next_20/Pre-20_0_4/Python_2/extras/Aimsun_Next_20_0_4_V2X_SDK_Windows_Python2_2021_08_12_14774095625.html (Last Visited: 12/26/2021)
(iii) V2X Framework
https://aimsun-releases.s3.amazonaws.com/Next_20/Pre-20_0_4/Python_2/extras/Aimsun_Next_20_0_4_V2XFramework_Windows_Python2_2021_08_12_14774095625.html (Last Visited: 12/26/2021)

The Aimsun V2X module provides an application example called "StopEngine", based on which users can develop more complicated V2X applications. In order to run this application, we need to install the following software:

(i) Visual Studio 2019. The community edition can be downloaded via the following link: https://visualstudio.microsoft.com/downloads/ (Last Visited: 04/06/2021)
(ii) Qt 5.14.2 (qt-opensource-windows-x86-5.14.2). The exe file can be downloaded via the following link: https://download.qt.io/archive/qt/5.14/5.14.2/ (Last Visited: 04/06/2021)

Note that, the above installation files as well as the following installation steps and settings are for the Windows 10 System.

3.1.2 Installation and setting up

3.1.2.1 Installation steps

The detailed installation steps are described below:

(i) Install Aimsun Next 20, V2X SDK and V2X Framework.
The V2X installation files should be installed under the same folder where the Aimsun core program is located/installed. After installation, the application example "StopEngine" is included inside the Aimsun program folder. However, to avoid potential writing restrictions while doing further development in "StopEngine", it is recommended to install Aimsun as well as the V2X components (SDK & Framework) to another folder, not to the default "Program

Files" folder under the "C" Drive. For example, we can create another folder named "Program Aimsun" under the "C" Drive as the file location.

After the installation is finished, the V2X module is located at "C:\Program Aimsun\Aimsun\Aimsun Next 20\include\aimsun_extensions\v2x". Below is a snapshot of the files inside the "v2x" folder.

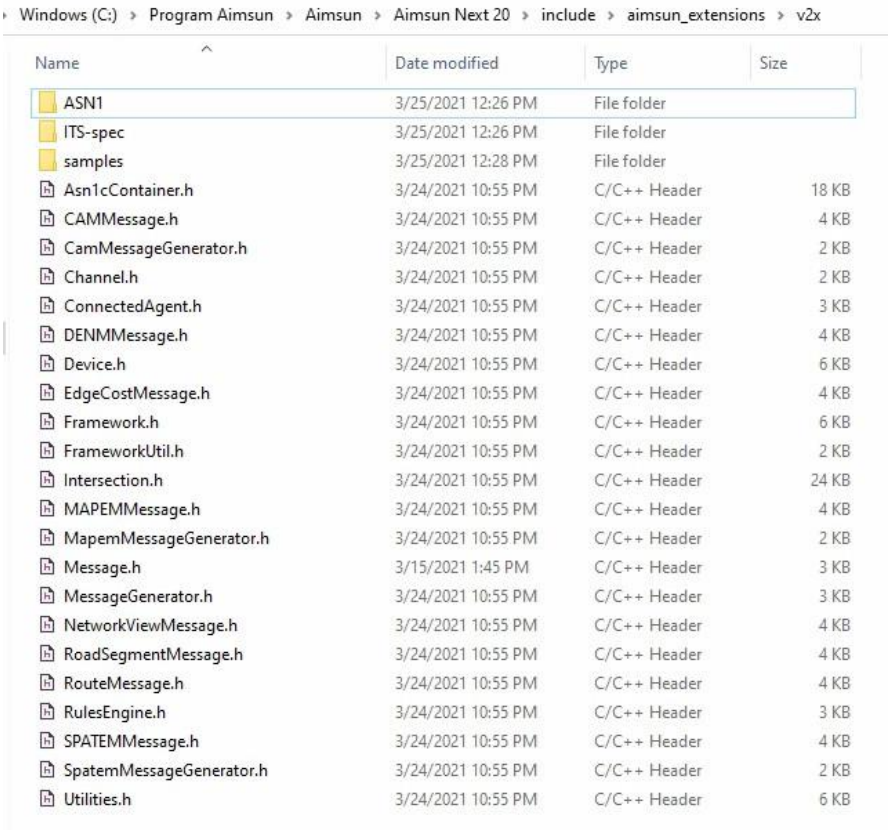

(ii) Install Qt 5.14.2.

(iii) Install Visual Studio 2019. Also install the right Windows SDK Version of your current Windows system, e.g., Windows 10.

(iv) Install "Qt Visual Studio Tools" as an extension in Visual Studio.
As shown below, in the Visual Studio Community Edition, click on "Extensions"→ "Manage Extensions" → "Online"→ Search for "Qt" → Install "Qt Visual Studio Tools".

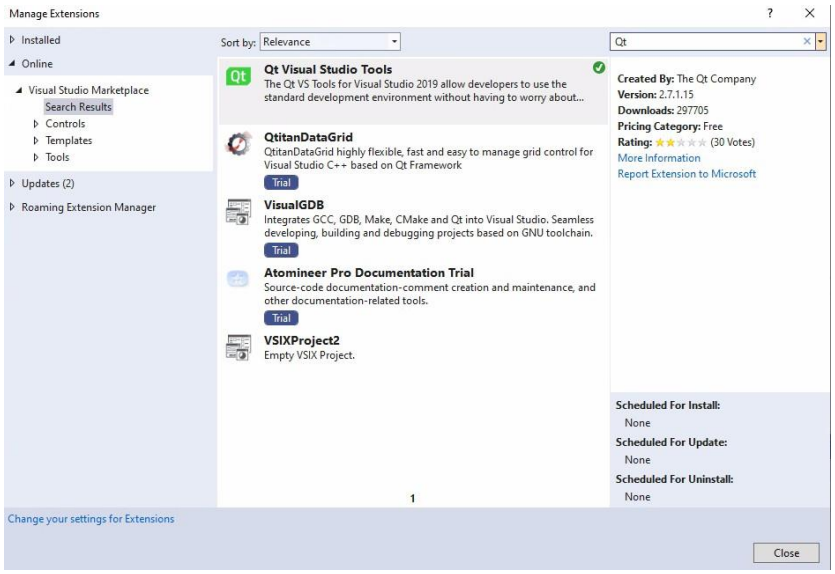

3.1.2.2 Setting up

Before setting up the V2X module, make sure all software components in the previous subsection have been installed correctly. Then the setup process is provided below:

(i) Access the "StopEngine" via the following path:
"..\Aimsun\Aimsun Next 20\include\aimsun_extensions\v2x\samples\StopEngine".

(ii) Start Visual Studio and configure the Qt Version in Qt VS Tools.
Click on "Extensions"→ "Qt VS Tools"→ "Qt Versions". In the Qt Version window, select the appropriate Qt installation, e.g., "msvc2017_64" in the Qt 5.14.2 folder, and add it as the default version.

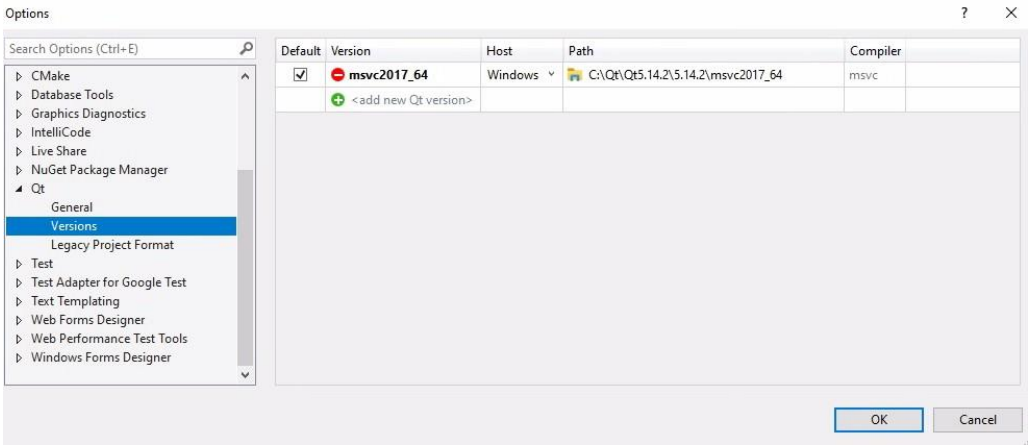

(iii) Open the Qt project file by clicking on "Extensions"→ "Qt VS Tools"→ "Open Qt Project File". Select the "StopEngineSample.pro" under the following path and compile it:
"..\Aimsun\Aimsun Next 20\include\aimsun_extensions\v2x\samples\StopEngine".

(iv) In Visual Studio, click on "Project"→ "Retarget Solution" and select the right Window SDK version of your current operation system.

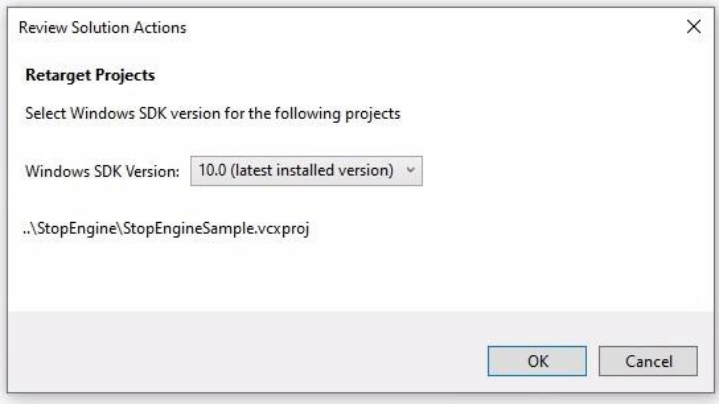

(v) In Visual Studio, click on "Project"→ "StopEngineSampleProperties". In the "StopEngineSample Property Pages" window, set the "Configuration" to be "Release" and the "Platform" according to your computer settings, e.g., "x64".

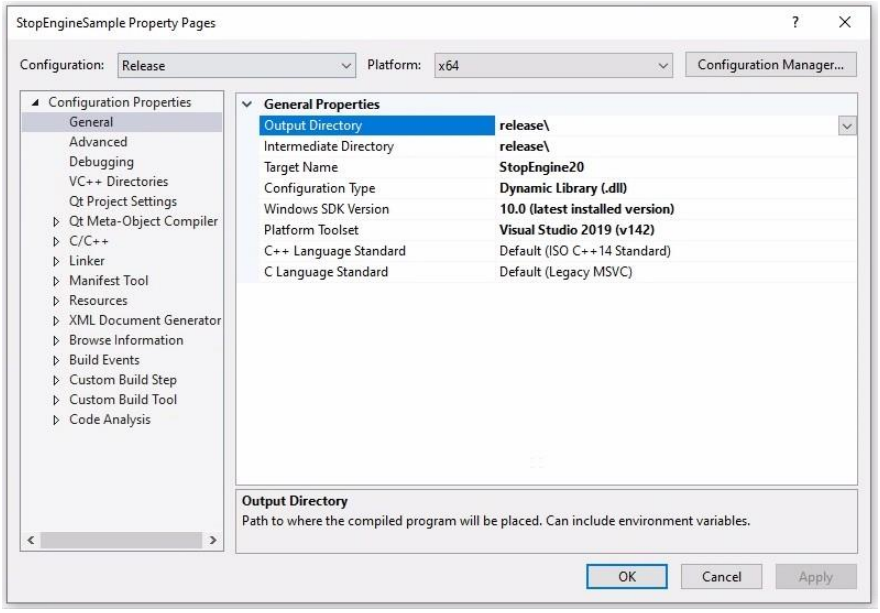

(vi) Create a new folder "dynamicAPIS" under "..\Aimsun\Aimsun Next 20\plugins".

(vii) Build the solution of "StopEngineSample".

(viii) Copy the generated "StopEngine20.dll" in the folder "..\Aimsun\Aimsun Next 20\include\aimsun_extensions\v2x\samples\StopEngine\release" alongside the "01_StopEngine.xml" file in the folder ".. \Aimsun\Aimsun Next 20\include\aimsun_extensions\v2x\samples\StopEngine" and place them inside "dynamicAPIS".

(ix) Open an Aimsun model and verify whether the dll is loaded properly. If yes, the V2X setup process should have concluded correctly.

3.2 The ACC/CACC module in Aimsun

The ACC/CACC module developed in Aimsun can be used to simulate the behaviors of AVs and CAVs. For a CAV equipped with ACC/CACC, there are five different vehicle control modes available, the selection of which depends on the measured gap and clearance to its leader. These five control modes are described below. Refer to (Aimsun Next, 2020c) for more details.

3.2.1 Five vehicle control modes

As mentioned, the ACC/CACC module consists of the following five modes: Cruise Control (CC) Speed Regulation mode, ACC Gap Regulation mode, CACC Gap Regulation mode, ACC/CACC Emergency Take Over mode, and Default Manual Driving mode.

3.2.1.1 Cruise Control (CC) Speed Regulation mode

When the clearance (i.e., distance) to the leader is longer than a user-defined threshold, the subject vehicle ii will use the CC speed regulation mode. Its acceleration is determined using the following equation:

$$aa_{ii} = kk_3(vv_{mmmm} - vv_{ii}) \tag{34}$$

where
aa_{ii}: recommended acceleration for vehicle ii;
vv_{mmmm}: free flow speed;
vv_{ii} : current speed of vehicle ii;
kk_3 : speed gain on the difference between the free flow speed and the subject vehicle's current speed.

3.2.1.2 ACC Gap Regulation mode

For an ACC-equipped vehicle, if the clearance to its leader is smaller than a user-defined threshold, it will use the ACC Gap Regulation mode. Similarly, for a CACC-equipped vehicle, if its leader is a human-driven vehicle, it will also use the ACC Gap Regulation mode. In such a case, the subject vehicle will use the following equation to update its acceleration:

$$aa_{ii} = kk_1(dd - TT_{ii}vv_{ii} - ll_{ii-1}) + kk_2(vv_{ii-1} - vv_{ii}) \tag{35}$$

where
kk_1 : distance gain on the position difference between the leading vehicle $ii - 1$ and the subject vehicle ii;
kk_2 : speed gain on the speed difference between the leading vehicle $ii - 1$ and the subject vehicle ii;
dd: distance between the subject vehicle's front bumper and the leading vehicle's front bumper;
ll_{ii-1} : length of the leading vehicle $ii - 1$;
vv_{ii-1} : current speed of the leading vehicle $ii - 1$;
TT_{ii}: desired time gap of the subject vehicle ii.

3.2.1.3 CACC Gap Regulation mode

For CACC-equipped vehicles, they can form platoons, which are groups of consecutive vehicles with smaller than normal time gaps between them. When a CACC-equipped vehicle is in a platoon, it will use the following equation to update its acceleration:

$$
\begin{aligned}
aa_{ii}(tt) &= \frac{vv_{ii}(tt) - vv_{ii}(tt - \Delta tt)}{\Delta tt} \\
vv_{ii}(tt) &= vv_{ii}(tt - \Delta tt) + kk_{pp}\, mm_{kk}(tt) + kk_{dd}\, \dot{m}_{kk}(tt) \\
mm_{kk}(tt) &= dd(tt - \Delta tt) - TT_{CCCCCCCC}\, vv_{ii}(tt - \Delta tt) - ll_{ii-1} \\
\dot{m}_{kk}(tt) &= vv_{ii-1}(tt - \Delta tt) - vv_{ii}(tt - \Delta tt) - TT_{CCCCCCCC}\, aa_{ii}(tt - \Delta tt)
\end{aligned}
\tag{36}
$$

where

Δtt: time step for each update;

$mm_{kk}(tt)$: time gap error;

$\dot{m}_{kk}(tt)$: speed error;

kk_{pp}: distance gain on the time gap error between the subject vehicle ii and the leading vehicle $ii - 1$;

kk_{dd}: speed gain on the speed gap error between the subject vehicle ii and the leading vehicle $ii - 1$;

$TT_{CCCCCCCC}$: constant time gap adopted by the CACC controller.

For a subject vehicle in a CACC platoon, it can be operated in two variants of Gap Regulation mode:

(i) When the leading vehicle's CACC platoon reaches its maximum length, the subject vehicle is operated in the CACC Leader Gap Regulation mode and a user-defined Time Gap Leader $TT_{CCCCCCC}^{Wmaddmr}$ will be used.

(ii) Otherwise, the subject vehicle is operated in the CACC Follower Gap Regulation mode and a user-defined Time Gap Follower $TT_{CCCCCCC}^{SSddwwddssrrrr}$ will be used.

3.2.1.4 ACC/CACC Emergency Take Over mode

In Aimsun, the Crash Avoidance Metrics Partnership (CAMP) forward collision warning algorithm (Kiefer et al., 2003; Liu et al., 2018) has been implemented to switch back to the Default Manual Driving mode if the algorithm detects a potential collision that cannot be handled by the ACC/CACC controller.

The CAMP algorithm will first determine the required deceleration $aa_{ii,rrrrrr}$ for the subject vehicle ii, which is designed to be a comfortable threshold to avoid a collision with the leading vehicle. Given the inputs of relative speed difference and leading vehicle's deceleration, the required deceleration $aa_{ii,rrrrrr}$ is computed using the following empirical equation:

$$
\begin{aligned}
aa_{ii,rrrrrr} &= -0.165 + 0.685 * aa_{ii-1} + 0.080\xi\xi - 0.00889 * (vv_{ii} - vv_{ii-1}) \\
\xi\xi &= \begin{cases} 1 & vv_{ii-1} > 0 \\ 0 & otherwise \end{cases}
\end{aligned}
\tag{37}
$$

where aa_{ii-1} is the deceleration of the leading vehicle $ii - 1$.

When $aa_{ii,rrrrrr} \geq 0$, it means the current gap is sufficient and thus the subject vehicle does not need to brake. When $aa_{ii,rrrrrr} < 0$, the CAMP algorithm will further calculate the required clearance (i.e., distance) $dd_{ii,rrrrrr}$ for the subject vehicle using the following equation:

$$dd_{ii,mmr} = \begin{cases} \max\{0, \frac{vv_i^2}{-2aa_{ii,mmr}} - \frac{vv_{ii-1}^2}{-2aa_{ii-1}}\} & \text{lmaddinRvmhuidlmsttqpssmacdiimr} \\ \max\{0, \frac{(vv_i - vv_{ii-1})^2}{-2(aa_{ii,mmr} - aa_{ii-1})}\} & \text{atthmneeiissm} \end{cases} \quad (38)$$

If the current clearance is smaller than $dd_{ii,rrrrrr}$, it indicates a collision will happen in the next few seconds and thus the CAMP algorithm will activate the Emergency Take Over mode and the subject vehicle will switch back to the default manual driving mode.

3.2.1.5 Default manual driving mode

When the ACC/CACC module is disabled due to safety constraints, the subject vehicle will follow the default control mode in Aimsun, which is the Gipps' model (Gipps, 1981). Refer to Section 2.5 for more detailed implementations of the Gipps' model in Aimsun.

3.2.2 Decision chart

During simulation, each simulated vehicle contains a dynamic column called "Cruise Control Status" to show which driving mode was used in the last time step. In Aimsun, an ACC/CACC-equipped vehicle can have five different modes:

- CC Speed Regulation
- ACC Gap Regulation
- CACC Platoon Leader Gap Regulation
- CACC Platoon Follower Gap Regulation
- Disabled (Default Manual Driving)

The decision chart of these five different modes is provided in Figure 3.

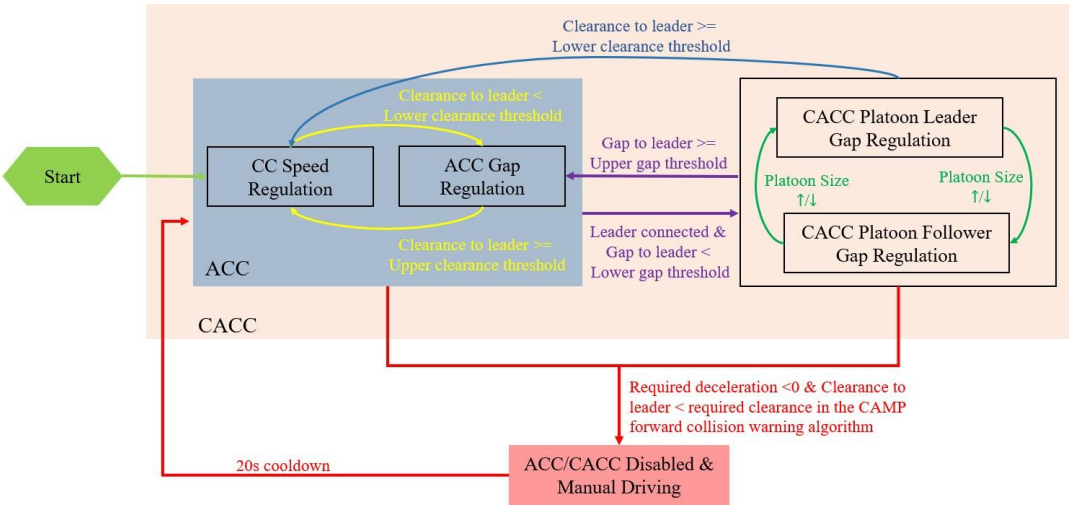

Figure 3: Decision chart of driving modes for ACC/CACC-equipped vehicles in Aimsun.

3.2.2.1 From *Start* to *CC Speed Regulation*

This transition occurs when an equipped vehicle is assigned into the transportation network and the ACC/CACC module is activated for the first time.

3.2.2.2 Switch between *CC Speed Regulation* and *ACC Gap Regulation*

An ACC/CACC-equipped vehicle will stay in the CC Speed Regulation mode in the following cases:

(i) There is no leader ahead;
(ii) It is not in a CACC platoon and the clearance to the leader is greater than a user-defined upper clearance threshold;
(iii) It was previously in a CACC platoon but the clearance to the leader (ACC/CACC-equipped) becomes greater than a user-defined lower clearance threshold.

When the subject vehicle detects its clearance to the leader is smaller than the user-defined lower clearance threshold, it will switch to the ACC Gap Regulation mode.

Similarly, when an ACC/CACC-equipped vehicle is in the ACC Gap Regulation mode and detects its clearance to the leader is greater than the user-defined upper clearance threshold, it will switch to the CC Speed Regulation mode.

When the clearance to the leader is between the upper and lower clearance thresholds, the subject vehicle will stay in either the CC Speed Regulation mode or the ACC Gap Regulation mode except the following cases:

(i) The leader is ACC/CACC-equipped and is connected, and the gap to the leader is smaller than the user-defined lower gap threshold. In this case, it will join the leader to form a CACC platoon.
(ii) The CAMP algorithm detects a potential collision. As a result, the ACC/CACC mode is disabled and the Default Manual Driving mode is used for the subject vehicle.

3.2.2.3 From CC *Speed Regulation/ACC Gap Regulation* to *CACC Platoon Gap Regulation*

Suppose the subject vehicle is currently in the ACC modes, either CC Speed Regulation or ACC Gap Regulation. It will join the leader to form a CACC platoon when:

(i) The leader is ACC/CACC-equipped;
(ii) Both the leader and the subject vehicle are connected;
(iii) The gap to the leader is smaller than the user-defined lower gap threshold.

Note that, jumping from the CC Speed Regulation mode straight to the CACC Platoon Gap Regulation modes is improbable if the Aimsun model has reasonable settings of upper/lower clearance and gap thresholds.

3.2.2.4 From *CACC Platoon Gap Regulation* to *ACC Gap Regulation/CC Speed Regulation*

Suppose the subject vehicle is currently in a CACC platoon, either as a leader or a follower.

- It will switch back to the ACC Gap Regulation mode when the gap to its leader is greater than the user-defined upper gap threshold.
- It will switch back to the CC Speed Regulation mode when its clearance to the leader becomes greater than the user-defined lower clearance threshold. In this case, the lower clearance threshold instead of the upper clearance threshold is used because it can help maintain platoon coherence by allowing the subject vehicle to switch back to the CC Speed Regulation mode as soon as possible. Plenty of simulation tests have been conducted by the Aimsun development team to conclude that the implemented option of lower clearance threshold is more stable and provides better results.

3.2.2.5 Switch between *CACC Platoon Leader and Follower Gap Regulation modes*

If the CACC platoon ahead of the subject vehicle reaches its maximum length, the subject vehicle will form a new platoon and serve as the leader. In this case, it will stay in the CACC Platoon Leader Gap Regulation mode. When a vehicle ahead of the subject vehicle leaves the platoon, the subject vehicle will switch to the CACC Platoon Follower Gap Regulation mode.

If the CACC platoon ahead of the subject vehicle doesn't reach its maximum length, the subject vehicle will stay in the CACC Platoon Follower Gap Regulation mode. When a vehicle ahead of the subject vehicle joins the platoon and the platoon reaches its maximum length, the subject vehicle will become the leader of a new platoon and switch to the CACC Platoon Leader Gap Regulation mode.

At every simulation step, the simulation engine will check conditional changes in the following order:

- First, check the "clearance to leader" condition. If fulfilled, the subject vehicle will switch to the CC Speed Regulation mode.
- Else, check the "gap to leader" condition. If fulfilled, the subject vehicle will switch to the ACC Gap Regulation mode.
- Else (neither of the above is true), check the platoon conditions and stay in either the CACC Platoon Leader Gap Regulation mode or the CACC Platoon Follower Gap Regulation mode.

3.2.2.6 From *ACC/CACC* to *Disabled (Manual Driving)*

In extreme cases, the implemented CAMP forward collision warning algorithm will detect a potential collision when (i) the required deceleration is negative, and (ii) the clearance to the leader is smaller than the required clearance. In this case, the Emergency Take Over mode will be activated and the subject vehicle will switch to the Default Manual Driving mode.

3.2.2.7 From *Disabled (Manual Driving)* to CC *Speed Regulation/ACC Gap Regulation*

When the ACC/CACC modes are disabled for the subject vehicle, there is a 20s cooldown period for it to be able to go into ACC/CACC modes again. This cooldown period is applied to consider the case that a driver will take over the vehicle to handle emergency situations and then judge whether it is safe to get back to the automatic driving modes.

3.2.3 Simulation settings

In order to enable the ACC/CACC module in simulations, we need to properly configure the key model parameters. More details about the settings are provided below.

3.2.3.1 Simulation time step and reaction time settings

In Aimsun, the ACC/CACC module has been implemented to work on autonomous vehicle simulation steps, which is 0.1s. Therefore, in order to see the impact of AVs/CAVs, we need to change the simulation time step in simulation experiments to be 0.1s.

For a simulation experiment shown below, the parameter "Simulation Step" under the "Reaction Time" tab should be set to 0.1s. Meanwhile, the parameter "Reaction Time Settings" should be set to "Variable (Different for Each Vehicle Type)". Considering a CAV can receive more traffic information from other connected CAVs and RSUs, we can set the parameters "Reaction Time", "Reaction Time at Stop", and "Reaction Time at Traffic Light" to be smaller than human-driven vehicles.

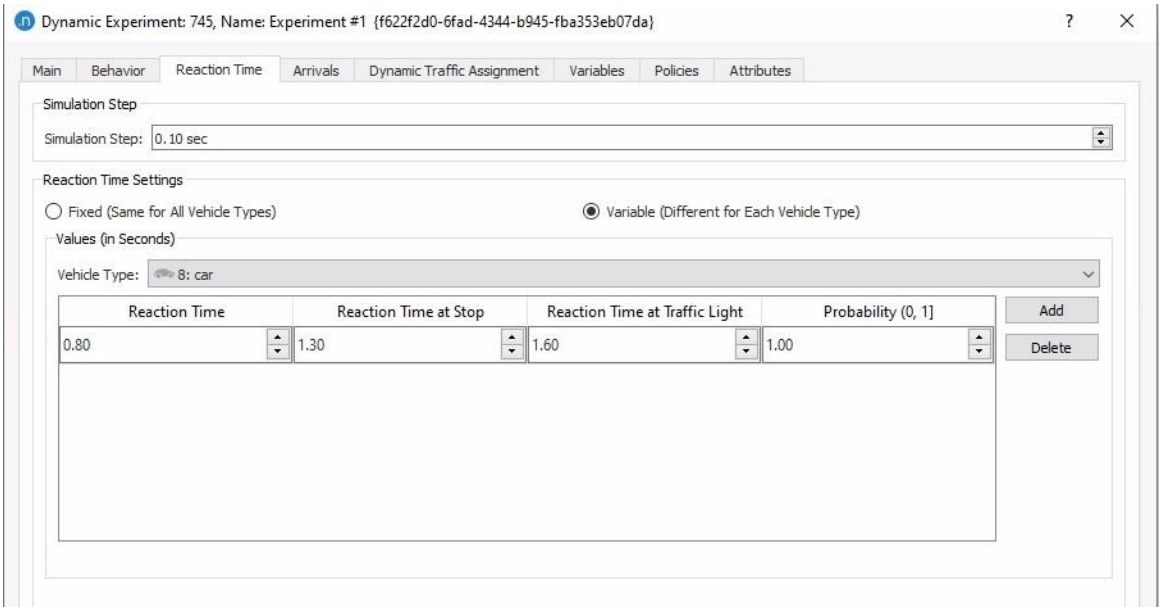

3.2.3.2 ACC/CACC vehicle settings

In Aimsun, we can set the parameters in the ACC/CACC module for any vehicle type and configure the percentages of vehicles equipped with ACC or CACC. In the Aimsun Graphical User Interface (GUI), click on "DEMAND DATA"→ "Vehicles" and double click on a vehicle type of interest, e.g., "car CAV" shown below.

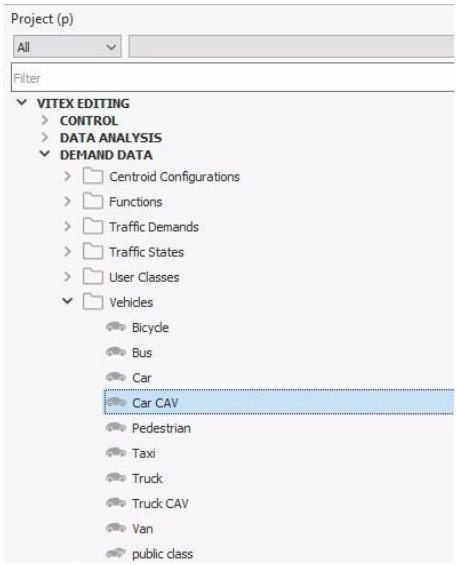

In the pop-up window, click on "Microscopic Model" → "Car-Following Model". Then we will see the place to edit the ACC/CACC model parameters, which is shown below.

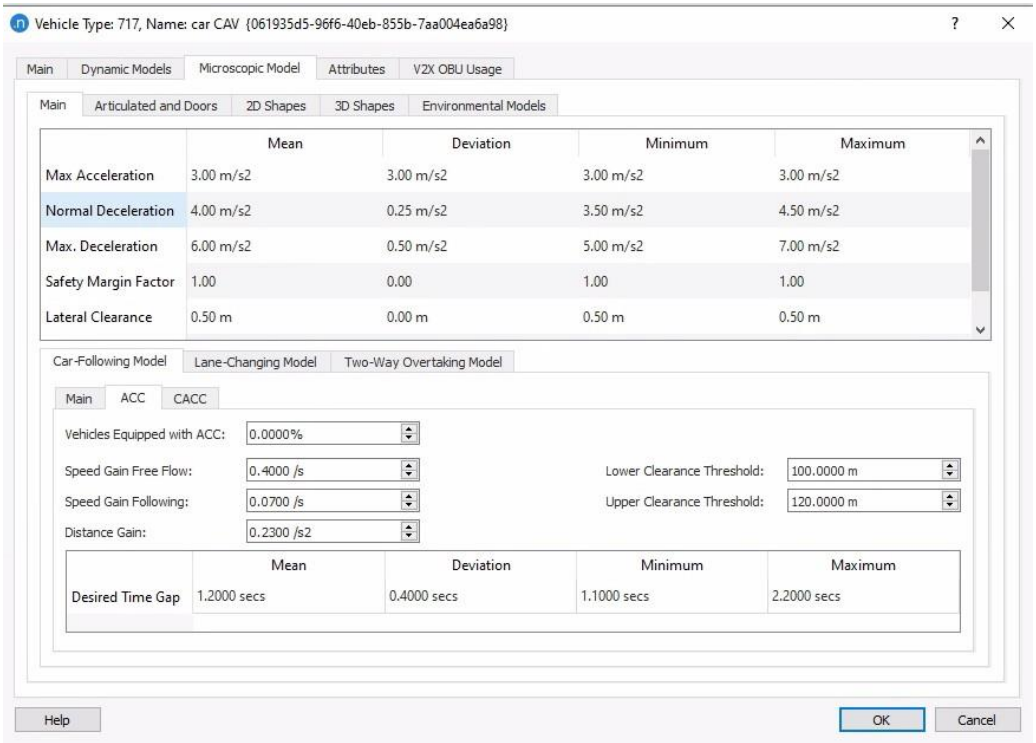

In the ACC configuration block, the available parameters are described below:

(i) "Vehicle Equipped with ACC": percentage of vehicles that are equipped with ACC.
(ii) "Speed Gain Free Flow": parameter kk_3 in Equation (34) under the CC Speed Regulation mode.
(iii) "Speed Gain Following": parameter kk_2 in Equation (35) under the ACC Gap Regulation mode.
(iv) "Distance Gain": parameter kk_1 in Equation (35) under the ACC Gap Regulation mode.

(v) "Desired Time Gap": parameter TT_{ii} in Equation (35) under the ACC Gap Regulation mode.

(vi) "Lower Clearance Threshold": parameter used to switch from the CACC Platoon Leader/Follower Gap Regulation modes to the CC Speed Regulation mode, or from the CC Speed Regulation mode to the ACC Gap Regulation mode in the Decision Chart.

(vii) "Upper Clearance Threshold": parameter used to switch from the ACC Gap Regulation mode to the CC Speed Regulation mode in the Decision Chart.

In the CACC configuration block shown below, the available parameters are described below:

(i) "Vehicles Equipped with CACC": percentage of vehicles that are equipped with CACC. Note that the sum of this percentage and the percentage of ACC-equipped vehicles cannot be greater than 100%.

(ii) "Speed Gain": parameter kk_{dd} in Equation (36) under the CACC Platoon Gap Regulation mode.

(iii) "Distance Gain": parameter kk_{pp} in Equation (36) under the CACC Platoon Gap Regulation mode.

(iv) "Time Gap Leader": constant time gap $TT_{cccccccc}$ in Equation (36) used in the CACC Platoon Leader Gap Regulation mode.

(v) "Time Gap Follower": constant time gap $TT_{cccccccc}$ in Equation (36) used in the CACC Platoon Follower Gap Regulation mode.

(vi) "Lower Gap Threshold": parameter used to switch from the CC Speed Regulation/ACC Gap Regulation modes to the CACC Platoon Leader/Follower Gap Regulation modes in the Decision Chart.

(vii) "Upper Gap Threshold": parameter used to switch from the CACC Platoon Leader/Follower Gap Regulation modes to the ACC Gap Regulation mode in the Decision Chart.

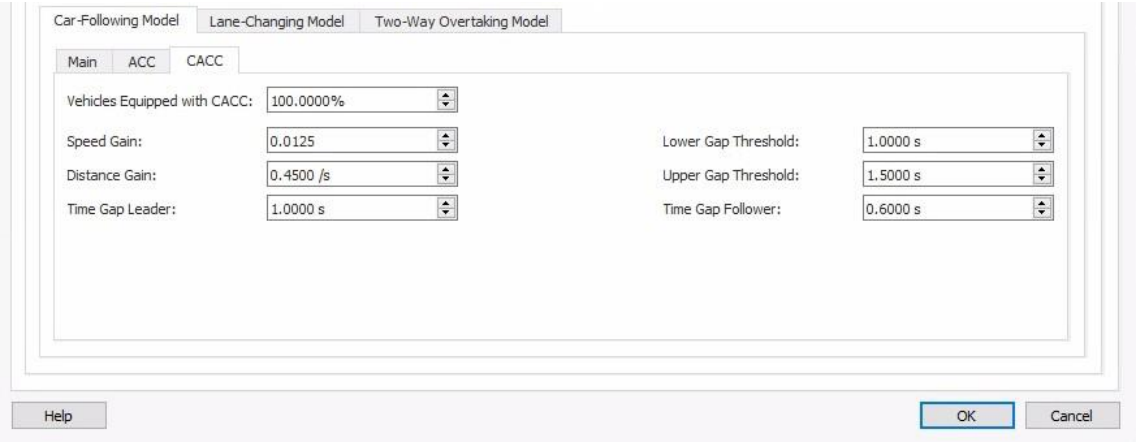

Note that, the above parameters can be tuned by users so as to regulate: (i) the car-following behavior of ACC/CACC equipped vehicles; (ii) the switches among different control modes in the Decision Chart.

3.2.3.3 Road type settings

When a vehicle is equipped with ACC/CACC, it will only be functional on the roads that allow it. Meanwhile, the CACC-equipped vehicles can form platoons with smaller time gaps between consecutive members. For a given road type, we can configure whether it allows ACC/CACC-equipped vehicles as well as the maximum platoon size for CACC-equipped vehicles.

In the Aimsun GUI, click on “INFRASTRUCTURE”→ “Road Types” and double click on a road type of interest, e.g., “Freeway” shown below.

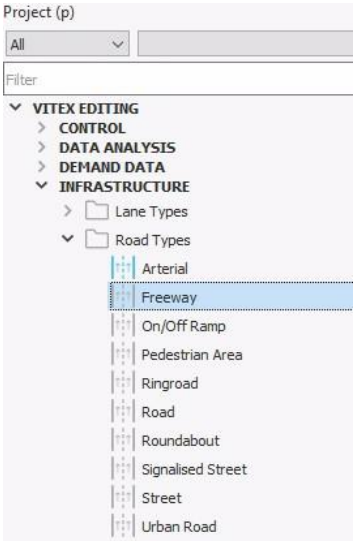

In the pop-up window, click on “Dynamic Models” → “Section Parameters”. The detailed settings for the road type “Freeway” are shown below. The attribute “ACC/CACC Allowed” should be checked (enabled), and the attribute “maximum CACC Platoon Size” can be set by the users with a reasonable number, e.g., 10 (vehicles).

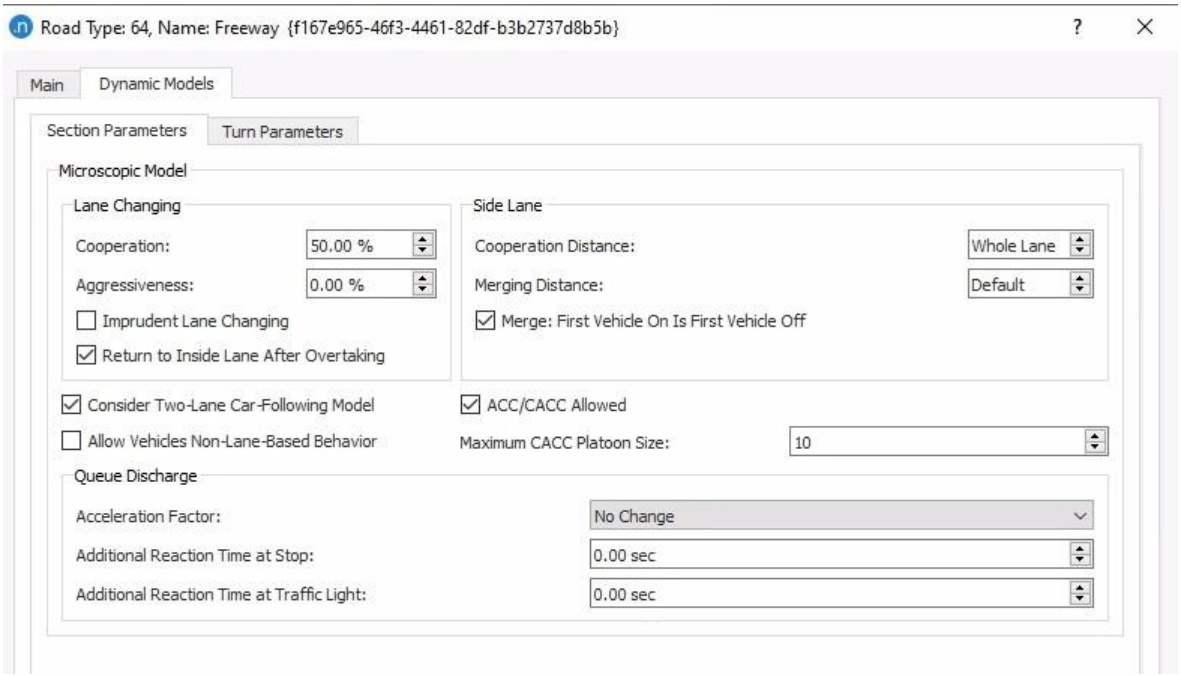

3.3 The V2X module in Aimsun

In this subsection, we will first illustrate key components and data flows in the V2X module implemented in Aimsun. Then we will provide detailed descriptions on the properties, creation, and settings of each component. For more information, refer to (Aimsun Next, 2020d; Aimsun Next, 2020e).

3.3.1 Architecture of the V2X module

3.3.1.1 Key components

As shown in Figure 4, the architecture of the V2X module in Aimsun consists of the following five major components:

(i) Message.
In the V2X module, messages can be passed between vehicles equipped with OBUs and RSUs. Some common types of messages, e.g., Cooperative Awareness Message (CAM), Decentralized Environmental Notification Message (DENM), Signal Phase and Timing Extended Message (SPATEM), and MAP Extended Message (MAPEM), have been implemented in the V2X SDK. Furthermore, new message types can be added to the V2X SDK using the V2X API, and they can be passed between equipped vehicles and RSUs in the same way as the existing message types.

(ii) Channel.
The communications channel implemented in the V2X module is a simulation representation of the radio hardware and protocols that provide communications among equipped vehicles and RSUs, e.g., a 5G cell-based communications network and a Wifi-based IEEE 802.11p protocol. The default channel object implemented in the V2X SDK is simple, which is a range-based message passing object with a stochastic probability of successful transmission. Therefore, more detailed communications settings and/or scenarios will require additional coding to the base channel, which is also doable using the V2X SDK.

(iii) On Board Unit (OBU).
The OBU implemented in the V2X module is the receiver and transmitter in an equipped vehicle. It can be configured to use one or more channels and to receive/transmit one or more messages to each channel.

(iv) Roadside Unit (RSU).
The RSU is the component that enables communications between equipped vehicles and road infrastructure, i.e., V2I/I2V communications. For a given RSU in the V2X module, users can configure the road network nodes it connects to, define the channels it can use and the message types it can receive and transmit. Meanwhile, users can connect the RSU to a TMC to exchange messages/information.

(v) Traffic Management Center (TMC).
The TMC implemented in the V2X module is the integrator of data from multiple RSUs and the manager of coordinated signal control and traffic management actions. The communications between the TMC and RSUs normally is different from that between equipped vehicles and RSUs, which may be based on wired links or dedicated radio channels.

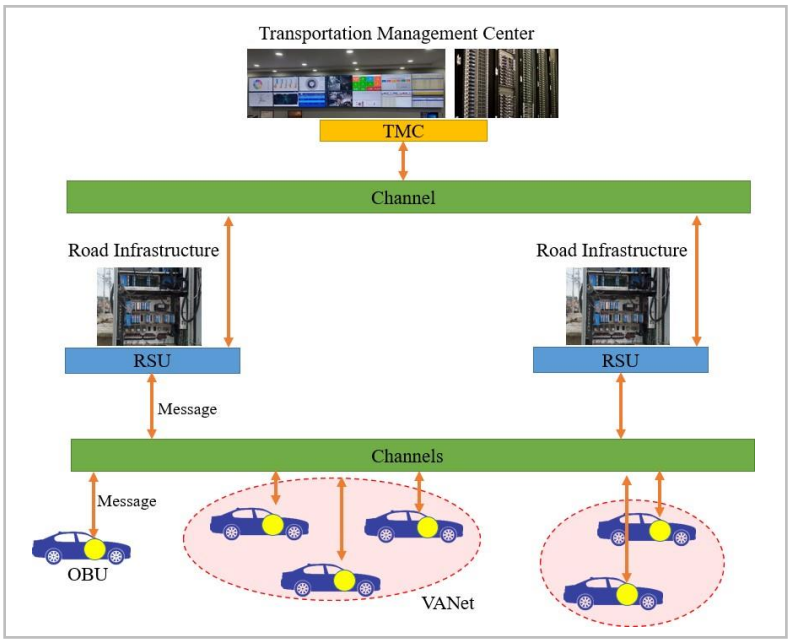

Figure 4: Architecture of the V2X module in Aimsun.

3.3.1.2 Data flows

The major data flows illustrated in Figure 4 and implemented in the V2X module can be described as follows:

(i) Equipped vehicles and RSUs can connect to other equipped vehicles and/or RSUs within their communications range. They can exchange information among themselves using selected message types (e.g., CAM) and communications channels.

(ii) The RSUs will gather all received messages and perform some local processing. They can send aggregated traffic information to the connected vehicles via selected message types, e.g., DENM. Meanwhile, they can send some vendor-specific aggregated messages to the TMC for further evaluations. Each RSU has its own "RSU Rules Engine", which manages the tasks of receiving/transmitting messages and performing local analysis.

(iii) The TMC will evaluate the information received from multiple RSUs and generate some actions. These actions will be relayed back to the equipped vehicles in the traffic network via the RSUs as well as to the traffic controllers and other ITS stations.

(iv) Each equipped vehicle has its own "Vehicle Rules Engine". The rule engine will manage the messages from other equipped vehicles and RSUs within vehicle's communications range, add the retrieved information to vehicle's existing knowledge of nearby traffic conditions, and influence vehicle's behavior.

3.3.2 Message Types

In the V2X module, some predefined V2X message types have been implemented to exchange information between equipped vehicles and RSUs. More details of these messages are provided below:

(i) Cooperative Awareness Message (CAM).

This message is defined by the European Telecommunications Standards Institute (ETSI) in standard TS 302 637-2. It provides information about the presence, activity, and position of ITS stations like RSUs and equipped vehicles. The frequency to generate this message is between 1HZ and 10HZ, depending on the activity of the ITS stations.

(ii) Decentralized Environmental Notification Message (DENM).

This message is defined by the European Telecommunications Standards Institute (ETSI) in standard 302 637-3. It aims to provide information about events or conditions that have potential impacts on road safety or traffic conditions. This message is often sent after an ITS station, e.g., RSU, has detected reportable conditions/events, e.g., traffic incident, from the received CAMs.

(iii) Signal Phase and Timing Extended Message (SPATEM).

This message is defined by the European Telecommunications Standards Institute (ETSI) in standard 103 301. It provides information about signal timings and predicted times of change. It is often accompanied with a MAPEM that provides topological information for decoding.

(iv) MAP Extended Message (MAPEM).

This message is defined by the European Telecommunications Standards Institute (ETSI) in standard 103 301. It is used to define the road and lane topology at a junction and provide necessary information to decode a SPATEM.

Besides the above message types, users can create new message types using the V2X API. For example, they can: (i) construct an abstract message type; (ii) define a format and add necessary attributes to the message type; (iii) add functions to create, send, and parse the messages.

3.3.3 V2X Channels

3.3.3.1 Key parameters

A channel represents a communications protocol, e.g., IEEE 802.11p, which is used to exchange information among ITS stations, e.g., equipped vehicles and RSUs. The channel implemented in the V2X module is a simplified version, which only focuses on reliability and range of communications and ignore some practical issues like package latency and loss caused by channel congestion and attenuation effect caused by buildings. The key parameters a channel in the V2X module considers are provided below:

(i) Latency

This parameter defines the delay in package transmission.

(ii) Range

This parameter defines the range of transmission, which will determine which ITS stations (e.g., equipped vehicles and RSUs) the subjected ITS station will connect to and communicate with. The range is defined as the distance between ITS stations, e.g., between equipped vehicles, regardless of road network connectivity and obstacles that may affect transmission.

(iii) Package Loss

This parameter defines the percentage of packages which are not received. When this value is not zero, the V2X module will consider this as the probability to discard a message during the transmission.

3.3.3.2 Channel creation and settings

In the Aimsun GUI, we can create a new channel from the "Project" menu. As shown in the following figure, click on "Project"→ "New"→ "V2X"→ "Channel".

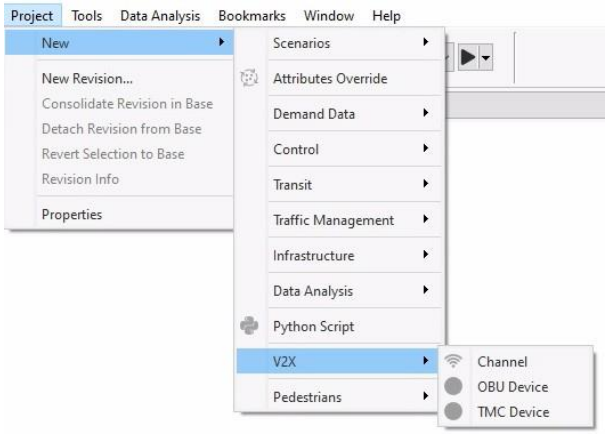

Then a new channel will be created in the location "Project (p)"→ "V2X"→ "Channels", which is shown below.

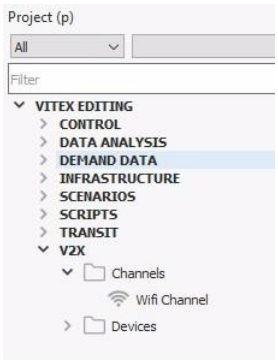

Double clicking on the new channel, a new window as shown below will pop up. We can change the name of the channel and configure the settings of "Latency", "Maximum Range", and "Package Loss (%)".

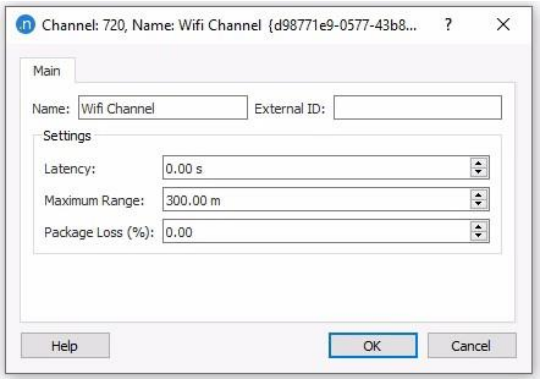

3.3.4 Vehicle On-Board Unit

In the V2X module, an On-Board Unit (OBU) is a simulation representation of message transmitter and receiver in the vehicle. It can be configured to connect to multiple channels and transmit/receive different message types on each channel.

To create a new OBU device, click on “Project”→ “New”→ “V2X”→ “OBU Device” as below.

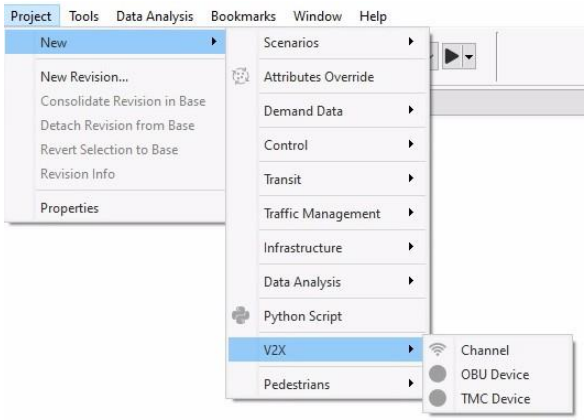

Then a new OBU will be created in the location “Project (p)”→ “V2X”→ “Devices”.

Double clicking on the new OBU device, a new window as shown below will pop up. We can change the OBU name and configure the channels it can connect to and the types of messages it can transmit and receive.

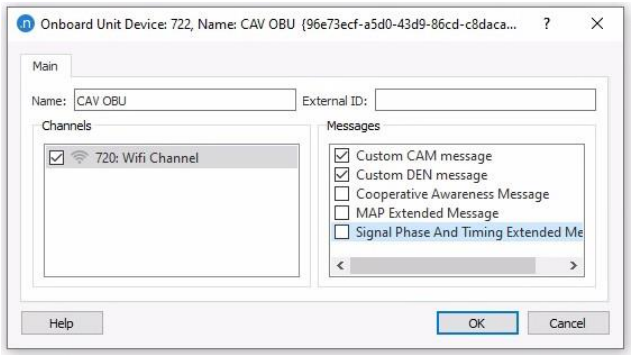

3.3.5 Roadside Unit

A Roadside Unit (RSU) is a physical device that exchanges information with equipped vehicles using the same channels and message types. It is often anchored at a fixed location with a predefined communications range. Therefore, it can connect to and receive traffic information from the equipped vehicles within its range. Meanwhile, it can connect to one or more road junctions and obtain necessary signal information from (or send control actions to) the traffic controllers. It also can perform some local processing and send aggregated information to the equipped vehicles or the TMCs it connects to.

A new RSU can be created from the "Tools" Toolbar, which is shown below. Click on the Wifi symbol and the symbol will change color, which means the function to create an RSU is activated.

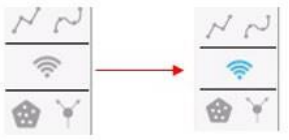

Click on the 2D map of a transportation network (in the Aimsun GUI) to define the location/center of the RSU and draw out a circle to the required radius. Once created, the position can be changed by selecting the object and dragging it to the targeted location, and the radius can be adjusted by selecting the circular boundary and resizing it. An example of an RSU centering at a signalized intersection is provided below.

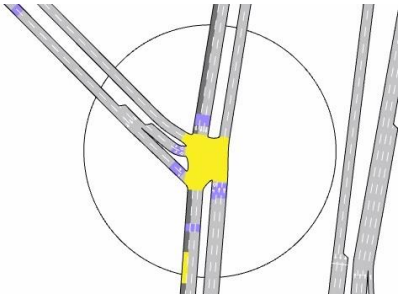

To configure the RSU connected to the road intersection, double click on the RSU object in the 2D map and a new window as shown below will pop up. In the "Connections" tab, first click on the "New" button and then click on the targeted node in the 2D map. If successful, a new node will appear inside the "Connections" box. The figure below also shows the new RSU is connected to the signalized intersection where it is located.

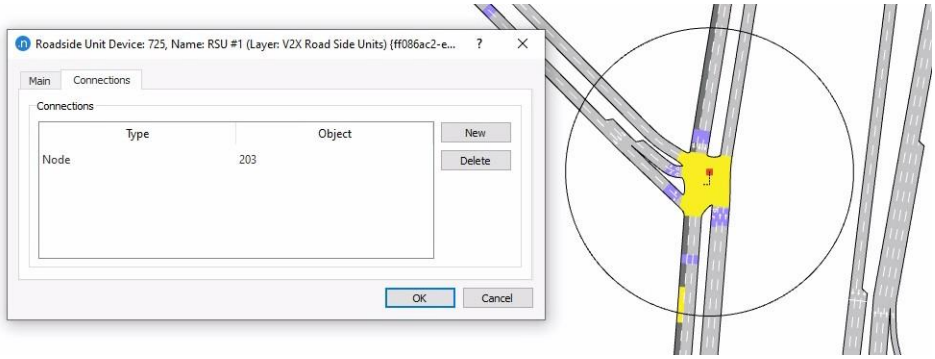

In addition, as shown below, users can rename the RSU in the "Main" tab and define communications channels as well as message types it can use.

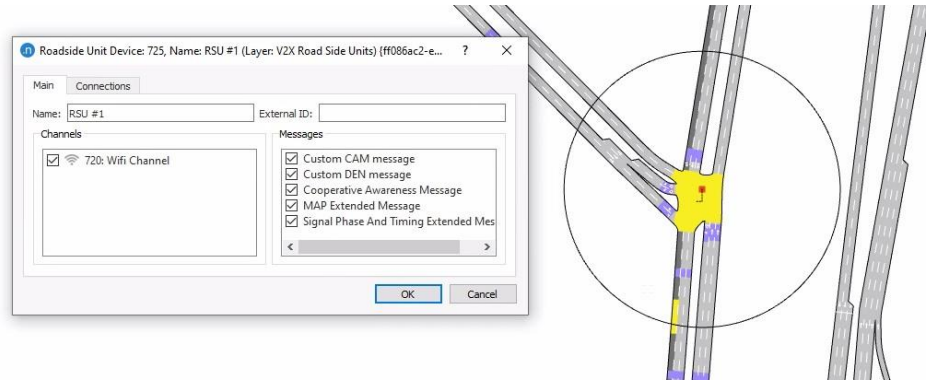

Note that, the radius of the RSU is just used for illustration purposes and has no impact on defining its communications range. The communications range of the RSU is the same as the communications rage of the channels it connects to. Ideally the radius should be drawn to be the same as the communications range, but it is not required. Therefore, the communications range of the channels, instead of the radius of the RSU, is used to detect the arrivals and exits of equipped vehicles in the V2X module.

3.3.6 Traffic Management Center

A Traffic Management Center (TMC) in the V2X module is used to process data from the connected RSUs, develop traffic management actions, and relay these actions to equipped vehicles and road devices (e.g., traffic controllers) via RSUs. The TMC has no visual representation or location in the Aimsun 2D window as it is just a control center not required to be in the modelled area (i.e., the transportation network opened in the Aimsun GUI).

To create a new TMC, click on "Project"→ "New"→ "V2X"→ "TMC Device", which is shown below.

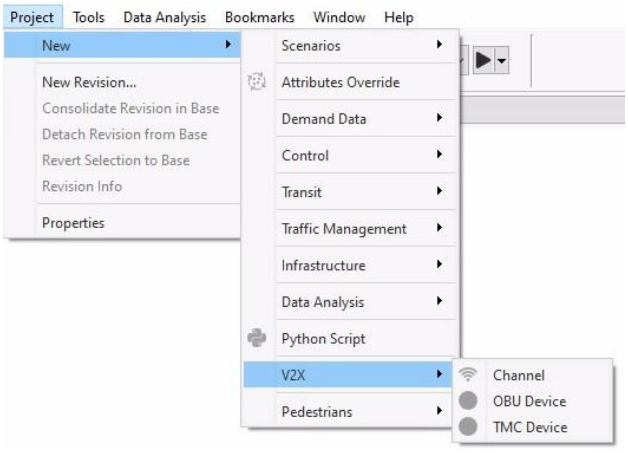

A new TMC will appear in the following location "Project (p)"→ "V2X"→ "Devices".

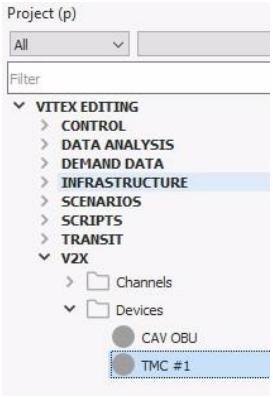

Double clicking on the new TMC object, a new window as shown below will pop up. In the "Road Side Units" tab, users can choose what RSUs it wants to connect to.

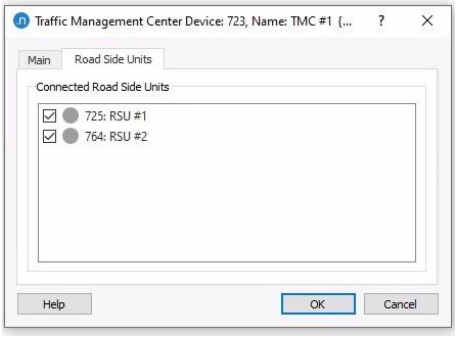

In order to allow the RSUs to function properly in Aimsun simulations, users need to make sure:

(i) The targeted RSUs are connected to a TMC;
(ii) The TMC is included in a dynamic scenario, which is shown below:

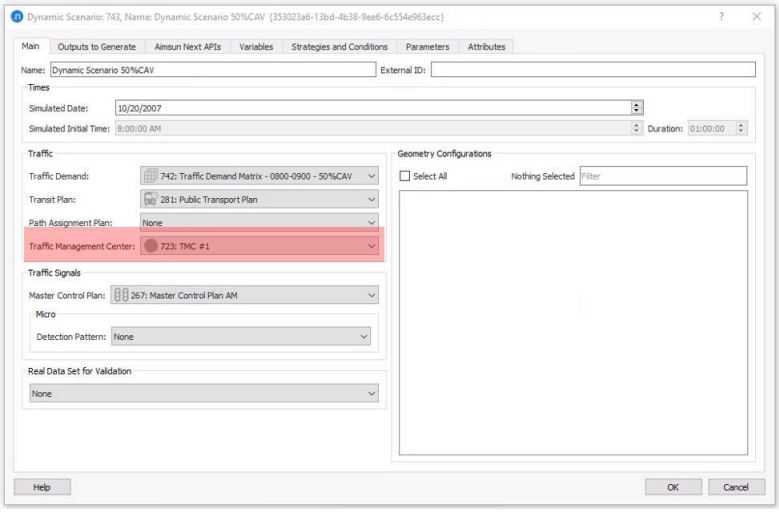

3.4 Steps to build an integrated microsimulation platform for CAVs in Aimsun

3.4.1 Architecture

In this subsection, we will provide detailed steps to build an integrated microsimulation platform for CAVs in Aimsun, the architecture of which is provided in Figure 5. As illustrated in Figure 5, the following functions will be enabled:

(i) At the vehicle control level, the ACC/CACC module will be used to control the longitudinal movements of CAVs. In particular, if the leading vehicle is a human-driven vehicle, the subject CAV will use ACC to control its movements. However, when its leader is a CAV, the subject CAV will join the platoon and use CACC to control its movements.

(ii) At the communications level, a CAV will send its traffic information to nearby connected RSUs via V2I communications. An RSU will collect all messages sent from CAVs within its communications range, perform some local analysis, and send information to its connected TMCs. Meanwhile, the RSU can broadcast detected traffic incidents/events and traffic management actions from TMCs to the CAVs within its communications range, which is known as I2V communications. In addition, once CAVs receive traffic incidents/events as well as traffic management actions from the RSU, it can broadcast this information to upstream CAVs via V2V communications.

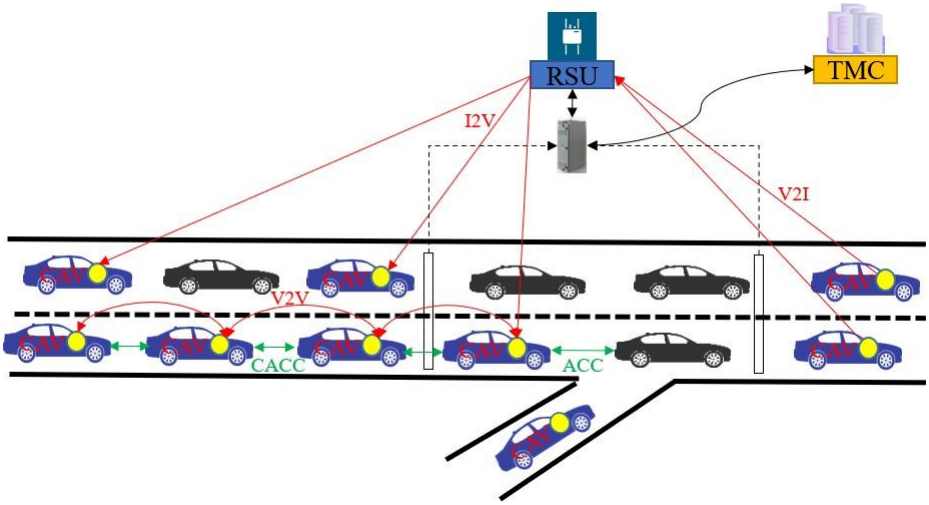

Figure 5: Architecture of a microsimulation environment for CAVs in Aimsun.

3.4.2 Existing issues

In Aimsun, there are two features available to build such a microsimulation environment for CAVs: (i) the ACC/CACC module, and (ii) the V2X module.

On the one hand, the ACC/CACC module only focuses on the control of longitudinal movements of AVs/CAVs, and the impact of V2V communications between CAVs is implicitly implemented in the

CACC control model (See Equation (36)). For a given vehicle type in Aimsum, e.g., “Car”, users can specify the percentages of vehicles equipped with ACC or CACC.

On the other hand, the V2X module is developed to mimic the communications flows between vehicles equipped with OBUs (e.g., CVs and CAVs) and other ITS stations (e.g., RSUs), which does not involve any control of vehicle-level movements. For a given vehicle type in Aimsum, e.g., “Car”, users can specify the percentage of vehicles equipped with OBUs.

However, due to the fact that these two features are developed independently, the assignment of vehicles equipped with ACC/CACC in the ACC/CACC module is independent from the assignment of vehicles equipped with OBUs in the V2X module. As a result, there will be inconsistency in the assignment of CAVs if they are not 100% equipped with both ACC/CACC and OBUs.

As shown below, if 10% of cars are CAVs, we should assign 0% equipped with ACC, 10% equipped with CACC, and 10% equipped with OBUs.

(i) 0% cars equipped with ACC

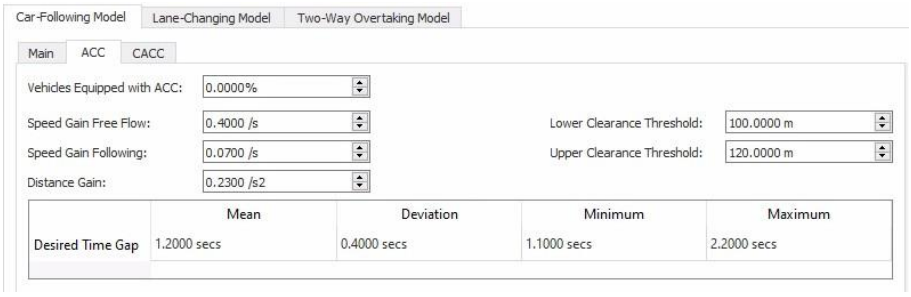

(ii) 10% cars equipped with CACC

(iii) 10% cars equipped with OBUs

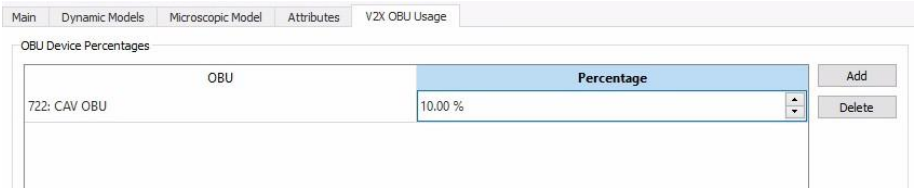

Unfortunately, the above procedure may fail to generate 10% CAVs equipped with both CACC and OBUs. The final assignment of vehicles can be any combinations with the total sum of 10% CACC and 10% OBUs, for example, 8% with both CACC and OBUs, 2% with CACC only, and 2% with OBUs only. Therefore,

these two features cannot be used at the same time with CAVs less than 100% in the current software design.

3.4.3 A practical solution

In order to build the architecture illustrated in Figure 5, we will provide a practical solution to bridge the gap between the above two features so as to have consistent vehicle assignments of CAVs. The proposed solution is divided into the following steps.

3.4.3.1 Create new vehicle types for CAVs

For each vehicle type, create a new type equipped with 100% CACC and OBUs. For example, for vehicle type "Car", we can create a new type called "Car CAV" equipped with 100% CACC and OBUs. Details are provided below.

(i) Create a new vehicle type called "Car CAV".

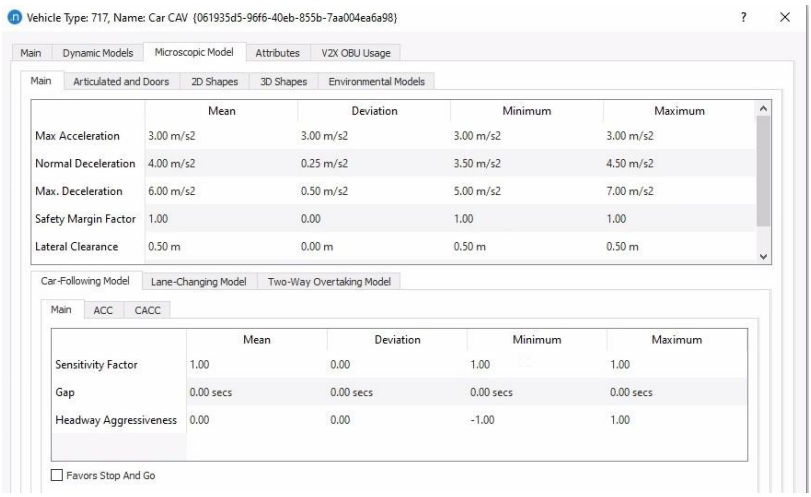

(ii) Set "Vehicles Equipped with ACC" to be 0%. Users can change the parameter settings in the "ACC" tab if needed.

a. Parameters in the ACC control modes: Speed Gain Free Flow, Speed Gain Following, Distance Gain, and Desired Time Gap.
b. Parameters in the Decision Chart: Lower Clearance Threshold, and Upper Clearance Threshold.

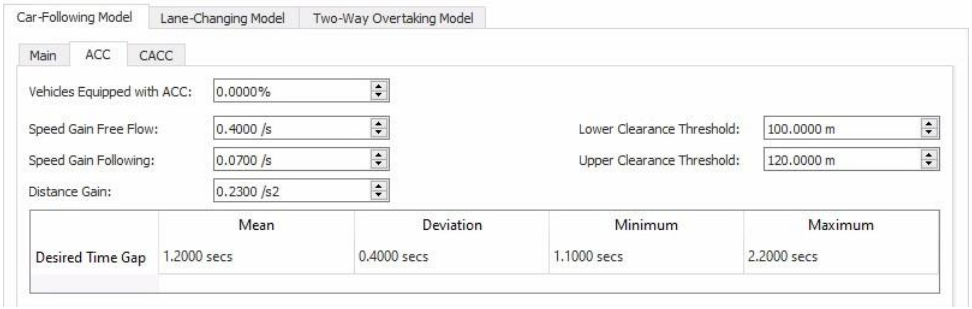

(iii) Set “Vehicles Equipped with CACC” to be 100%. Users can change the parameter settings in the “CACC” tab if needed.

a. Parameters in the CACC control modes: Speed Gain, Distance Gain, Time Gap Leader, and Time Gap Follower.
b. Parameters in the Decision Chart: Lower Gap Threshold, and Upper Gap Threshold.

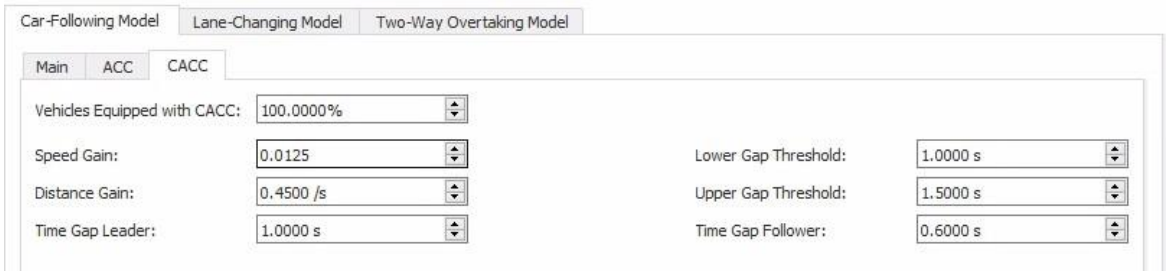

(iv) In the “V2X OBU Usage” tab, pick an available OBU in the transportation system, e.g., “CAV OBU”, and set the parameter “Percentage” to be 100%.

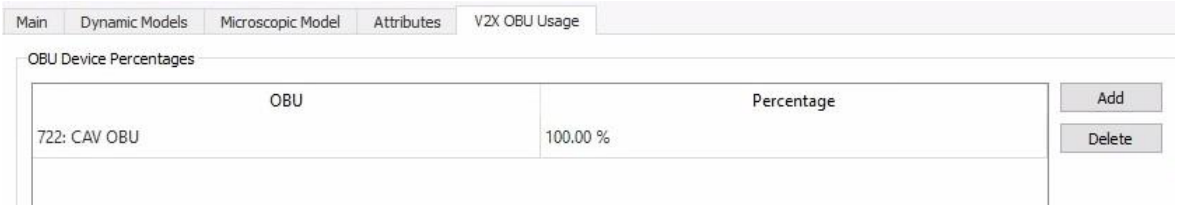

Users can follow the above procedure to create new CAVs equipped with 100% CACC and OBUs for other vehicle types, e.g., “Truck CAV” for “Truck”. Users can also adjust the parameter settings to consider the differences, e.g., time gap, between vehicle types, e.g., “Car” vs. “Truck”.

3.4.3.2 Adjust OD matrices for CAVs with different penetration rates

Once new CAV vehicle types have been created, users need to adjust the OD matrices according to their penetration rates. For example, consider the vehicle types “Car” and the following original OD matrix “Car Matrix – 0800–0900”.

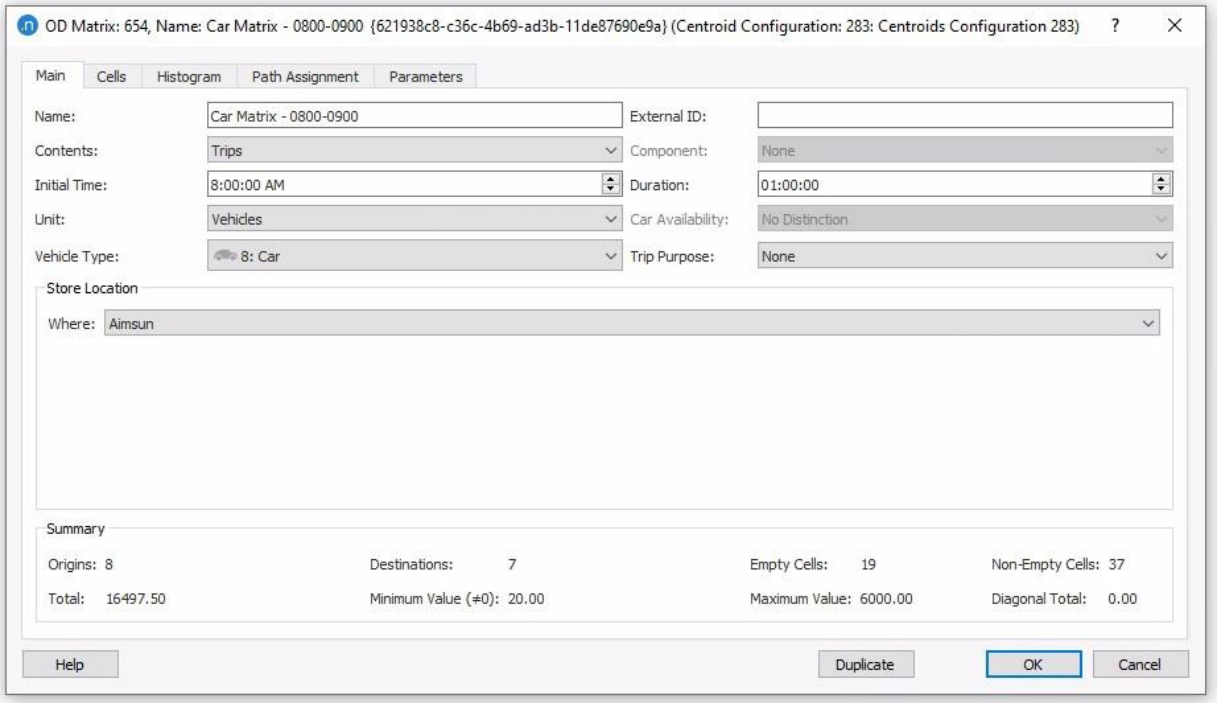

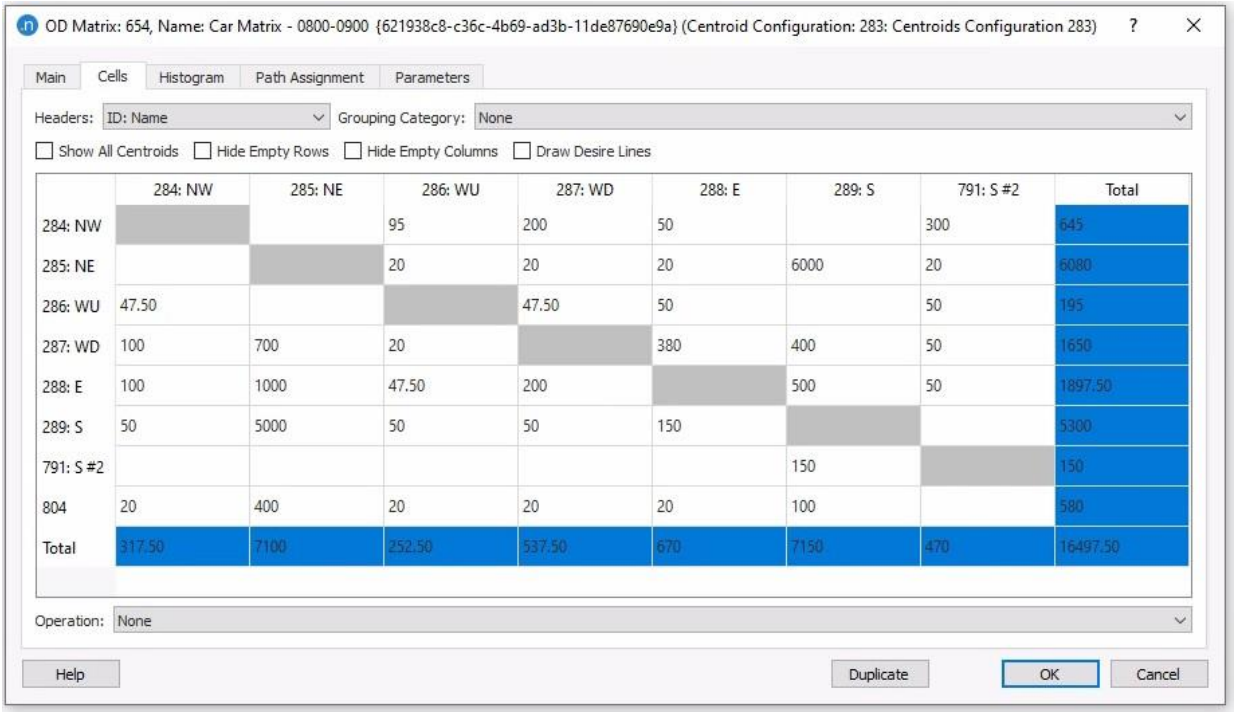

	284: NW	285: NE	286: WU	287: WD	288: E	289: S	791: S #2	Total
284: NW			95	200	50		300	645
285: NE			20	20	20	6000	20	6080
286: WU	47.50			47.50	50		50	195
287: WD	100	700	20		380	400	50	1650
288: E	100	1000	47.50	200		500	50	1897.50
289: S	50	5000	50	50	150			5300
791: S #2						150		150
804	20	400	20	20	20	100		580
Total	317.50	7100	252.50	537.50	670	7150	470	16497.50

If the penetration rate of Car CAVs is 20%, then users need to split the original OD matrix into two:

(i) A new OD matrix “Car CAV Matrix - 0800-0900 - 20%” for Car CAVs with 20% of the original demand, which is shown below:

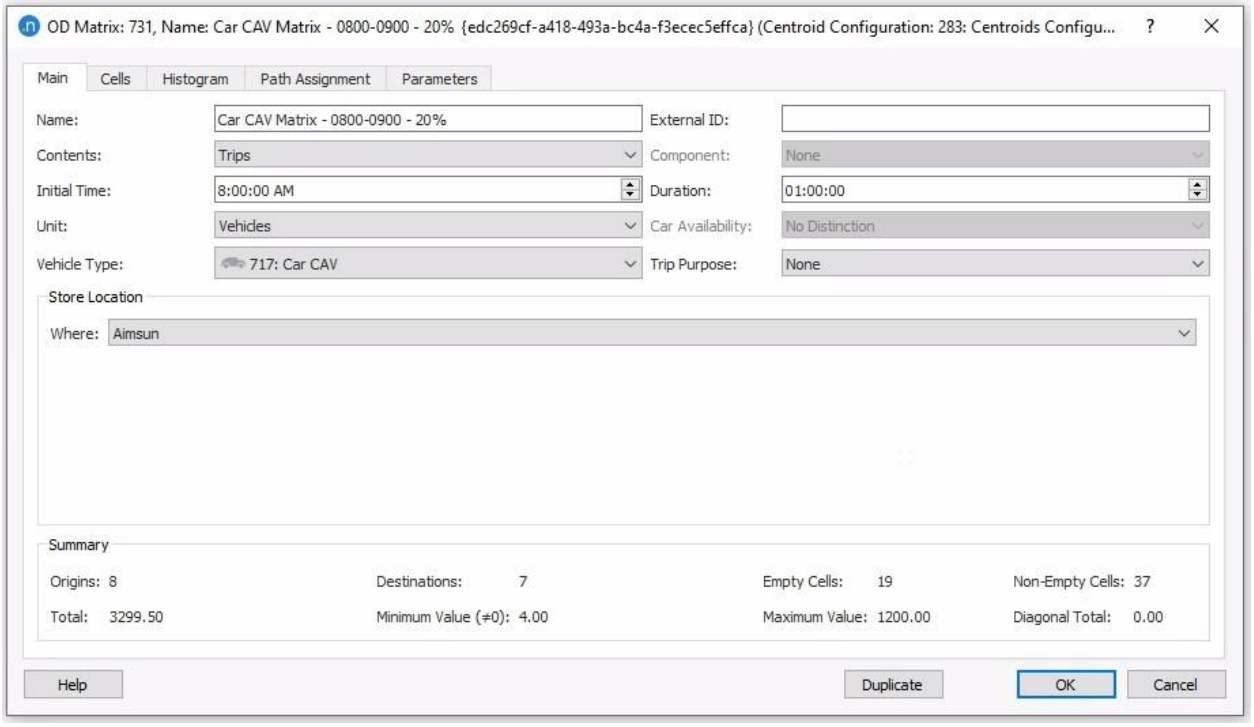

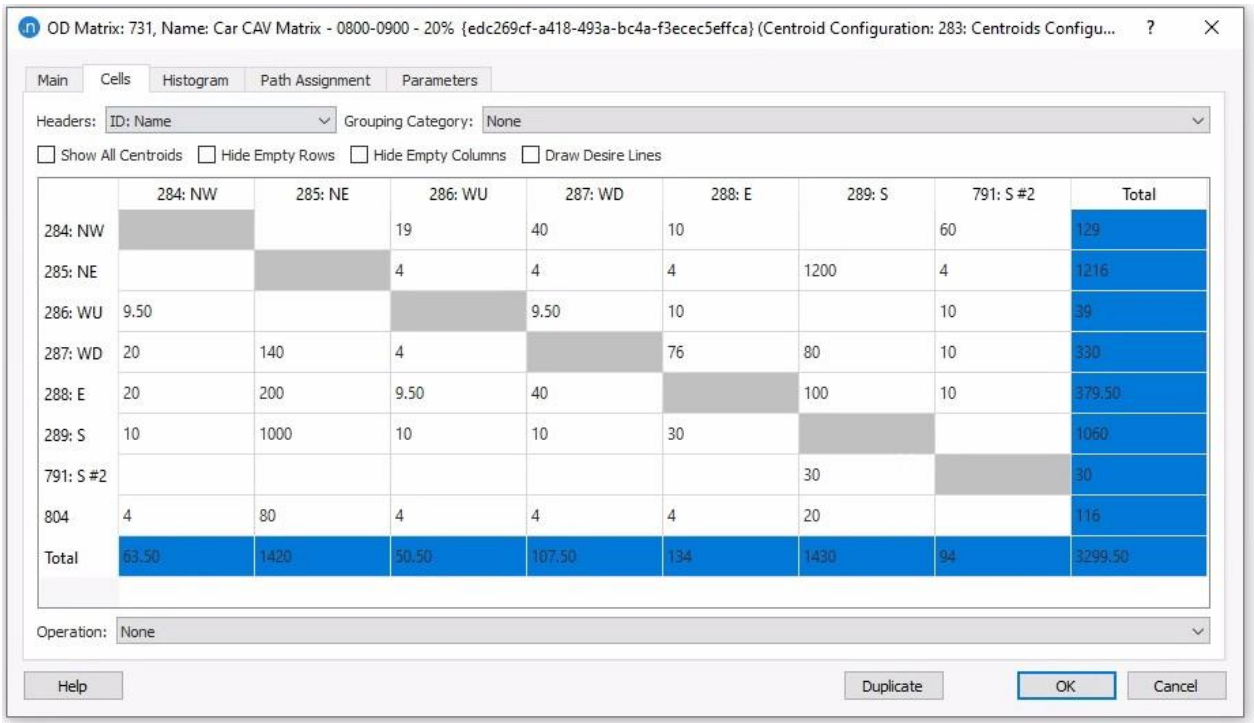

	284: NW	285: NE	286: WU	287: WD	288: E	289: S	791: S #2	Total
284: NW			19	40	10		60	129
285: NE			4	4	4	1200	4	1216
286: WU	9.50			9.50	10		10	39
287: WD	20	140	4		76	80	10	330
288: E	20	200	9.50	40		100	10	379.50
289: S	10	1000	10	10	30			1060
791: S #2						30		30
804	4	80	4	4	4	20		116
Total	63.50	1420	50.50	107.50	134	1430	94	3299.50

(ii) A new/adjusted OD matrix “Car Matrix - 0800-0900 - 80%” for Cars with 80% of the original demand, which is shown below:

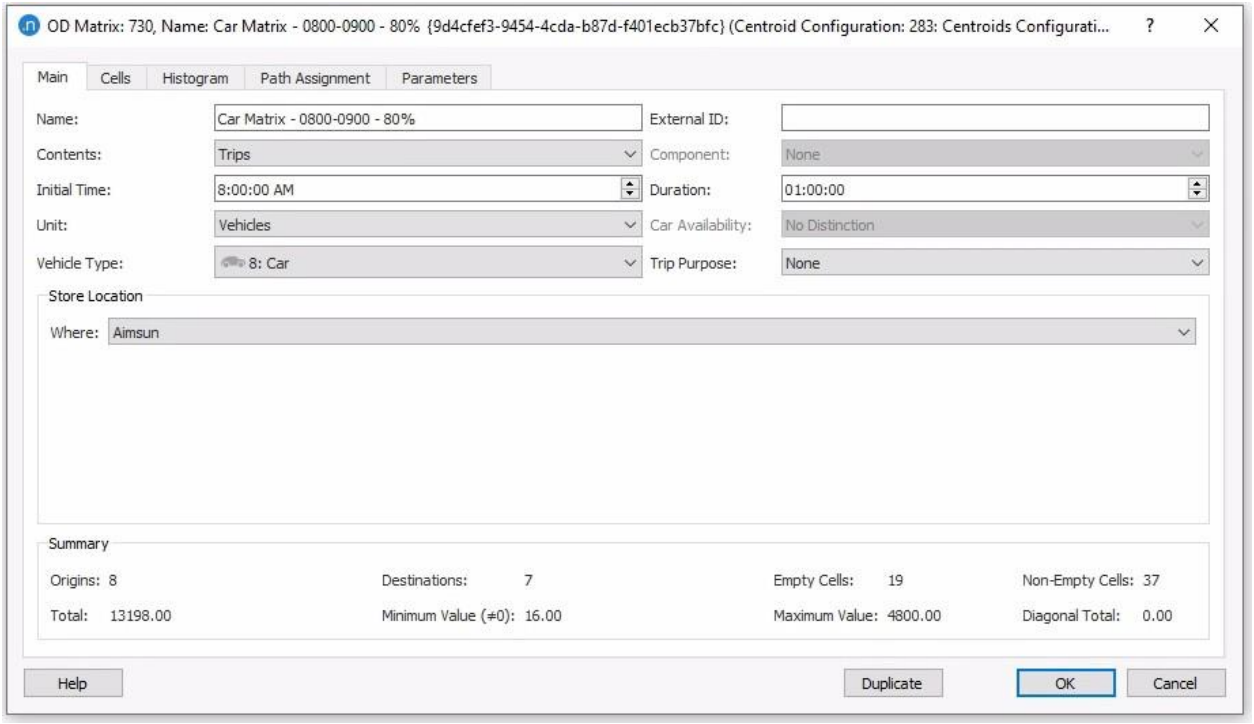

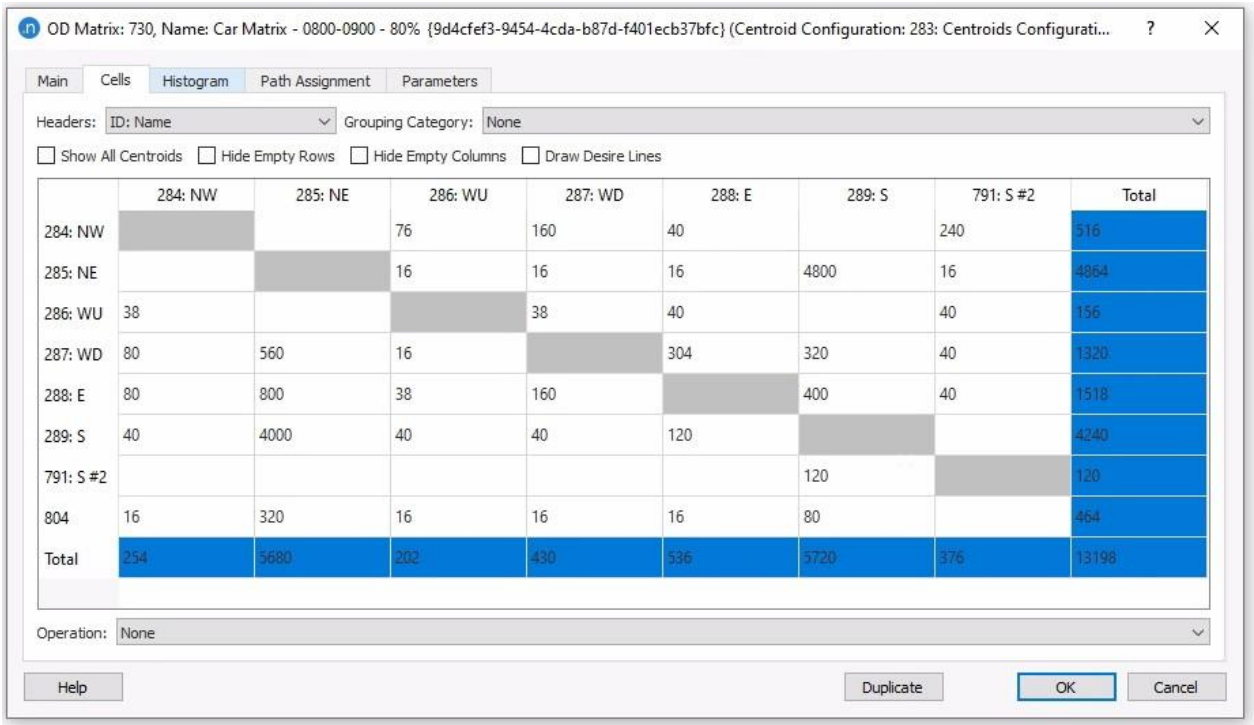

	284: NW	285: NE	286: WU	287: WD	288: E	289: S	791: S #2	Total
284: NW			76	160	40		240	516
285: NE			16	16	16	4800	16	4864
286: WU	38			38	40		40	156
287: WD	80	560	16		304	320	40	1320
288: E	80	800	38	160		400	40	1518
289: S	40	4000	40	40	120			4240
791: S #2						120		120
804	16	320	16	16	16	80		464
Total	254	5680	202	430	536	5720	376	13198

In addition, as shown below, users can follow the above procedure to create new OD matrices for different types of CAVs, e.g., Truck CAV, with different penetration rates, e.g., 50%.

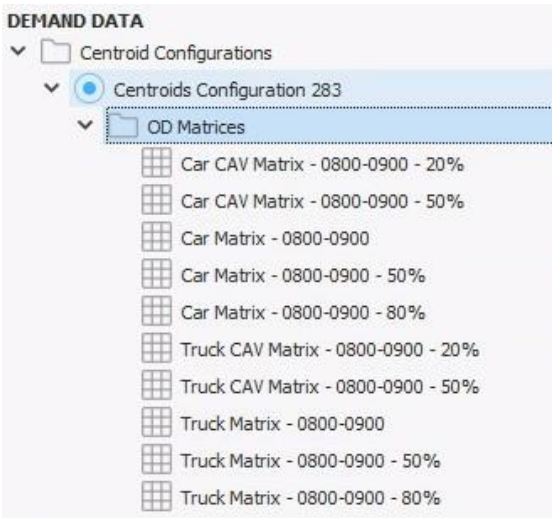

3.4.3.3 Create demand profiles for mixed traffic

Once OD matrices for both CAVs and human-driven vehicles have been created, users can create demand profiles for mixed traffic with different penetration rates of CAVs.

For example, without CAVs, the original "Traffic Demand Matrix - 0800-0900" can be constructed as below with two different vehicle types, Car and Truck.

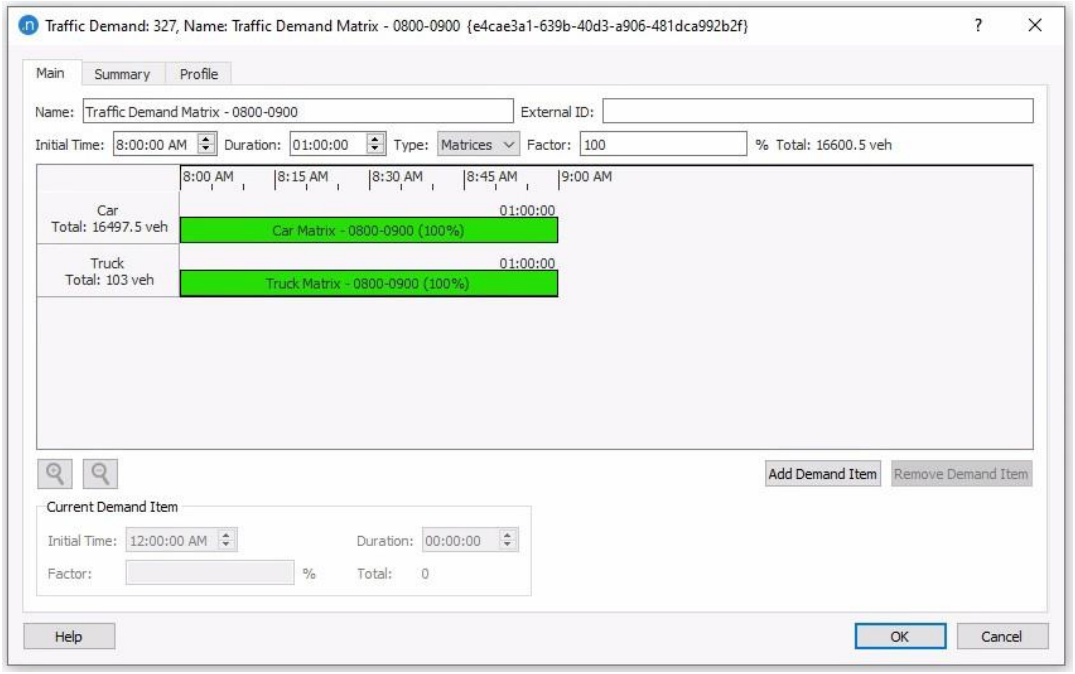

With 20% CAVs for both Car and Truck, a new matrix "Traffic Demand Matrix - 0800-0900 - 20%CAV" can be constructed as below:

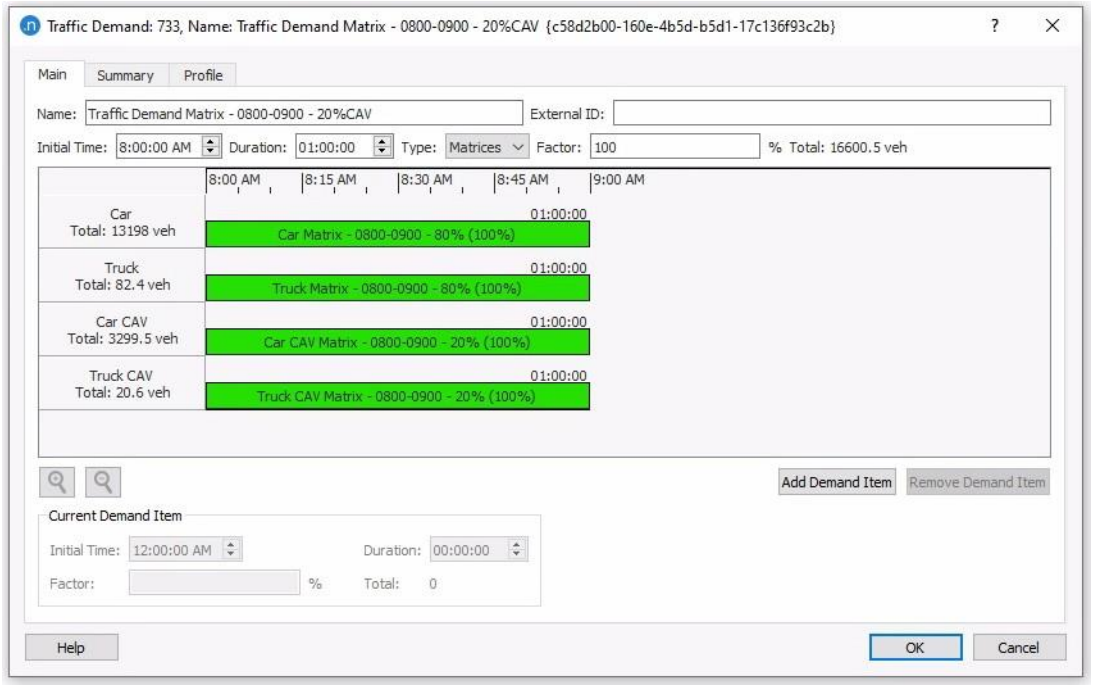

To simulate future traffic with increased demand, users can change the percentage in the parameter "Factor" to be greater than 100%, e.g., 120%. An example of the matrix "Traffic Demand Matrix - 0800-0900 - 20%CAV - Demand 120%" is provided below.

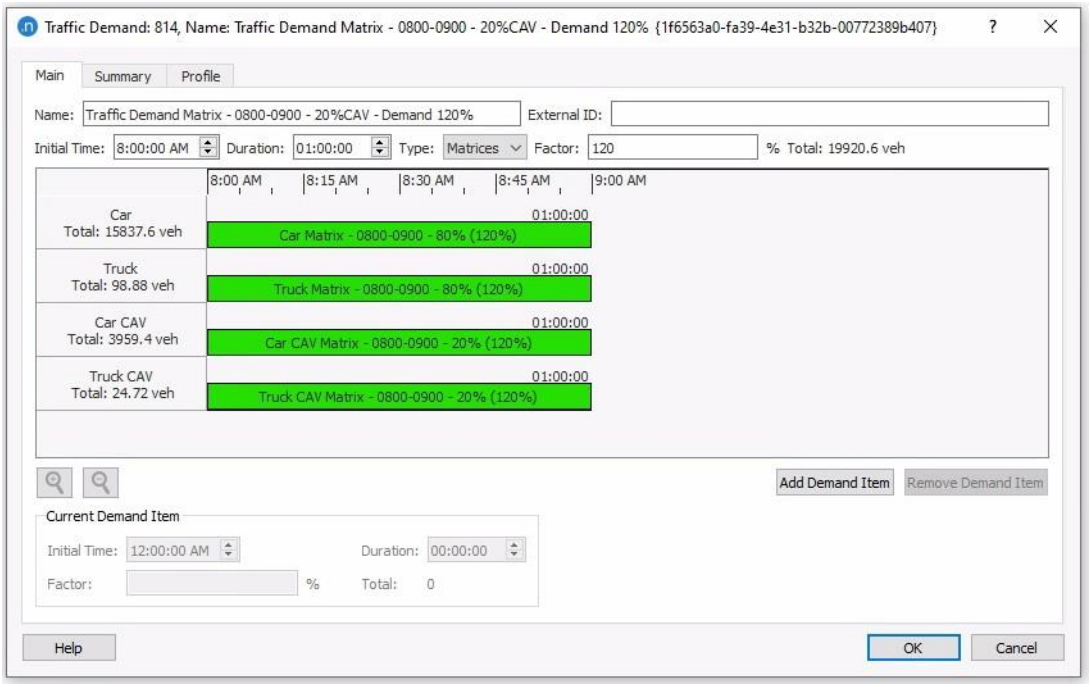

Users can follow the same procedure to create many different Traffic Demand Matrices with different percentages of CAVs. An example is provided below:

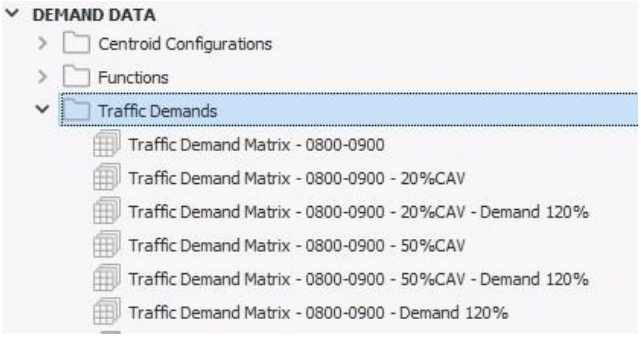

3.4.3.4 Create simulation scenarios for mixed traffic

3.4.3.4.1 Settings for road types

Before creating simulation scenarios for mixed traffic, users need to make sure the ACC/CACC module is set up correctly in the road types in the transportation network. For example, for the "Freeway" road type, users should enable the option "ACC/CACC Allowed" under the "Dynamic Models" tab in the following window:

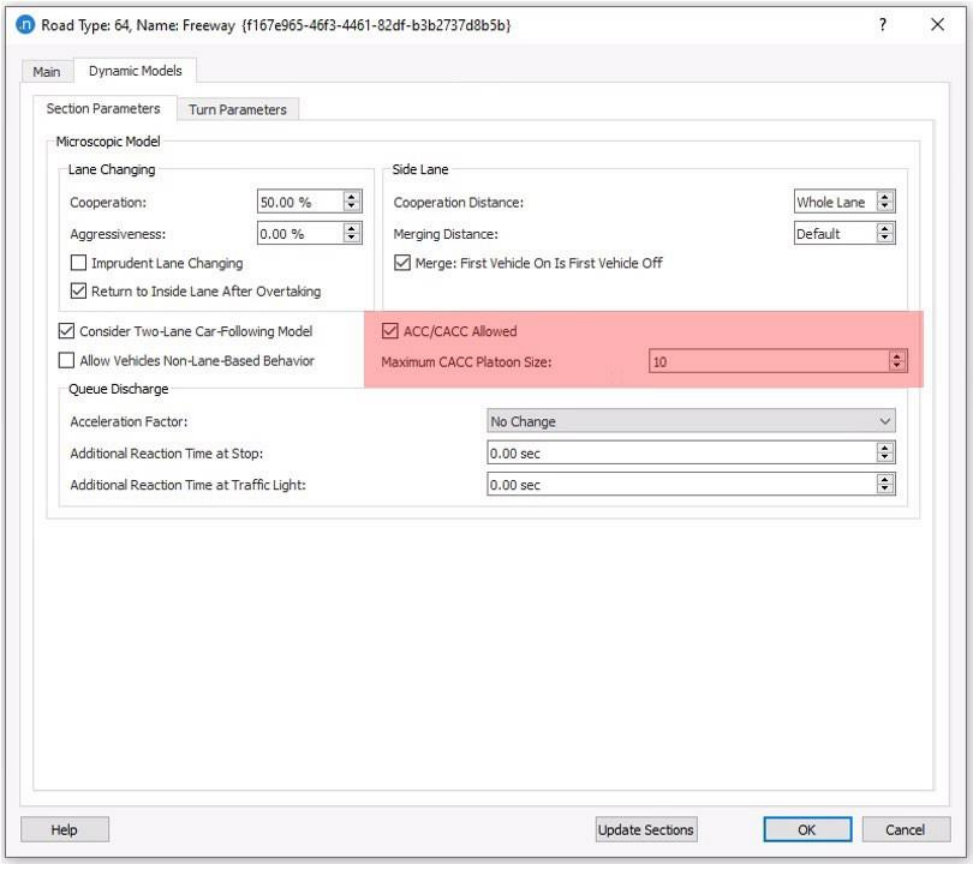

Meanwhile, users can change the "Maximum CACC Platoon Size" to a value that is appropriate for different road types, e.g., platoon size of 10 for "Freeway". Furthermore, users can follow the same procedure to enable ACC/CACC on other road types in the transportation network.

3.4.3.4.2 Settings for dynamic scenarios

As an example, consider the following Dynamic Scenario "Dynamic Scenario - 0800-0900 - 20%CAV" for mixed traffic with 20% CAVs.

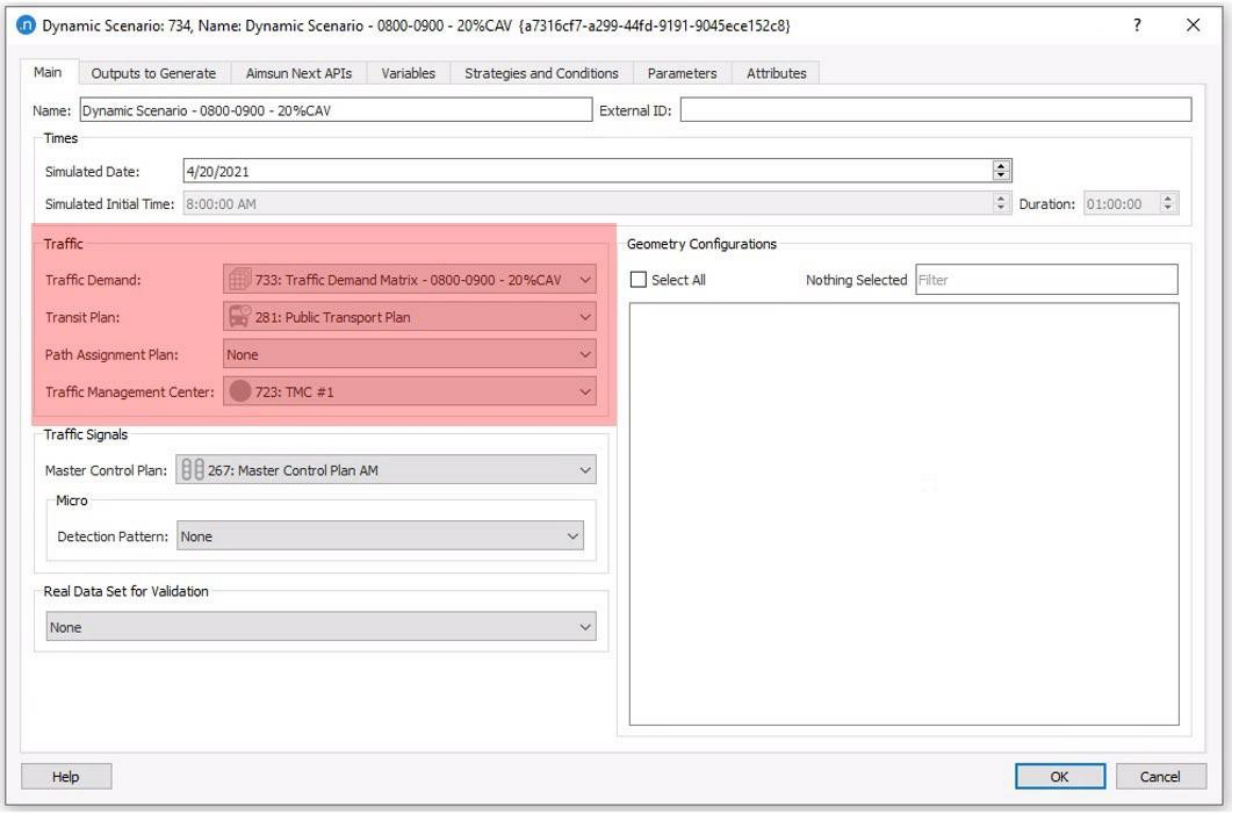

Under the "Main" tab, users need to adjust the following settings in the "Traffic" block to enable the ACC/CACC and V2X modules:

(i) "Traffic Demand": select the demand matrix for the same time period with 20% CAVs.

(ii) "Traffic Management Center": select the TMC that connects to multiple RSUs in the network. This is required to make sure the RSUs in the selected TMC can function properly. If no TMC is selected, the RSUs won't work during simulations.

For other parameters, users can edit them according to their simulation requirements/settings.

3.4.3.4.3 Settings for dynamic experiments

Once a Dynamic Scenario has been created, users can create Dynamic Experiments to simulate the mixed traffic environment. In order to make sure the ACC/CACC module can run properly, users need to make some adjustments in a selected Dynamic Experiment. For example, for the following Dynamic Experiment "Experiment #1", we need to adjust the settings under the "Reaction Time" tab.

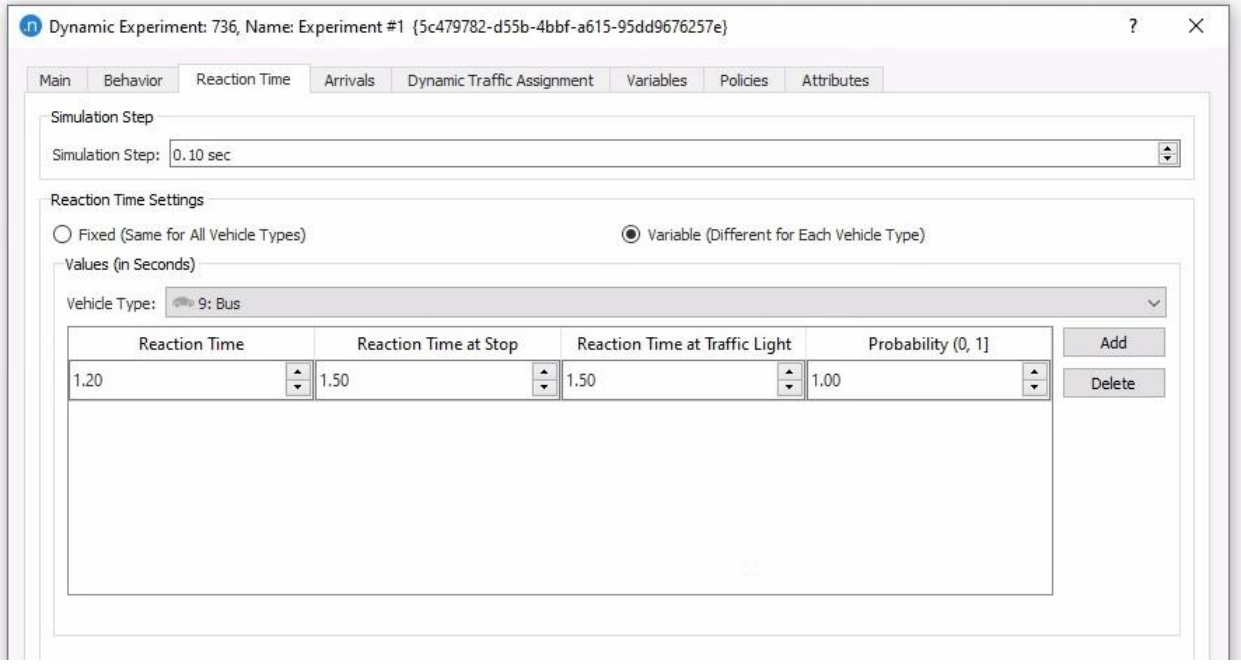

In particular, users need to change the "Simulation Step" to be 0.1s in order to allow the ACC/CACC control module to work properly. Furthermore, users need to choose "Reaction Time Settings" to be "Variable (Different for Each Vehicle Type)" to allow different vehicle types to have different reaction times. As an example, below are the reaction time settings for four vehicle types: Car, Car CAV, Truck, Truck CAV.

- Car
    - Reaction time: 0.8s
    - Reaction time at stop: 1.2s
    - Reaction time at traffic light: 1.6s
- Car CAV
    - Reaction time: 0.4s
    - Reaction time at stop: 0.8s
    - Reaction time at traffic light: 1.0s
- Truck
    - Reaction time: 1.5s
    - Reaction time at stop: 2.0s
    - Reaction time at traffic light: 2.5s
- Truck CAV
    - Reaction time: 1.0s
    - Reaction time at stop: 1.5s
    - Reaction time at traffic light: 2.0s

For other parameters, users can change the settings according to their simulation requirements/settings.

3.5 Discussion

In this section, we provided a tutorial on how to build an integrated microsimulation platform for mixed traffic with CAVs in Aimsun. In particular, we used the newly-developed ACC/CACC and V2X modules in Aimsun to build such a platform. In Section 3.1, we first provided detailed steps to install required software components, which mainly include the core Aimsun Next 20 software, the V2X SKD and Framework, Visual Studio, and Qt. Next in Section 3.2, we provided a summary of the ACC/CACC module implemented in Aimsun. Especially, we focused on the available ACC/CACC control modes as well as the decision chart on how these modes switch between each other. Then in Section 3.3 we introduced the key components in the V2X module implemented in Aimsun, which include Messages, Channels, OBUs, RSUs, and TMCs. We discussed the properties of these components and provided detailed steps on how to create and set them up properly in microsimulation.

However, given that the two modules, ACC/CACC and V2X, are developed separately, there exists inconsistency in vehicle assignments if both modules are used with the current software design for mixed traffic, e.g., with 10% CAVs. Therefore, in Section 3.4 we provided a practical solution that bridges the gap between these two modules so as to build the integrated microsimulation platform for mixed traffic with any percentages of CAVs. In particular, we provided detailed steps on: (i) how to create new vehicle types of CAVs, (ii) how to create new OD matrices for CAVs with different penetration rates, and (iii) how to create demand profiles and dynamic simulation scenarios for mixed traffic with different penetration rates of CAVs.

In the rest of this report, we will use this integrated microsimulation platform to evaluate system-level impacts of CAV applications on different transportation networks. For freeways, we will evaluate the performance of different freeway speed harmonization algorithms with CAVs. For arterials, we would like to understand how traffic light optimal speed advisory algorithms can help improve traffic. For corridor networks, i.e., with both freeways and arterials, we would like to know how route guidance using CAVs can help mitigate congestion caused by non-recurrent traffic incidents on freeways. Moreover, users can use this integrated microsimulation platform to develop their CAV applications and evaluate their corresponding performance.

This page left blank intentionally

4. Simulation results of CAV applications in small networks

In Section 3, we have developed an integrated microsimulation platform in Aimsun that can mimic the real-world mixed traffic environment with CAVs. More specifically, this microsimulation platform integrates the ACC/CACC module with the V2X module in Aimsun and has two levels of functionalities:

- At the vehicle control level: the ACC/CACC module is used to control CAV's longitudinal movements.
- At the communications level: the V2X module is used for V2I/I2V and V2V communications with standard message formats, e.g., SPaT (SAE J2735-201603), MAP (SAE J2735-201603), CAM (ETSI TS 302 637-2), and DENM (ETSI 302 637-3) messages.

In this section, we would like to demonstrate how to apply this integrated microsimulation platform to evaluate network-level impacts of CAV applications. In particular, three applications with CAVs are selected for demonstration purposes: (i) freeway speed harmonization with CAVs, (ii) route guidance with CAVs for traffic incident management, and (iii) traffic light optimal speed advisory with CAVs. For each application, we have implemented the required workflows to enable the communications between RSUs and CAVs as well as algorithms to regulate CAV's driving behaviors and route choice decisions. In order to assess their performance, we have generated three different subnetworks from the original I-210 network: (i) a Freeway-Only subnetwork for the application of freeway speed harmonization with CAVs; (ii) a Freeway-and-Arterial Combined subnetwork for the application of route guidance with CAVs for traffic incident management; and (iii) an Arterial-Only subnetwork for the application of traffic light optimal speed advisory with CAVs. In the rest of this section, we will provide detailed descriptions on the implementation of these CAV applications as well as some simulation results in the subnetworks.

In Section 4.1, we first provide detailed parameter settings in the ACC/CACC module, which include the settings of simulation time step, vehicle reaction time, parameters in the ACC and CACC control modes, and road types. These settings will be kept the same for all simulation studies in this project (both in this section and Section 5).

In Section 4.2, we present the system architecture and the communications workflow for the application of freeway speed harmonization with CAVs. For demonstration purposes, we select three different algorithms with minor revisions to incorporate CAVs, which are the rule-based algorithm in (Talebpour et al., 2013), the VSL-VSA algorithm in (Lu et al., 2015; Hale et al., 2016), and the C-VSLS in (Grumert et al., 2015). Then we describe the network settings in the Freeway-Only subnetwork and conduct various simulation scenarios under different demand levels and percentages of CAVs to assess the performance of these three algorithms.

In Section 4.3, we present the system architecture and the communications and incident management workflows for the application of route guidance with CAVs for traffic incident management. In order to mimic CAV's route choice decisions when new detour routes are available, we revise and implement the route choice algorithm in (Samimi Abianeh et al., 2020) to consider the impacts of lane index (inner lanes vs. shoulder lanes) and vehicle types (car vs. truck) on the decision-making step. Next, we describe the network settings and scenario design in the Freeway-and-Arterial Combined subnetwork. In particular, we consider two traffic accidents occurring at the same location but with different levels of severity: (i) a major

traffic accident in the AM peak between 7AM and 8AM; and (ii) a minor traffic accident in the PM peak between 4PM and 5PM. Under these settings, we conduct simulations with 30% and 50% CAVs to evaluate how this type of information sharing can help mitigate congestion when traffic incidents occur.

In Section 4.4, we present the system architecture and the communications workflow for the application of traffic light optimal speed advisory. For demonstration purposes, we revise and implement the Green Light Optimal Speed Advisory (GLOSA) application proposed in (Katsaros et al., 2011). Then we describe the network settings in the Arterial-Only subnetwork and conduct various simulation scenarios under different time periods (e.g., 7AM—8AM and 4PM—5PM), demand levels (e.g., 80% -- 120%), and percentages of CAVs (0% – 100%) to assess the performance of the GLOSA algorithm.

In Section 4.5, we summarize our findings with some future research directions.

4.1 Parameter settings in the ACC/CACC module

In order to activate the ACC/CACC module during simulations and generate reasonable results, we need to properly configure some key model parameters in Aimsun. More detailed settings are provided in the following subsections. Note that these settings are kept the same for all simulation scenarios in the rest of this report.

4.1.1 Simulation time step and reaction time settings

As implemented in Aimsun, we need to set the simulation time step to be 0.1s in order to see the impact of AVs/CAVs. Meanwhile, considering a CAV can receive more traffic information from nearby CAVs and RSUs, we can have different "Reaction Time Settings" for different vehicle types. In particular, there are three reaction times considered in Aimsun: Reaction Time, Reaction Time at Stop, and Reaction Time at Traffic Light. In Table 1, we list the reaction time settings for the vehicle types used in the I-210 network and the subnetworks.

Table 1. Reaction time settings for different vehicle types.

Vehicle Type	Reaction Time	Reaction Time at Stop	Reaction Time at Traffic Light
Car	0.8s	1.2s	1.6s
Car CAV	0.4s	0.8s	1.0s
Car HOV	0.8s	1.2s	1.6s
Car HOV CAV	0.4s	0.8s	1.0s
Truck Medium	1.5s	2.0s	2.5s
Truck Medium CAV	1.0s	1.5s	2.0s
Truck Heavy	2.0s	2.5s	3.0s
Truck Heavy CAV	1.5s	2.0s	2.5s

Here "Truck Medium" stands for "Truck – Medium Duty" with an average length of 30 ft in Aimsun, and "Truck Heavy" stands for "Truck – Heavy Duty" with an average length of 60ft in Aimsun.

4.1.2 Settings of ACC/CACC control modes

As shown in Figure 3, the ACC mode is embedded in the CACC mode for CAVs. Therefore, for a selected CAV vehicle type, e.g., "Car CAV", we need to set the percentage of ACC-enabled vehicles (i.e., AVs) to 0% but the percentage of CACC-enabled vehicles (i.e., CAVs) to 100%. Example of parameter settings for the vehicle type "Car CAV" in Aimsun is provided in Figure 6.

In addition, more parameter settings in the ACC/CACC control modes are listed in Table 2. Refer to Figure 6 for the corresponding parameter names.

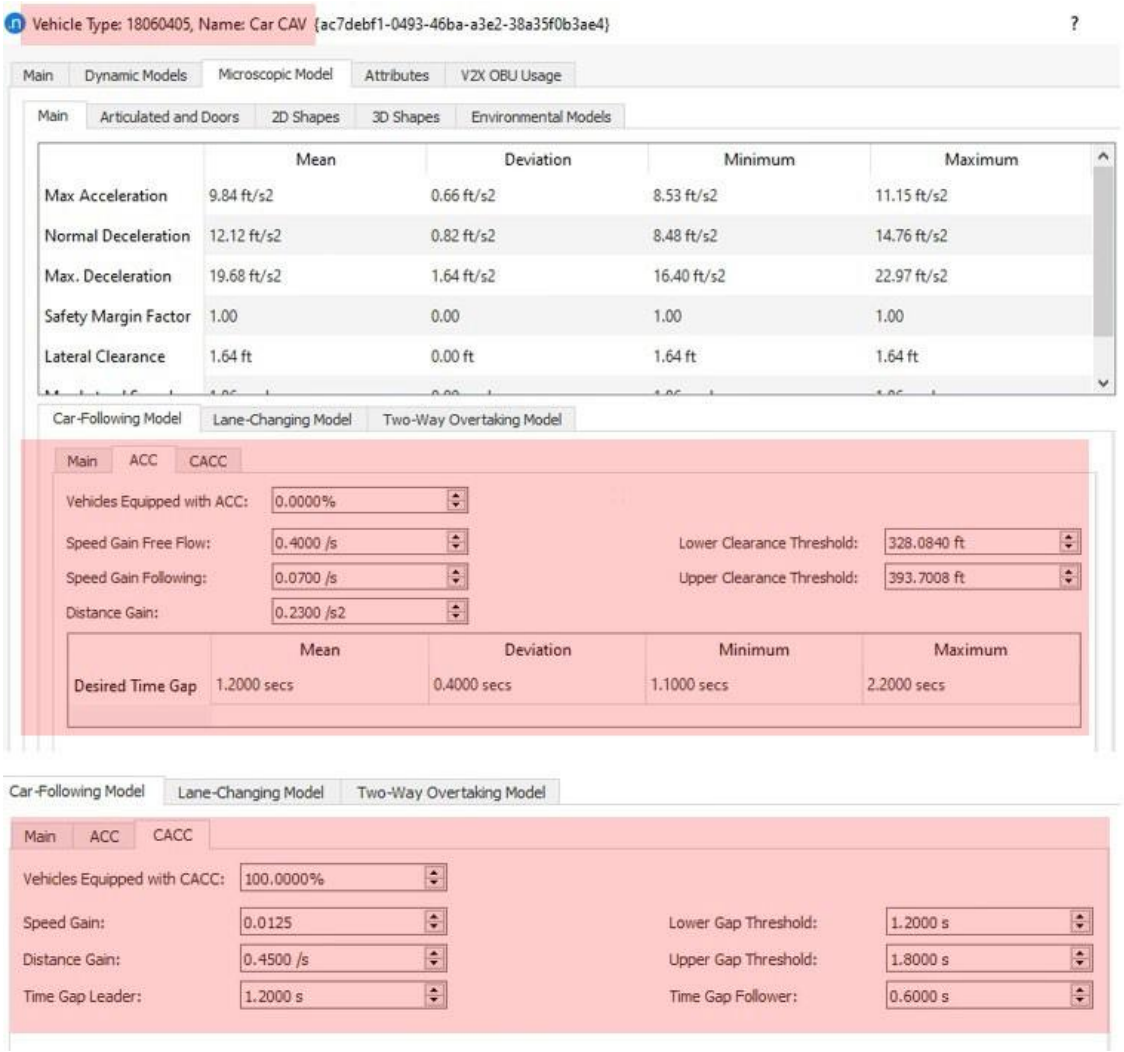

Figure 6. Example of parameter settings for the vehicle type "Car CAV" in Aimsun.

4.1.3 Road type settings

When a vehicle is equipped with ACC/CACC, it will only be functional on the roads that allow it. Meanwhile, the CACC-equipped vehicles can form platoons with smaller time gaps between consecutive members. For a given road type, we can configure whether it allows ACC/CACC-equipped vehicles as well as the maximum platoon size for CACC-equipped vehicles.

In our simulation setting, we enable ACC/CACC for all road types which include freeway, arterial, on/off ramp, etc. For simplicity, we also apply the same value, i.e., 10, to all road types as the maximum platoon size for CACC-equipped vehicles.

Table 2. Parameter settings in the ACC/CACC control modes.

ACC		
Parameters	Value	
Speed Gain Free Flow	0.400/s (Default)	
Speed Gain Following	0.0700/s (Default)	
Distance Gain	0.2300/s^2 (Default)	
Desired Time Gap	1.200 secs (Default)	
Lower Clearance Threshold	100m (Default)	
Upper Clearance Threshold	120m (Default)	
CACC		
Parameters	Value	
Speed Gain	0.0125 (Default)	
Distance Gain	0.4500/s (Default)	
Time Gap Leader	Car CAV:1.2s Truck Medium CAV: 1.5s	Car HOV CAV: 1.2s Truck Heavy CAV: 2.0s
Time Gap Follower	Car CAV:0.6s Truck Medium CAV: 1.2s	Car HOV CAV: 0.6s Truck Heavy CAV: 1.5s
Lower Gap Threshold	Car CAV:1.2s Truck Medium CAV: 1.5s	Car HOV CAV: 1.2s Truck Heavy CAV: 2.0s
Upper Gap Threshold	Car CAV:1.8s Truck Medium CAV: 2.0s	Car HOV CAV: 1.8s Truck Heavy CAV: 2.5s

4.2 Application: Freeway speed harmonization with CAVs

In this subsection, we demonstrate how to apply the integrated microsimulation platform to the application of freeway speed harmonization with CAVs. More details are provided below.

4.2.1 System architecture

In Figure 7, we provide the system architecture of freeway speed harmonization with CAVs. In this system architecture, V2I/I2V communications between RSUs and CAVs and V2V communications among CAVs are enabled. We also consider RSUs can receive real-time detector measurements within the targeted speed harmonization zone either from local controllers or from the TMC.

4.2.1.1 Communications workflow

In this application, the communications workflow is described as follows:

- RSUs are enabled to collect traffic measurements of vehicle counts, occupancies, and speeds from loop detectors installed inside the speed harmonization zone, either directly from local controllers or from the TMC.

- In the downstream section of the speed harmonization zone, e.g., the section after the on-ramp merging gore in Figure 7, CAVs are sending CAM messages with their current speeds to the connected RSUs at a user-defined interval, e.g., 0.1 second.
- Meanwhile, RSUs are collecting CAV speeds from the received CAM messages. At a user-defined interval, e.g., 10 seconds, they will use the collected CAV speeds as well as traffic measurements from the detectors as inputs into the selected speed harmonization algorithm to generate new speed limits.
- At a user-defined interval, e.g., 0.1 second, the RSUs will broadcast DENM messages with the most up-to-date recommended speed limits to the CAVs in the upstream section of the speed harmonization zone, e.g., the section before the on-ramp merging gore in Figure 7.
- For the CAVs in the upstream section of the speed harmonization zone, they will receive the DENM messages and parse the information inside. Once they get a new recommended speed limit, they will apply it as the desired travelling speed. Whether they can successfully update their speeds with the speed limit depends on whether the surrounding environment allows them to do so. Once they manage to update their speeds, they will keep the recommended speed limits for a user-defined interval, e.g., 1 second, unless other triggers, e.g., emergency takeover, are activated.
- In addition, a variable called "Time-To-Live" (TTL) is included in the DENM messages, which is used to allow the number of "hops" that a DENM message can be propagated upstream. If TTL is greater than 1, a CAV which receives a DENM message will subtract the TTL by 1 and then broadcast the message to other CAVs within its communications range.

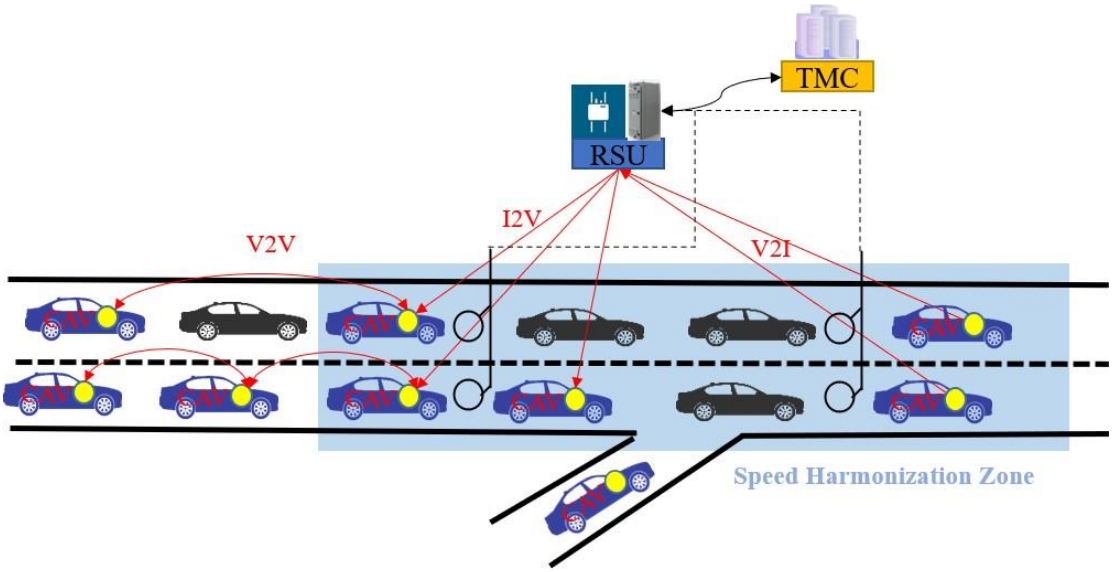

Figure 7. System architecture of freeway speed harmonization with CAVs.

The CAM messages sent from CAVs to RSUs contain the following attributes:

- Current road link ID;
- Current vehicle speed;
- Vehicle type.

For the DENM messages sent from RSUs to CAVs or from CAVs to CAVs, it contains the following attributes:

- Recommended speed limit;
- Road link IDs which the recommended speed limit is applied to;
- TTL.

4.2.1.2 Selected algorithms

In our current deployment, we have implemented the following speed harmonization algorithms: (i) a rule-based speed harmonization algorithm in (Talebpour et al., 2013); (ii) a variable speed limit (VSL) and advisory (VSA) algorithm in (Lu et al., 2015; Hale et al., 2016); and (iii) a cooperative variable speed limit system (C-VSLS) in (Grumert et al., 2015).

4.2.1.2.1 A rule-based speed harmonization algorithm

The rule-based speed harmonization algorithm is the one proposed in (Talebpour et al., 2013) with some minor revisions. Basically, the logit can be summarized below:

- A high speed limit will be recommended when both flow and density are low or when both flow and speed are high.
- A low speed limit will be recommended when traffic is congested with low speeds.
- Medium speed limits will be recommended when traffic is in the transition regime, which is between the free-flow and congested regimes.

The decision tree revised from the one in (Talebpour et al., 2013) is illustrated in Figure 8.

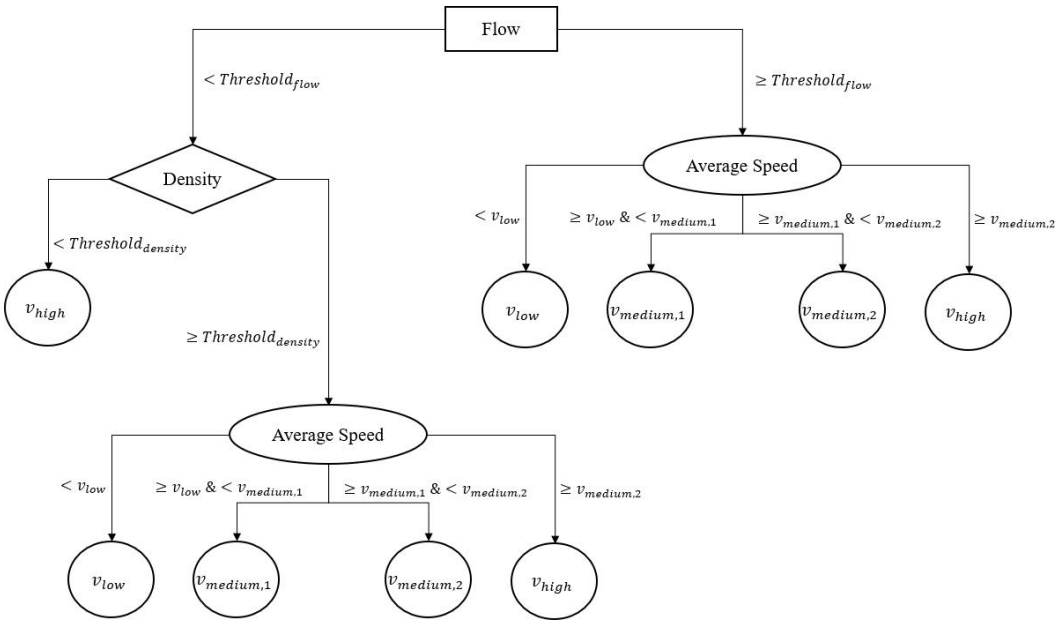

Figure 8: Decision tree of the rule-based speed harmonization algorithm.

4.2.1.2.2 A variable speed limit (VSL) and advisory (VSA) algorithm

The VSL-VSA algorithm implemented in our framework is the one proposed in (Lu et al., 2015; Hale et al., 2016). The proposed algorithm aims to delay traffic breakdown and improve throughputs for heavy traffic through two different operations: (i) in the upstream of a bottleneck, recommend lower speed limits to reduce the ingress flow, but (ii) at the bottleneck location, recommend higher speed limits to increase the egress flow. Therefore, at a bottleneck location mm, the recommended speed limit is calculated as:

$$\begin{gathered} bb_{ss}(tt) = \alpha\alpha_{ss}\, \bar{u}_{s}(tt) \\ \alpha\alpha_{ss} \in [1.1, 1.5]; \text{ default value: } \alpha\alpha_{ss} = 1.3 \end{gathered} \tag{39}$$

where $u_s(tt)$ is the measured speed at freeway section mm.

At the immediate upstream, the recommended speed limit is calculated as:

$$\begin{gathered} bb_{ss+1}(tt) = \begin{cases} vv_{rrrrrrr} & iii\ \bar{O}_{ss}(tt) \le OOcccc_{ssss} \\ \beta\beta_{ss}\, u_{s}(tt) & iiii\ \bar{O}_{ss}(tt) > OOcccc_{ssss} \end{cases} \\ \beta\beta_{ss} \in [0.7, 0.9]; \text{ default value: } \beta\beta_{ss} = 0.8 \end{gathered} \tag{40}$$

where O_{cc} is the measured occupancy at the bottleneck location mm, and $OOcccc_{ssss}$ is the occupancy threshold at which traffic is close to the capacity flow.

4.2.1.2.3 A cooperative variable speed limit system (C-VSLS)

The cooperative variable speed limit system (C-VSLS) implemented in our framework is the one proposed in (Grumert et al., 2015) with some minor revisions to incorporate I2V/V2I communications. This algorithm was an extension to the existing variable speed limit system (VSLS) (van Toorenburg and de Kok, 1999) and aimed to harmonize traffic flow and reduce vehicle emissions. Through I2V/V2I communications, information about the variable speed limit will be received at an earlier point in time in the C-VSLS. For each CAV, its future speed will be determined by the speed limit recommended by the VSLS as well as its current speed and position.

In the VSLS, the mean speed $vv_{dd,ssrraaii}$ at detector dd is calculated as:

$$\frac{1}{vv_{dd,ssrraaii}(tt+1)} = \alpha\alpha \frac{1}{vv_{dd,ssrraassmmrrrrdd}} + (1 - \alpha\alpha)\frac{1}{vv_{dd,ssrraaii}(tt)} \tag{41}$$

where $vv_{dd,ssrraassmmrrrrdd}$ is the measured speed at detector dd, and $\alpha\alpha$ is a smoothing parameter between 0 and 1. If the mean speed $vv_{dd,ssrraaii}$ goes below $vv_{ssh\ rrrrssh\ ddyydd,yydds\ s}$, e.g., 45km/h, the closest variable speed limit sign near the detection point is set to be $vv_{WWW,yydds\ s}$, e.g., 60 km/h, while the upstream two variable speed limit signs are set to $vv_{WWW,ssrrddiimms\ s}$, e.g., 80km/h, and $vv_{WWW,h\ iitth}$, e.g., 100 km/h, respectively. In contrast, if the mean speed $vv_{dd,ssrraaii}$ increases back to $vv_{ssh\ rrrrssh\ ddyydd,h\ iitth}$, e.g., 55km/h, all related variable speed limit signs are updated to $vv_{rrrrrrr}$, e.g., 120km/h.

Instead of using variable speed limit signs, we have implemented a different approach for CAVs by dividing the speed harmonization zone into multiple sub-zones. As shown in Figure 9, the speed harmonization zone is divided into three sub-zones according to a user-defined distance threshold $dd_{ssh\ rrrrssh\ ddyydd}$. A CAV is in Zone 1 when its distance to the downstream reference detectors dd is smaller than $dd_{ssh\ rrrrssh\ ddyydd}$, and the speed limit $vv_{WWW,yydds\ s}$ is applied. When the distance dd satisfies the condition, $dd_{ssh\ rrrrssh\ ddyydd} \le dd < 2 * dd_{ssh\ rrrrssh\ ddyydd}$, the CAV

is in Zone 2 and the speed limit $vv_{WWW,ssrrddiimmss}$ is applied. When the distance dd satisfies the condition, $dd \geq 2 * dd_{sshrrrrsshddyydd}$, the CAV is in Zone 3 and the speed limit $vv_{VVVVV,hiitth}$ is applied.

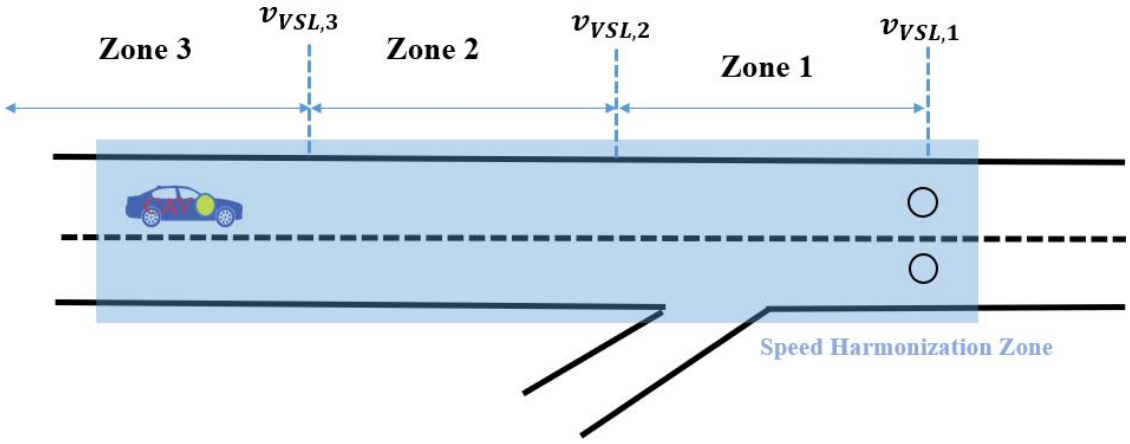

Figure 9. Settings of speed harmonization zones in the C-VSL algorithm.

Then the recommended individual speed limit $vv_{ii,VVVVV}$ for CAV ii is calculated as follows:

$$\begin{aligned} aa_{ii} &= \frac{vv_{WWW,jj}^2 - vv_{ii}^2}{2dd_{iijj}} \\ vv_{WWW,ii} &= vv_{ii} + aa_{ii}TT \\ vv_{WWW,ii} &= \max\{vv_{WWW,jj}, \min\{VV_{ssaamm}, vv_{WWW,ii}\}\} \end{aligned} \tag{42}$$

where

$vv_{VVVVV,jj}$: recommended speed limit for the speed harmonization Zone $jj \in \{1,2,3\}$,

dd_{iijj} : distance to the downstream end of Zone jj when CAV ii receives a recommended speed limit,

VV_{ssaamm}: maximum speed on the road,

TT: time interval to update the speed limits,

vv_{ii} : CAV's current speed.

Once $vv_{VVVVV,ii}$ is calculated, CAV ii will use it as the desired speed to adjust its current speed.

4.2.3 Freeway-Only subnetwork

4.2.3.1 Network settings and scenario design

As shown in Figure 10, the selected Freeway-Only subnetwork for the application of speed harmonization with CAVs is a 5-mile-long freeway portion at the I-605/I-210 interchange. It consists of 274 sections/links and 182 nodes, with a total of 102 lane miles. Inside the network, there are three RSUs installed at the following weaving sections:

- I-210 WB @ Irwindale Ave
- I-210 WB @ Vernon Ave
- I-210 EB @ Azusa Ave

These three locations are selected because traffic is generally congested in the AM peak period, especially in the WB direction.

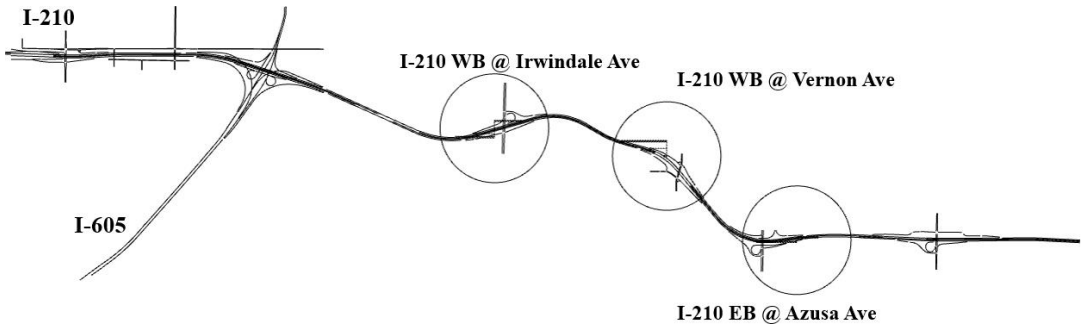

Figure 10: Freeway-Only subnetwork for the application of speed harmonization with CAVs.

In Figure 11, we show the settings of the speed harmonization zone at the weaving section at I-210 WB @ Irwindale Ave. The circle stands for the communications range of the RSU, which is set to be 1640 feet (500 meters) in this network. For simplicity, we consider an ideal case with zero latency and zero package loss rate for the RSU to collect/distribute messages from/to CAVs within its communications range.

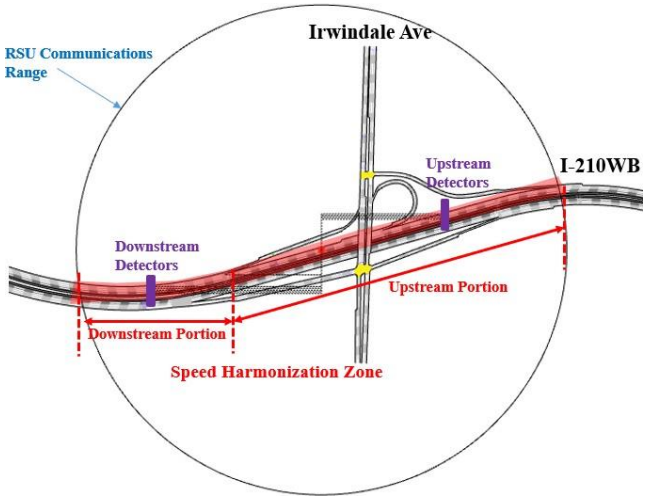

Figure 11. Settings of the speed harmonization zone at the waving section at I-210 WB @ Irwindale Ave.

In our system design, we divide the speed harmonization zone into two different portions according to the merging gore location at the weaving section: (i) a downstream portion which is after the merging gore, and (ii) an upstream portion which is before the merging gore. In the downstream portion, CAVs will send CAM messages with their speeds to the RSU, and the RSU will use this information as one of the inputs into the speed harmonization algorithm. In the upstream portion, the RSU will broadcast DENM messages with a recommended speed limit, and the CAVs will use it as the desired speed to adjust their current speeds. In addition, downstream and upstream detectors on the freeway mainline are connected to the RSU to provide 1-minute vehicle count, occupancy, and speed data as inputs into the speed harmonization algorithm.

The selected simulation period is 1 hour, from 7AM to 8AM. During this period, traffic in the Freeway-Only subnetwork is congested, especially in the WB direction of I-210. To further evaluate the performance of the speed harmonization algorithms, we consider additional scenarios with heavier traffic congestion by increasing the original traffic demand level to 110%.

For each RSU, the interval to send DENM messages is 0.1s, and the TTL is 1. The interval to collect CAM messages from CAVs and update the speed limit is 10s. For each CAV, it will check whether it connects to an RSU at the frequency of every 1s. Once connected, it sends out CAM messages with speed information every 0.1s and updates its speed limit every 1s. After the CAV disconnects from an RSU, it will stop sending CAM messages and keep its speed limit for an additional interval of 1s.

In the downstream portion of the speed harmonization zone, we use the following weighted function to fuse the speed data from CAVs with the speed measurement from the detectors:

$$vv_{ddddssiissssrrrraass} = ee * vv_{CCCCVV,aavvtt} + (1 - ee) * vv_{dd} \quad (43)$$

where

$vv_{ddddssiissssrrrraass}$: fused speed;

ee: coefficient which ranges between 0 and 1;

$vv_{CCCCVV,aavvtt}$: average speed of the CAVs;

vv_{dd}: measured speed from the detectors.

However, in the upstream portion of the speed harmonization zone, if speed information is needed in the speed harmonization algorithm, only the measured speeds from the detectors will be used.

Table 3: Parameter settings of the three speed harmonization algorithms in the Freeway-Only subnetwork.

Speed Harmonization Algorithm	Parameter	Value
Rule-Based	$TTTTTTTTTTTTdd_{jjmmff}$	1500 veh/hr/ln
	$TTTTTTTTTTTTdd_{aaaaaaaaaa}$	15 veh/km/ln
	vv_{mmff}	54 km/hr
	$vv_{mmTTddddmm,11}$	72 km/hr
	$vv_{mmTTddddmm,22}$	90 km/hr
	vv_{mmaaxx}	108 km/hr
VSL-VSA	$\alpha\alpha_{mm}$	1.4
	$\beta\beta_{mm}$	0.9
	$CCCCCC_{mmff}$	25%
C-VSLS	$\alpha\alpha$	0.5
	$vv_{aaaaaaaaaa,mmff}$	45 km/hr
	$vv_{aaaaaaaaaa,mmaaxx}$	55 km/hr
	$vv_{WWW,mmff}$	60 km/hr
	$vv_{WWW,mmTTddddmm}$	80 km/hr
	$vv_{WWW,mmaaxx}$	100 km/hr
	vv_{ffffrr}	120 km/hr
	$dd_{aaaaaaaaaa}$	300 meters

4.2.3.2 Results

For the simulations in the Freeway-Only subnetwork, we have activated the above three speed harmonization algorithms with the parameter settings listed in Table 3. In addition, the coefficient ee is the same across all three speed harmonization algorithms, which is set to be 0.2.

We have conducted various simulation scenarios under different congestion levels and penetration rates of CAVs. For each scenario, e.g., 100% demand level and 20% CAVs, the random seed in each simulation replication is the same across the baseline model and the three selected speed harmonization algorithms. Here, the baseline model is the one without speed harmonization, but the ACC/CACC module is activated.

Table 4: Vehicle delays under different speed harmonization algorithms in the Freeway-Only subnetwork.

Demand Level	CAV %	Delay (sec/km)						
		Baseline	Rule-Based	Diff (%)	C-VSLS	Diff (%)	VSL-VSA	Diff (%)
100%	0%	40.04						
	20%	32.22	32.68	-1.43	***32.05***	***0.53***	33.15	-2.89
	40%	26.91	***26.66***	***0.93***	***26.46***	***1.67***	***26.67***	***0.89***
	60%	22.62	22.7	-0.35	***22.48***	***0.62***	***22.43***	***0.84***
	80%	22.67	***22.18***	***2.16***	22.84	-0.75	***22.02***	***2.87***
	100%	24.85	***24.8***	***0.20***	***24.74***	***0.44***	***24.25***	***2.41***
110%	0%	51.96						
	20%	50.35	50.75	-0.79	***50.12***	***0.46***	51.66	-3.07
	40%	43.68	***43.24***	***1.01***	43.79	-0.25	44.39	-1.63
	60%	35.94	36.01	-0.19	36.65	-1.98	***35.91***	***0.08***
	80%	31.91	***31.5***	***1.28***	32.06	-0.47	***30.08***	***5.73***
	100%	29.03	***28.69***	***1.17***	***28.85***	***0.62***	***27.69***	***4.62***

Note: in the above table, the "Green" means the delay was reduced while the "Red" means the delay was increased.

In Table 4, we provide vehicle delays under different speed harmonization algorithms in the Freeway-Only subnetwork. According to the results in the table, we find that none of the speed harmonization algorithms can beat the baseline model in all scenarios. Each speed harmonization algorithm can only perform well under certain traffic conditions and CAVs percentages.

- For the baseline model, significant delay reduction is achieved as the percentage of CAVs increases, which indicates that the ACC/CACC model is the major contributor to the delay reduction in the network. However, we do notice that when the demand level is 100% and the percentage of CAVs is greater than 60%, traffic delay slightly increases as the percentage of CAVs increases. This indicates two things. First, the Freeway-Only subnetwork reaches its best performance when the percentage of CAVs is about 60%. Second, the settings in the ACC/CACC model are more conservative than those in the default car-following model. Therefore, it is less "efficient" under normal free-flow traffic conditions.

- For the Rule-Based speed harmonization algorithm, it seems it only can perform well under high CAV percentages, e.g., at 80% or higher. However, even with this high percentage of CAVs, the delay improvement is small, which is between 1% and 2%. In addition, the results also show that the performance of the Rule-Based speed harmonization algorithm degrades as the percentage of CAVs reaches 100%.
- For the C-VSLS speed harmonization algorithm, results indicate that it only works well under relatively light traffic congestion and low CAV percentages, e.g., at 100% demand level with 40% CAVs. However, as shown in the table, its improvement on vehicle delay is small, which is below 2%.
- For the VSL-VSA speed harmonization algorithm, results show that it only works well with high percentages of CAVs, e.g., at 80% or higher. Overall, the improvement on vehicle delay is larger than 2% and is more obvious when traffic is more congested. For example, when the demand level is 110% and the percentage of CAVs is 80%, the improvement can reach 5.73%.

In summary, the results in Table 4 only represent the settings in the speed harmonization zones and the parameters in Table 3, which may not be optimal. To better access the performance of the speed harmonization algorithms, in the future we need to conduct thorough analysis to understand where, when, and how to activate speed harmonization with the consideration of the following factors:

- Road geometry: Different road geometries will require different settings in the speed harmonization zones as well as different parameters in the speed harmonization algorithms. For example, a freeway section near a freeway interchange will be different from a freeway section with multiple on-ramps and off-ramps.
- Existing detector placement and control settings: In field deployment, detector placement varies a lot among different weaving sections. Some weaving sections have both sets of upstream and downstream detectors, while other sections may only have one set of the detectors, either the upstream ones or the downstream ones. As a result, we need to choose the right speed harmonization algorithms that can fit into the detector placement at the study network. In addition, when ramp metering exists, the metering rate may also impact the performance of the speed harmonization algorithms.
- Traffic demand and OD patterns: As shown in Table 4, traffic demand is a key factor that will lead to different levels of congestion and therefore impact the performance of the speed harmonization algorithms. Besides that, sometimes even with the same traffic demand, different OD patterns will lead to significantly different levels of traffic congestion. For example, at a weaving section near a freeway interchange, a substantial number of lane-changing vehicles will negatively reduce the capacity in the downstream and create a traffic bottleneck with heavy congestion. However, this may not occur when the same traffic demand is applied to other weaving sections. Therefore, this difference in OD patterns, for sure, will impact the performance of the speed harmonization algorithms.
- Settings of speed harmonization zones: The settings of speed harmonization zones are closely related to the road geometry as well as the upstream and downstream detector locations. Different coverage of the upstream and downstream portions will impact the collection of speed information and the broadcasting of speed limits, which will lead to different performance in the speed harmonization algorithms.

- Settings in the RSU: Besides the communications range of the RSU, other parameters such as latency and package loss rate may also impact the performance of the speed harmonization algorithms.
- Settings in the V2I/I2V communications: In particular, how frequent an RSU collects speed information and broadcasts speed limits would impact CAVs' decisions and therefore the performance of the speed harmonization algorithms.
- Parameter settings in the speed harmonization algorithms: Each speed harmonization algorithm has its own set of parameters to adjust. These parameters may need to be updated if other factors like road geometry, speed harmonization zones, and RSUs are changed.

4.3 Application: Route guidance with CAVs for traffic incident management

In this subsection, we demonstrate how to apply the integrated microsimulation platform to the application of route guidance with CAVs for traffic incident management. More details are provided below.

4.3.1 System architecture

In Figure 12, we show the system architecture of route guidance with CAVs for traffic incident management. In this application, we are interested in how we can detour CAVs to designated arterial routes to mitigate congestion caused by freeway incidents.

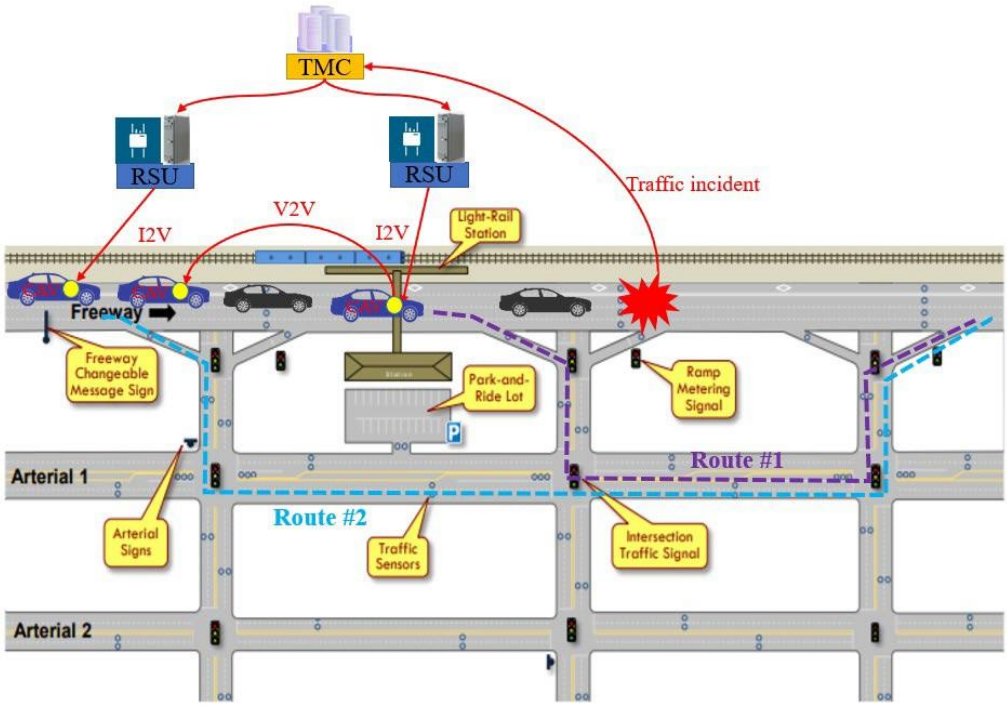

Figure 12. System architecture of route guidance with CAVs for traffic incident management.

4.3.1.1 Workflows

This architecture consists of two separated workflows, i.e., incident management workflow and communications workflow, the details of which are provided below.

4.3.1.1.1 Incident management workflow

Consider a traffic incident occurs at a certain location on a freeway at time tt. The current design of the incident management workflow is described as below:

- The workflow will kick off when this incident is reported to the TMC with a delay time Δtt_1, i.e., at time $tt + \Delta tt_1$.
- After a decision period Δtt_2, i.e., at time $tt + \Delta tt_1 + \Delta tt_2$, the TMC generates a response plan that includes detour routes and new signal timing plans at the intersections and ramp meters involved in the detour routes. CMSs are currently not included in the workflow but will be considered in future development. The TMC will send out control commands to activate the new timing plans at the involved intersections and ramp meters along the detour routes.
- Suppose it takes Δtt_3 to clear the incident since it is occurred. Then at time $tt + \Delta tt_3$, a new update is sent to the TMC to indicate the incident is cleared.
- Then the TMC will respond and generate a termination plan with all involved intersections and ramp meters back to Time-Of-Day (TOD) control. A delay time of Δtt_4 will be used to make sure the majority of detoured vehicles have enough time to get back to the freeway from the detour routes. That means at time $tt + \Delta tt_3 + \Delta tt_4$, the TMC will send out control commands to the involved intersections and ramps to change back to TOD control.

Here we have $\Delta tt_1 + \Delta tt_2 < \Delta tt_3$. Note that the current incident management workflow is a simplified version for demonstration purposes as it considers no updates, e.g., changes in number of lanes blocked or in detour routes, during the incident period. In the future, we will develop a more comprehensive incident management workflow that considers multiple incident updates or even multiple incidents on the freeway.

4.3.1.1.2 Communications workflow

In the design of the communications workflow, we only consider the communications between RSUs/TMC and CAVs. Also, the messages sent from RSUs/TMC to CAVs are DENM messages which contain the following major attributes:

- Incident link ID, which tells where the incident is located;
- Recommended detour route ID;
- List of link IDs involved in the recommended detour route;
- Current number of detoured CAVs within the communications range of the RSU;
- Allowed number of detoured CAVs within the communications range of the RSU;
- Number of lanes on the freeway mainline.

The first three attributes contain necessary information regarding the incident and the detour routes, while the last three are extended attributes designed for CAVs to determine the probability to take the detour route or not.

In addition, in our current implementation, once a CAV updates its path with the recommended detour route, it will start to send confirmation messages (via CAM messages) with the detour route ID to its connected RSU(s) at a user-defined interval, e.g., 1s. RSUs will receive these CAM messages and update the corresponding number of detoured CAVs in each route within their communications ranges. Through controlling the number of detoured CAVs inside the coverage of the RSUs, we can avoid unexpected congestion along the detour routes.

The detailed procedures of the communications workflow are described below:

- Once the TMC generates a response plan, it will immediately share the recommended detour routes with the RSUs in the upstream of the incident location.
- If the number of detoured CAVs does not reach the allowed number within its communications range, the RSUs will then broadcast DENM messages with detour route information to the CAVs at a user-defined interval, e.g., 1s.
- For a CAV receiving the DENM messages, it will parse the information inside and determine whether its route is impacted or not. If yes, it will further determine whether to update its route with the recommended one according to the route choice algorithms.
- In addition, V2V communications is enabled as an optional choice. A variable called "Time-To-Live" (TTL) is used to calculate the allowable number of "hops" that a DENM message can be propagated upstream. If TTL is greater than 1, a CAV will subtract the TTL by 1 and broadcast the DENM message to other CAVs within its communications range.
- For CAVs that have applied the recommended detour route, they will send CAM messages with the detour route id to their connected RSUs at a user-defined interval, e.g., 1s. For RSUs, they will receive and parse these CAM messages and update the current number of detoured CAVs for the corresponding detour route within their communications ranges. Once a CAV disconnects from the RSUs, they will stop sending these CAM messages.

4.3.1.2 Selected route choice algorithm

Once a CAV is informed via the DENM messages that its current route is impacted by a downstream traffic incident, it has the option to determine whether to take the recommended detour route or not. In (Samimi Abianeh et al., 2020) drivers of connected vehicles are informed about the traffic congestion and can determine whether to take the new route or not. To model driver's willingness to change routes, the following normal distribution function is used:

$$PP_{mmddnnssrr} = \alpha\alpha \times \frac{\exp\left(-\frac{nn^2}{2 \times \sigma\sigma^2}\right)}{\sqrt{2\pi\pi} \times \sigma\sigma} \quad (44)$$

where
$\alpha\alpha$: a constant to adjust the probability function;
nn: number of rerouted vehicles on each link;
$\sigma\sigma$: standard deviation of the normal distribution.

Note that the above equation implies the following two modeling considerations:

- The variable $\alpha\alpha$ can be used to simulate the case that vehicles on inner lanes will have a lower probability to reroute.
- The variable nn implicitly models the case that a higher number of rerouted vehicles will result in a lower probability to choose the alternative route.

Besides the above two modeling considerations, we further consider the following cases:

- A global compliance rate (between 0% and 100%) is chosen to consider not all vehicles are willing to detour.
- Compared with passenger cars, trucks have a lower probability to detour.

Therefore, in our current modeling framework, we propose the following algorithm to mimic driver's decision on whether to take the detour routes or not.

$$
\begin{aligned}
PP_{mmddmmssrr} &= II_{yyaaiirr} \times II_{ssmmddkk} \times II_{ddrrssddmmrr} \times PP_0, \\
II_{yyaaiirr} &= 1 - \xi\xi \frac{(ll-1)}{LL}, \\
II_{ssmmddkk} &= \begin{cases} 1-\beta\beta & iiii\ iitt\ iiss\ aa\ ttrrkk, \\ 1 & oottkk\ mmeeiissmm, \end{cases} \\
II_{ddrrssddmmrr} &= 1 - \frac{mm_{ddrrssddmmrr}}{NN_{ddrrssddmmrr}}
\end{aligned}
\tag{45}
$$

where

PP_0: global compliance rate for all vehicles, which takes values in $[0\%, 100\%]$;

ll: current lane ID of the CAV, which is numbered from the rightmost (i.e., 1) to the leftmost (i.e., L);

LL: number of lanes on the road link where the CAV is located at;

$\xi\xi$: smoothing factor for lane impacts, which takes values in $[0, 1]$;

$\beta\beta$: reduction factor for trucks, which takes values in $[0, 1]$;

$mm_{ddrrssddmmrr}$: number of detoured CAVs in the communications range of an RSU;

$NN_{ddrrssddmmrr}$: maximum number of CAVs in the communications range of an RSU that are allowed to detour.

4.3.2 Freeway-and-Arterial Combined subnetwork

4.3.2.1 Network settings and scenario design

As shown in Figure 13, the selected Freeway-and-Arterial Combined subnetwork mainly consists of: (i) a freeway section starting from SR-134@Orange Grove Blvd to I-210@Rosemead Blvd; (ii) five major paralleled arterial streets, including Walnut St, Corson St, Maple St, Villa St, and Foothill Blvd. There is an RSU installed at the weaving section at I-210E@Lake Ave with a communications range of 2462ft (approximately 750 meters), which is denoted as the black circle in Figure 13. Note that the communications range in this network is of a reasonable setting and is longer than the one in the Freeway-Only subnetwork just for demonstration purposes and to cover enough area to detour traffic.

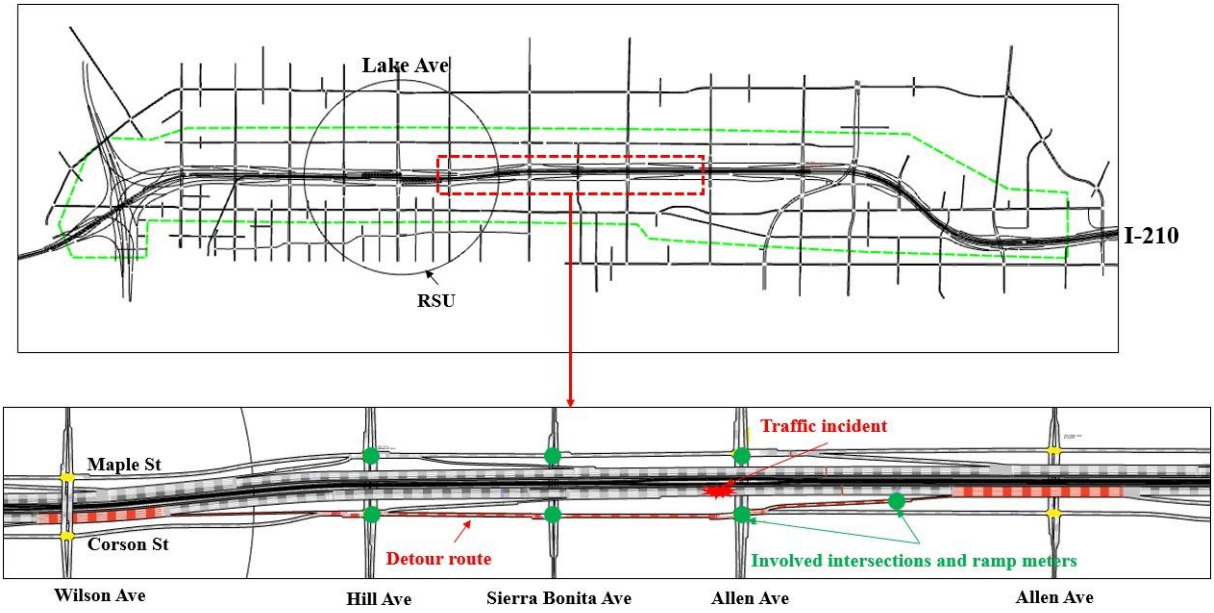

Figure 13: Freeway-and-Arterial Combined subnetwork for the application of route guidance with CAVs for traffic incident management.

During the AM peak, traffic is more congested in the WB direction than in the EB direction. However, it is oppositive during the PM peak: traffic is more congested in the EB direction than in the WB direction. Therefore, as shown in Figure 13, in our scenario design, we consider two traffic accidents at the same location, i.e., at I-210EB @ Allen Ave, but with different levels of severity:

- A major traffic accident in the AM peak between 7AM and 8AM;
- A minor traffic accident in the PM peak between 4PM and 5PM.

Note that the AM and PM peak periods are longer than 1 hour. But due to long simulation times when the V2X module is activated in this study network, we only conduct simulations for 1 hour for demonstration purposes.

The settings of the major traffic accident in the AM peak are described below:

- At 7:05 AM, a car accident occurs at I-210EB @ Allen Ave and blocks three left lanes (i.e., Lane 1 to Lane 3) for about 20 minutes.
- At 7:25AM, two lanes (i.e., Lane 2 and Lane 3) are opened and only the leftmost lane (i.e., Lane 1) is still blocked for another10 minutes, till 7:35AM.
- At 7:35AM, the accident is cleared and no lane is blocked.

The settings of the minor traffic accident in the PM peak are described below:

- At 4:05PM, a car accident occurs at I-210EB @ Allen Ave and blocks two left lanes (i.e., Lane 1 and Lane 2) for about 15 minutes.
- At 4:20PM, one lane (i.e., Lane 2) is opened and only the leftmost lane (i.e., Lane 1) is still blocked for another 15 minutes, till 4:35PM.

- At 4:35PM, the accident is cleared and no lane is blocked.

The incident management workflow is described below:

- We consider there is a delay of 2 minutes when the TMC receives the accident report and generates a response plan, e.g., a new detour route and new signal control plans for intersections and ramp meters involved in the detour route. That means, the TMC will kick off the response plan at 7:07AM for the major traffic accident in the AM peak and at 4:07PM for the minor traffic accident in the PM peak.
- We also consider there is a delay of 2 minutes to terminate the response plan after the accident is cleared. That means, the TMC will terminate the response plan at 7:37AM for the major traffic accident in the AM peak and at 4:37PM for the minor traffic accident in the PM peak.
- After the response plan is terminated, the signal control plans along the detour route will switch back to their normal TOD control plans.

As shown in Figure 13, the detour route used in this scenario is a short one, which takes the following sequence of links: I-210EB @ Wilson Ave → Off-ramp → Corson St @ Hill Ave → Corson St @ Sierra Bonita Ave → Corson St @ Allen Ave → On-ramp → I-210EB @ Craig Ave. Along this detour route, three signalized intersections are involved: Corson St @ Hill Ave, Corson St @Sierra Bonita Ave, and Corson St @ Allen Ave. Therefore, new signal timing plans are used to accommodate the eastbound detoured traffic. For simplicity, despite the very different traffic demand patterns in the AM and PM peaks, we apply the same detour route and the same new timing plans for the two aforementioned traffic accidents. An example of the new timing plan at the intersection of Corson St @ Hill Ave is provided in Figure 14, which shows longer green times are provided to the EB through traffic (Phase 5).

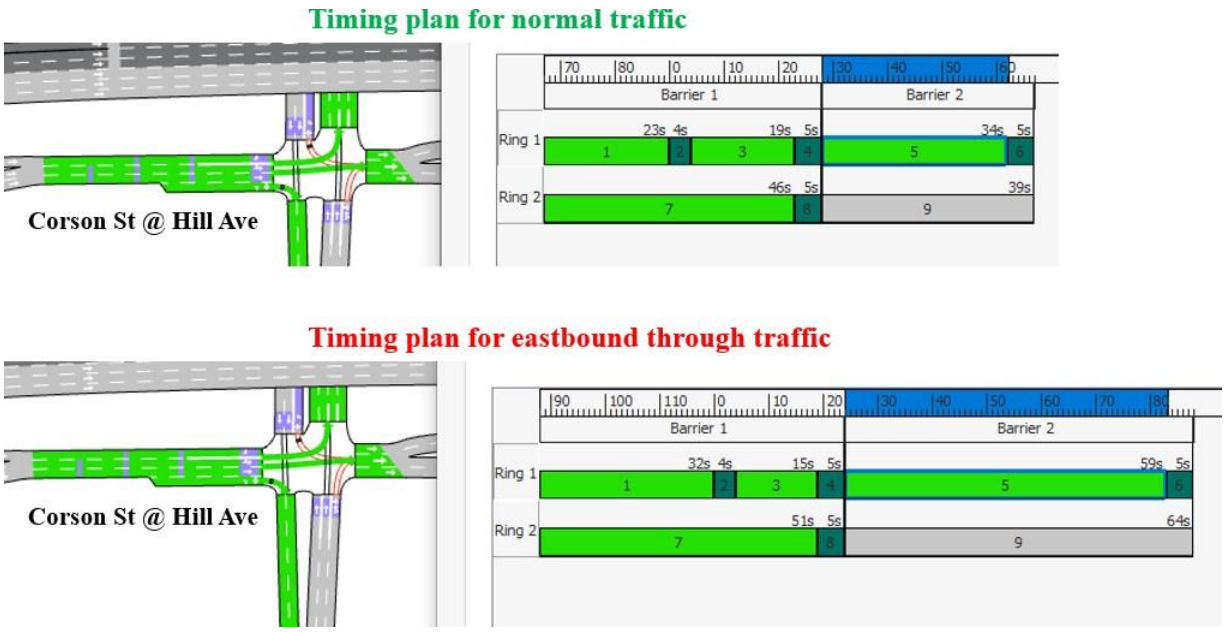

Figure 14: New timing plan for the detoured traffic at the intersection of Corson St @ Hill Ave.

Considering potential impacts on the neighboring intersections, especially those connected to the I-210WB, new timing plans to accommodate the westbound through traffic are used. Therefore, new timing plans are used for the following three intersections: Maple St @ Hill Ave, Maple St @Sierra Bonita Ave, and Maple St @ Allen Ave. An example of the new timing plan at the intersection of Maple St @ Hill Ave is provided in Figure 15, which shows longer green times are provided to the WB through traffic (Phase 5).

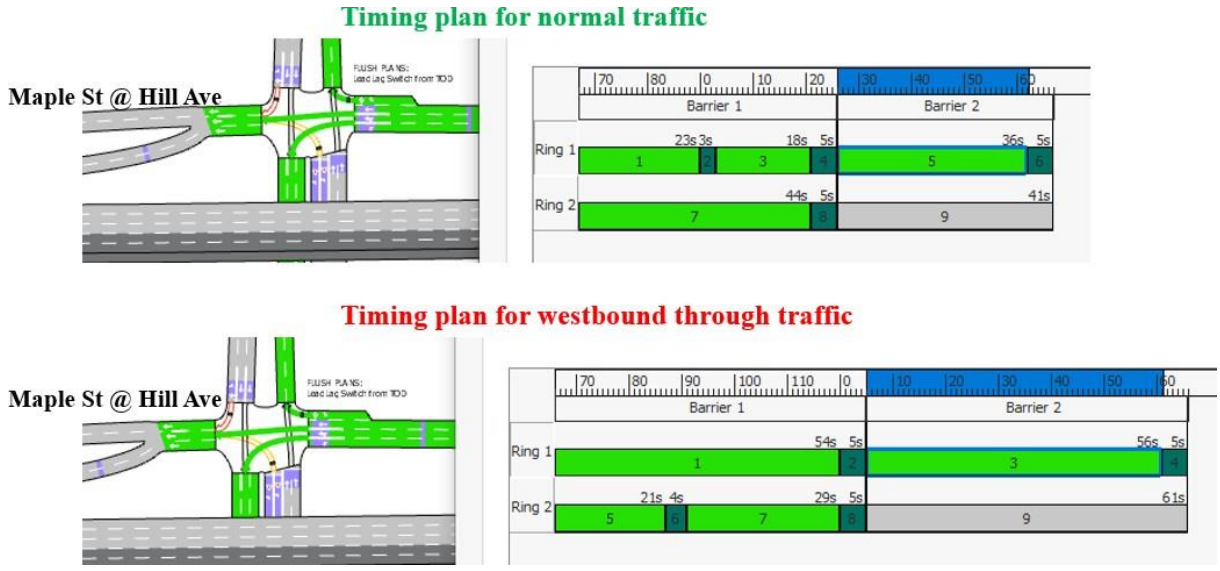

Figure 15: New timing plan for the westbound through traffic at the intersection of Maple St @ Hill Ave.

Regarding the ramp meter at I-210EB@Craig Ave, the metering rate is set to be 1200 veh/hr/ln to accommodate the detoured traffic, which is constant during the whole simulation period.

For the aforementioned major and minor traffic accidents, the communications workflow is described below:

- Once the TMC generates a response plan, we consider the RSU in the upstream of the accident location will immediately receive the detour route information and start to broadcast it to the CAVs within its communications range. That means, the RSU will start to broadcast DENM messages with detour route information at 7:07AM for the major traffic incident in the AM peak and at 4:07PM for the minor traffic incident in the PM peak.
- Similarly, when the TMC terminates the response plan, the RSU will stop broadcasting DENM messages immediately. That means the RSU will stop broadcasting DENM messages at 7:37AM for the major traffic incident in the AM peak and at 4:37PM for the minor traffic incident in the PM peak.
- When the response plan is still active, the RSU will broadcast the DENM messages to the CAVs within its communications range at a user-defined interval and meanwhile keep track of the number of CAVs which have decided to take the detour route.
- For CAVs first entering the communications range of the RSU, they will receive the detour route information from the RSU via the DENM messages. They will decide whether to take the detour route or not based on two conditions: (i) the number of detoured CAVs does not reach the maximum

number; and (ii) the route choice algorithm allows them to take the detour route. Once a CAV has decided to take the detour route, it will send CAM messages to its connected RSUs to confirm the detour route it takes. If the CAV have decided not to take the detour route, it will ignore the following DENM messages unless a new detour route is proposed. Once the CAV disconnects from the RSUs, it will stop sending the CAM messages.

4.3.2.2 Results

In the Freeway-and-Arterial Combined subnetwork, we have activated the selected route choice algorithm with parameter settings listed in Table 5. For the RSU, the time interval to broadcast DENM messages is 0.1s, the time interval to check the number of detoured CAVs within its communications range is 1s, the time interval to check active detour routes is 60s, and the TTL is 1. For CAVs, the time interval to send CAM messages is 0.1s.

Table 5: Parameter settings in the Freeway-and-Arterial Combined subnetwork.

Parameter	Value
Global compliance rate for all vehicles: PP_{00}	100%
Smoothing factor for lane impacts: $\xi\xi$	0.5
Reduction factor for trucks: $\beta\beta$	25%
Maximum number of CAVs allowed to detour: NN_{max}	30 vehicles

Due to long simulation times when the V2X module is activated in the Freeway-and-Arterial Combined subnetwork, we only conducted simulations for two different percentages of CAVs, i.e., 30% and 50%, for demonstration purposes. In Figure 16, we provide the speed heatmaps with and without route guidance for the major traffic accident in the AM peak period with 30% CAVs. As shown in the figure, the case without route guidance has a long vehicle queue in the EB direction at the end of simulation, i.e., at 8AM, while traffic is relatively uncongested in the case with route guidance. Similar patterns can be found in the speed heatmaps with and without route guidance for the minor traffic accident in the PM peak period with 50% CAVs, which is shown in Figure 17. Note that with 50% CAVs, traffic in the EB direction is not very congested in the PM peak period, and therefore, it is as expected that the minor traffic accident will not generate a long residual queue at the end of simulation, i.e., at 5PM, for the case without route guidance.

In Table 6, we summarize the delay and speed improvement with route guidance for the AM and PM traffic accidents. According to the simulation results, we do find that better improvement can be achieved with higher percentages of CAVs. For the case of 50% CAVs, the network-level delay reduction is over 3%, while the network-level speed improvement is over 1.5%, for both the AM and PM traffic accidents. Considering the size of the network and the fact that only a short detour route is used, this delay and speed improvement is promising. However, we also notice that the case with 30% CAVs in the PM traffic accident does have lower delay reduction and speed improvement. That is because in the PM peak, traffic in the EB is still congested with 30% CAVs. Even with a small traffic accident, a long vehicle queue will form quickly on the mainline freeway. It is very possible that the vehicle queue is so long that it prohibits the detoured CAVs to exit the freeway freely. As a result, it significantly degrades the performance of route guidance with CAVs.

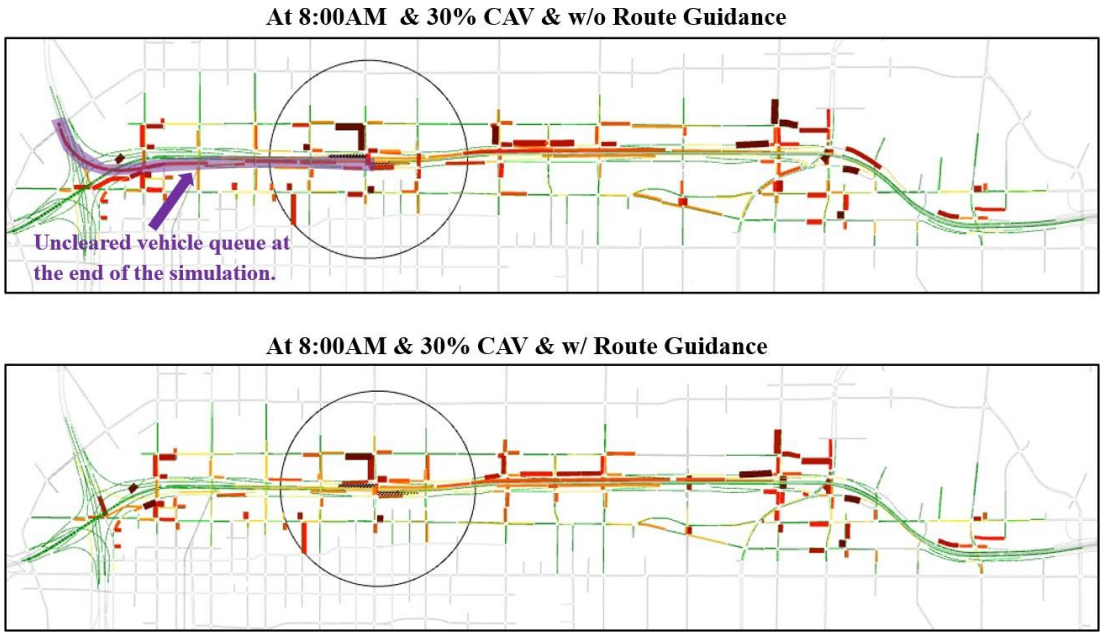

Figure 16. Speed heatmaps w/ & w/o route guidance for the AM major traffic accident with 30% CAVs.

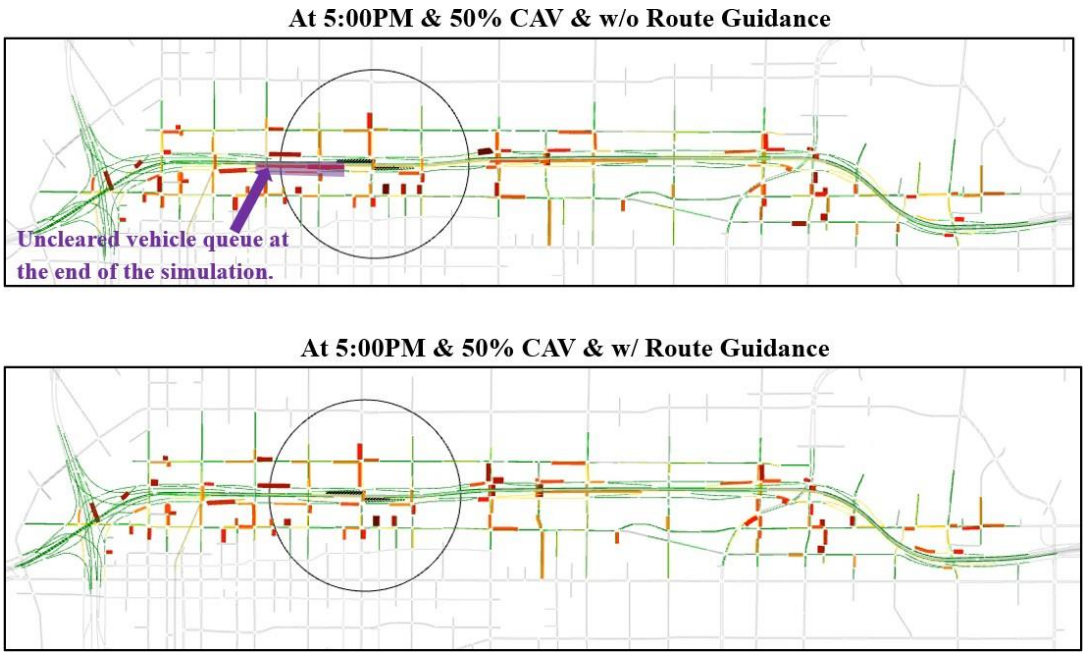

Figure 17. Speed heatmaps w/ & w/o route guidance for the PM minor traffic accident with 50% CAVs.

Table 6. Delay and speed improvement with route guidance for the AM and PM traffic accidents.

Major traffic accident in the AM peak (7AM – 8AM)						
CAV (%)	**Delay** w/o Route Guidance (sec/km)	**Delay** w/ Route Guidance (sec/km)	**Improvement** (%)	**Harmonic Speed** w/o Route Guidance (km/hr)	**Harmonic Speed** w/ Route Guidance (km/hr)	**Improvement** (%)
30%	73.81	71.33	3.36%	24.67	25.12	1.82%
50%	66.97	64.66	3.45%	25.91	26.36	1.74%
Minor traffic accident in the PM peak (4PM – 5PM)						
CAV (%)	**Delay** w/o Route Guidance (sec/km)	**Delay** w/ Route Guidance (sec/km)	**Improvement** (%)	**Harmonic Speed** w/o Route Guidance (km/hr)	**Harmonic Speed** w/ Route Guidance (km/hr)	**Improvement** (%)
30%	74.01	73.24	1.04%	24.31	24.45	0.58%
50%	64.13	62.16	3.07%	26.09	26.49	1.53%

In summary, the above examples demonstrate the potential of integrating CAVs into existing ICM systems to help mitigate traffic congestion. Especially, it reveals the benefits of sharing detour route information with road users, which is not limited to CAVs but should include those who can receive real-time traffic information, e.g., navigation app users. In the future, we will extend the current framework to study policies and schemes of information sharing with navigation app users so as to manage traffic incidents more efficiently and effectively. Also, we will improve the current framework with more complete features to handle multiple traffic incidents and detour routes.

4.4 Application: Traffic light optimal speed advisory with CAVs

In this subsection, we demonstrate how to apply the integrated microsimulation platform to the application of traffic light optimal speed advisory with CAVs. More details are provided below.

4.4.1 System architecture

In Figure 18, we show the system architecture of the application of traffic light optimal speed advisory with CAVs. In this application, I2V communications is enabled. Therefore, an RSU can get real-time signal information from the connected intersection signal controller and broadcast this information via SPaT and MAP messages to the CAVs within its communications range. CAVs will receive this real-time traffic signal information via the SPaT and MAP messages and adjust their approaching speeds according to the optimal speed advisory algorithms. With this framework, we would like to understand whether intersection performance can be improved if CAVs can dynamically adjust their speeds according to the real-time traffic signal information.

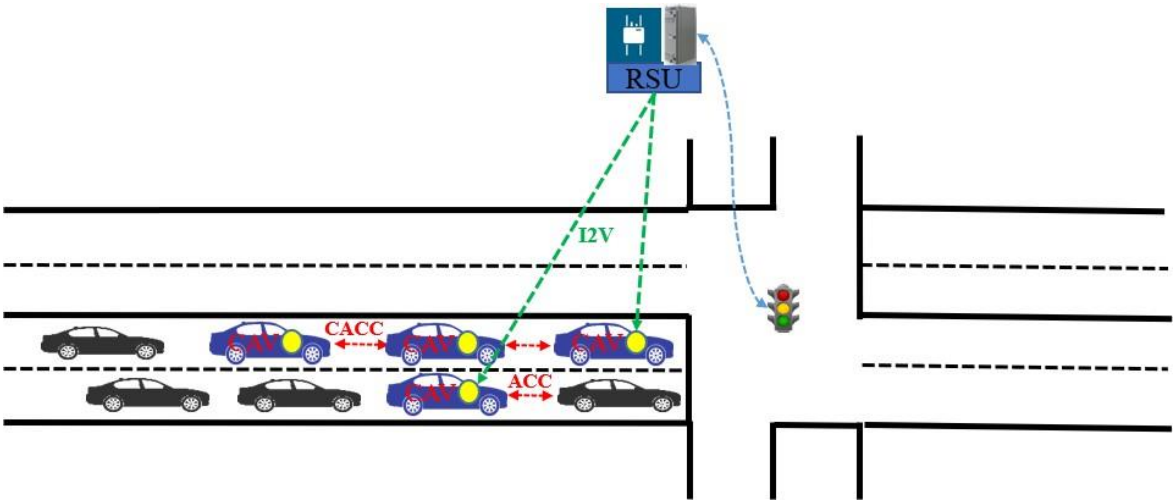

Figure 18. System architecture of traffic light optimal speed advisory with CAVs.

4.4.1.1 Communications workflow

In this application, the communications workflow at a signalized intersection is described as below:

- An RSU is connected to the intersection controller and is able to receive real-time signal information.
- The RSU has the MAP information of the intersection. Therefore, it can construct the MAP message according to the SAE J2735-201603 standard and broadcast it to the CAVs within its communications range at a user-defined interval, e.g., 1s.
- The RSU can also construct the SPaT message according to the SAE J2735-201603 standard and broadcast it to the CAVs within its communications range at a user-defined interval, e.g., 0.1s.
- CAVs within the communications range of the RSU will receive and parse the SPaT and MAP messages and obtain the intersection signal phase and map information. In this study, since CAVs are allowed to form platoons on arterial streets, only the leader of a CAV platoon or individual CAVs will use this real-time signal phase and map information as inputs into the optimal speed advisory algorithms and adjust their speeds according to the advised speeds.

4.4.1.2 Selected optimal speed advisory algorithm

According to (Guo et al., 2019), advanced traffic control at arterial intersections under connected and/or autonomous vehicles can be divided into the following three categories:

- **C1: Driver guidance control systems based on signal and vehicle data**. Such systems provide instructions to drivers/AVs to properly operate vehicles so as to minimize fuel consumptions, reduce travel delays, etc.
- **C2: Optimization of signal timings and phases based on data from CAVs.** Such a category includes actuated signal control, platoon-based signal control, and planning-based signal control.
- **C3: Signal-vehicle coupled control (SVCC) systems with CAVs.** Such systems aim to optimize both vehicle and signal timings/phases to achieve better performance at intersections.

Considering the readiness of the above control categories as well as the scope of our study, we focus on the studies in the first category **C1**. For demonstration purposes, we implement the Green Light Optimal Speed Advisory (GLOSA) application proposed in (Katsaros et al., 2011) in the Arterial-Only subnetwork with minor revisions.

In our implementation of the GLOSA algorithm, RSUs attached to traffic lights will periodically broadcast SPaT and MAP messages to nearby vehicles. For each CAV, it receives these SPaT and MAP messages and determines its actions based on the predicted traffic light status when it reaches the intersection.

- When the predicted traffic status is green, it should continue with the goal to reach the maximum speed limit.
- When the predicted traffic status is red, it calculates its speed so as to reach the next green phase.

At time tt, a CAV will calculate the projected time to reach the traffic light through the following equation,

$$TT_{pprrddjjrrddssrrdd} = \begin{cases} \dfrac{dd_{ssddVVssddppbbooaarr}}{vv_0} & eehhrrmmnnooaa = 0 \\ -\dfrac{vv_0}{aa} + \dfrac{\sqrt{vv_0^2 + 2aa\, dd_{ssddVVssddppbbooaarr}}}{aa} & eehhrrmmnnooaa \neq 0 \end{cases} \quad (46)$$

where

$dd_{ssddVVssddppbbooaarr}$: distance to the intersection stopbar;

vv_0: vehicle speed averaged over $[tt - \Delta TT_{aavvtt}, tt]$;

aa: vehicle acceleration averaged over $[tt - \Delta TT_{aavvtt}, tt]$.

Meanwhile, the CAV can calculate the current signal status $II_{ssiittiiaaggddmmrrrriiss}$ (i.e., GREEN or RED) and the remaining time $TT_{rrrrssaaiiii}$ for its movement (i.e., left turn, through, and right turn) according to the latest SPaT and MAP messages. Using the following logit, it will determine whether it can cross the intersection or not, i.e., $II_{ddrrddssss} = \{YYYYSS, NNoo\}$. If yes, it will calculate the expected time $TT_{rrrrmmppprrddssrrdd}$ to cross the intersection.

- When $II_{ssiittiiaaggddmmrrrriiss}$ is GREEN
  - If $TT_{pprrddjjrrddssrrdd} < TT_{rrrrssaaiiii}$, the CAV can cross the intersection within the remaining green time. Therefore, we set $II_{ddrrddssss} = YYYYSS$, and $TT_{rrrrmmppprrddssrrdd} = TT_{pprrddjjrrddssrrdd}$.
  - Else the traffic light will turn red when the CAV reaches the intersection. Therefore, we set $II_{ddrrddssss} = NNOO$, and $TT_{rrrrmmppprrddssrrdd} = TT_{rrrrssaaiiii}$. Note that $TT_{rrrrmmppprrddssrrdd}$ here is just an estimate and the actual expected time should be longer than that.
- When $II_{ssiittiiaaggddmmrrrriiss}$ is RED
  - If $TT_{pprrddjjrrddssrrdd} < TT_{rrrrssaaiiii}$, the traffic light remains red when the CAV reaches the intersection. Therefore, we set $II_{ddrrddssss} = NNOO$, and $TT_{rrrrmmppprrddssrrdd} = TT_{rrrrssaaiiii}$.
  - Else, the traffic light turns green when the CAV reaches the intersection. Therefore, we set $II_{ddrrddssss} = YYYYSS$, and $TT_{rrrrmmppprrddssrrdd} = TT_{pprrddjjrrddssrrdd}$.

When the CAV calculates a set of $\{II_{ddrrddssss}, TT_{rrrrmmppprrddssrrdd}\}$, it will adjust its speed according to the following logit:

- If $II_{ddrrddssss}$ is NO, it will keep its current speed since it is not able to cross the intersection without stopping.
- Else the CAV will apply the following advised speed $vv_{aaddvviissrrdd}$ as its desired speed.

$$vv_{aaddvviissrrdd} = \max\{vv_{ssaarrttrrssrrdd}, vv_{ssiiii}\} \& \min\{vv_{ssaarrttrrssrrdd}, vv_{ssaarrmm}\}$$
$$vv_{ssaarrttrrssrrdd} = \frac{2 * dd_{ssddVVssddppbbaarr}}{TT_{rrmmppmmddssrrdd}} - vv_0 \quad (47)$$

where vv_{ssiiii} and $vv_{ssaarrmm}$ are the permitted min and max speed limits.

In addition, to avoid any potential conflicts with other vehicles when a CAV is too close to the intersection, the CAV is only allowed to perform the GLOSA algorithm when its distance to the stopbar is greater than a certain distance threshold, i.e., $dd_{ssddVVssddppbbaarr} > dd_{sshrrrrsshddyydd,ssssddppbbaarr}$. Also, the GLOSA algorithm does not consider the case when it is too close to its leader if it exists, which will make the advised speed invalid and might even cause unexpected collisions. Therefore, we only allow the CAV to perform the GLOSA algorithm when its distance to the leader is greater than a certain threshold, i.e., $dd_{ssddVVrraaddrrrr} > dd_{shrrrrshddyydd,yyrraaddrrrr}$.

4.4.2 Arterial-Only subnetwork

4.4.2.1 Network settings and scenario design

As shown in Figure 19, the selected Arterial-Only subnetwork consists of 13 arterial intersections along Orange Grove Blvd in the City of Pasadena, CA, from Orange Grove Blvd @ Raymond to Orange Grove Blvd @ Martelo Ave with a total of 21 lane miles. As indicated in the figure, ten of the intersections are signalized, while the rest three are stop-controlled. There are four RSUs installed at the following four intersections: Orange Grove Blvd @ Los Robles Ave, Orange Grove Blvd @ Lake Ave, Orange Grove Blvd @ Hill Ave, and Orange Grove Blvd @ Allen Ave. We consider these RSUs have a communications range of 985ft (300 meters) with zero latency and zero package loss rate.

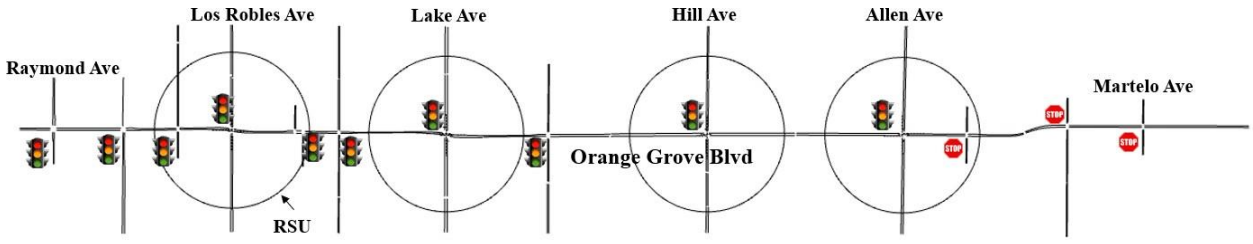

Figure 19. Arterial-Only subnetwork for the application of traffic light optimal speed advisory.

For the above four intersections equipped with RSUs, the coordinated traffic direction is the north-south direction. That means we may expect long vehicle delay in this Arterial-Only subnetwork as traffic in the east-west direction may experience frequent stops at the intersections. Regarding the signal settings, the left-turn settings vary a lot among these four intersections and are listed below:

- Orange Grove Blvd @ Los Robles Ave
  - Northbound & southbound: permitted left turns; coordinated
  - Eastbound & westbound: protected-permitted left turns

- Orange Grove Blvd @ Lake Ave
    - Northbound & southbound: protected-permitted left turns; coordinated
    - Eastbound & westbound: protected-permitted left turns
- Orange Grove Blvd @ Hill Ave
    - Northbound & southbound: permitted left turns; coordinated
    - Eastbound & westbound: permitted left turns
- Orange Grove Blvd @ Allen Ave
    - Northbound & southbound: permitted left turns; coordinated
    - Eastbound & westbound: permitted left turns

In order to assess the performance of the GLASO algorithm, we select two simulation periods in this study: one is from 7AM to 8AM while the other is from 4PM to 5PM on Weekdays. In addition, we change the traffic demand level by $\pm$10% and $\pm$20% to evaluate the performance of the GLOSA algorithm under various traffic conditions. We also vary the percentage of CAVs in the network so as to see how the network performance is changed as the percentage of CAVs increases.

4.4.2.2 Results

In the Arterial-Only subnetwork, we have activated the GLOSA algorithm with parameter settings listed in Table 7. For each RSU, it constructs the SPaT and MAP messages according to the SAE J2735-201603 standard. The interval to send the MAP messages is 1s, while the interval to send the SPaT messages is 0.1s. For each CAV, the interval to perform the GLOSA algorithm and maintain the advised speed is 2s.

We have conducted various simulations under different time periods, demand levels, and percentages of CAVs. Results in the AM period from 7AM to 8AM are provided in Table 8, while results in the PM period from 4PM to 5PM are provided in Table 9. Here the baseline scenarios are those with only ACC/CACC enabled.

As shown in the tables, we find that even though the GLOSA algorithm provides better performance for most of the scenarios, the improvement is very minor. The delay reduction is less than 1% for most of the cases, with a few exceptions over 1%. There are several factors that may lead to this low performance improvement, which are explained below.

- Uncoordinated intersections in the Arterial-Only subnetwork. In the Arterial-Only subnetwork, the coordination at the four signalized intersections equipped with RSUs are in the north-south direction, which means traffic in the east-west direction is being interrupted with frequent stops which contributes to the network-level vehicle delay. Meanwhile, this low performance improvement indicates it is difficult to reduce vehicle delay caused by poor signal timings through adjusting the speeds of CAV leaders and thus the vehicles behind.
- Settings of permitted left turn movements. At the four intersections equipped with RSUs, only the four left-turn movements at the intersection Orange Grove Blvd @ Lake Ave and the eastbound & westbound left turn movements at the intersection Orange Grove Blvd @ Los Robles Ave are protected-permitted. When a left-turn movement is permitted, it makes the green time information inside the SPaT messages unreliable since a left-turn CAV may not be able to cross the intersection due to the conflicting traffic in the opposite direction when it reaches the stopbar. Unfortunately,

this situation is unavoidable at the current moment since the implemented GLOSA algorithm doesn't explicitly handle this issue.

- Existence of vehicle queue at the intersections. In the GLOSA algorithm, the calculation of the expected time to the stopbar doesn't consider the existence of vehicle queues at the intersection approach. Therefore, even though the algorithm predicts the CAV can cross the intersection without stopping, the CAV may have to stop due to the existence of vehicle queues.
- Impacts from other traffic movements at the intersection approach. At an intersection approach, one traffic movement is often impacted by other traffic movements, especially when traffic is congested or when lane blockage occurs. For example, left-turn lane blockage often occurs with insufficient green times or inappropriate signal settings (e.g., permitted left turns) for high left-turn flows. In this case, it not only significantly degrades the performance of the GLOSA algorithm for the left-turn vehicles, but also negatively forces other vehicles to slow down or even stop.

Table 7: Parameter settings in the Arterial-Only subnetwork.

Parameter	Value
Time interval to average speed and acceleration ΔT_{avg}	0.5s
Distance threshold to the stopbar $dl_{stopbar}$	50 meters
Distance threshold to the leader dl_{leader}	15 meters
Minimum speed v_{min}	5 m/s
Maximum speed v_{max}	1.1 v_{free}

Table 8. Vehicle delay under different demand levels and percentages of CAVs in the AM period.

7AM -- 8AM											
CAV %	Method	80% Demand		90% Demand		100% Demand		110% Demand		120% Demand	
		Delay (sec/km)	Diff (%)	Delay (sec/km)	Diff (%)	Delay (sec/km)	Diff (%)	Delay (sec/km)	Diff (%)	Delay (sec/km)	Diff (%)
0%	Baseline	49.14		50.41		55.78		59.96		69.25	
20%	Baseline	47.86		50.31		54.86		58.54		64.43	
	GLOSA	47.91	-0.10	*50.05*	*0.52*	*54.85*	*0.02*	58.60	-0.10	*63.97*	*0.71*
40%	Baseline	46.85		49.55		51.04		57.32		64.16	
	GLOSA	*46.74*	*0.23*	*49.34*	*0.42*	*50.82*	*0.43*	57.39	-0.12	*63.67*	*0.76*
60%	Baseline	45.48		47.60		50.16		55.23		59.36	
	GLOSA	*45.45*	*0.07*	*47.56*	*0.08*	50.34	-0.36	*54.98*	*0.45*	60.18	-1.38
80%	Baseline	44.12		45.84		49.63		52.58		57.88	
	GLOSA	*43.93*	*0.43*	45.98	-0.31	*49.23*	*0.81*	53.01	-0.82	*57.01*	*1.50*
100%	Baseline	43.11		45.06		47.63		49.49		54.86	
	GLOSA	*42.91*	*0.46*	*44.99*	*0.16*	*47.24*	*0.82*	*49.07*	*0.85*	55.04	-0.33

Note: in the above table, the "Green" means the delay was reduced while the "Red" means the delay was increased.

Table 9. Vehicle delay under different demand levels and percentages of CAVs in the PM period.

4PM -- 5PM											
CAV %	Method	80% Demand		90% Demand		100% Demand		110% Demand		120% Demand	
		Delay (sec/km)	Diff (%)	Delay (sec/km)	Diff (%)	Delay (sec/km)	Diff (%)	Delay (sec/km)	Diff (%)	Delay (sec/km)	Diff (%)
0%	Baseline	50.70		54.06		56.34		61.78		74.36	
20%	Baseline	49.23		52.52		55.27		58.01		66.81	
	GLOSA	*49.17*	*0.12*	52.64	-0.23	*54.93*	*0.62*	*57.80*	*0.36*	*66.69*	*0.18*
40%	Baseline	49.27		50.73		53.13		56.86		63.38	
	GLOSA	*49.11*	*0.32*	*50.72*	*0.02*	**53.37**	-0.45	*56.35*	*0.90*	*62.51*	*1.37*
60%	Baseline	47.21		49.74		52.99		55.35		59.46	
	GLOSA	*47.16*	*0.11*	*49.36*	*0.76*	*52.98*	*0.02*	55.37	-0.04	*59.36*	*0.17*
80%	Baseline	46.33		48.67		50.50		52.45		57.44	
	GLOSA	*46.20*	*0.28*	*48.53*	*0.29*	*50.47*	*0.06*	*51.87*	*1.11*	*57.21*	*0.40*
100%	Baseline	44.82		46.02		48.79		50.88		54.63	
	GLOSA	*44.69*	*0.29*	*45.83*	*0.41*	*48.49*	*0.61*	*50.46*	*0.83*	*53.79*	*1.54*

Note: in the above table, the "Green" means the delay was reduced while the "Red" means the delay was increased.

Therefore, the factors mentioned above should be considered when we develop new algorithms/methods to use CAVs to improve intersection performance. If methods in the first category "*Driver guidance control systems based on signal and vehicle data*" are not able to provide satisfactory outcomes, we need to proceed to the next levels to develop methods in the second "*Optimization of signal timings and phases based on data from CAVs*" or third "*Signal-vehicle coupled control (SVCC) systems with CAVs*" categories.

4.5 Discussion

In this section, we demonstrated how to apply the integrated microsimulation platform to study the network-level impacts of CAV applications. In particular, we implemented the following three applications with CAVs: (i) freeway speed harmonization with CAVs; (ii) route guidance with CAVs for traffic incident management, and (iii) traffic light optimal speed advisory with CAVs. We have successfully implemented the required workflows for each of the applications using the functions provided by the V2X and other modules in Aimsun. To help evaluate the performance of these three applications, we generated three different subnetworks from the original I-210 network: (i) a Freeway-Only subnetwork for the application of freeway speed harmonization with CAVs, (ii) a Freeway-and-Arterial Combined subnetwork for the application of route guidance with CAVs for traffic incident management, and (iii) an Arterial-Only subnetwork for the application of traffic light optimal speed advisory with CAVs.

For the application of freeway speed harmonization with CAVs, we implemented three different algorithms for demonstration purposes, which are the rule-based algorithm in (Talebpour et al., 2013), the VSL-VSA algorithm in (Lu et al., 2015; Hale et al., 2016), and the C-VSLS in (Grumert et al., 2015). We tested their

performance in the Freeway-Only subnetwork under different combinations of demand levels and percentages of CAVs in the morning peak period from 7AM to 8AM. Simulation results showed that these three algorithms have very different performance. The rule-based algorithm and the VSL-VSA algorithm tend to have better performance when the percentage of CAVs is high, e.g., 80% or higher, while the C-VSLS tends to have better performance with a relatively low percentage of CAVs, e.g., about 40%, and under light traffic congestion. Regarding the level of improvement, the rule-based algorithm and the C-VSLS can only achieve a relatively small delay reduction between 1% and 2%, while the VSL-VSA algorithm can achieve a relatively large delay reduction between 2% and 6%. Note that these conclusions are drawn based on the particular settings in the Freeway-Only subnetwork. In reality, many factors may impact the performance of the speed harmonization algorithms. These factors include, but are not limited to: road geometries, existing detector placement and control settings, traffic demand and OD patterns, settings of speed harmonization zones, settings in the RSU, settings in the V2I/I2V communications, and parameter settings in the speed harmonization algorithms. Therefore, in the future, more analysis is required in order to fully understand where, when and how to activate speed harmonization with CAVs.

For the application of route guidance with CAVs for traffic incident management, we have implemented two different workflows: (i) an incident management workflow to manage different stages of a traffic incident and the activation and termination of response plans; (ii) a communications workflow to manage the information exchange between RSUs and their connected CAVs. We also revised the algorithm in (Samimi Abianeh et al., 2020) to mimic CAV's route choice decisions with considerations of potential impacts from lane index (e.g., inner lanes vs. shoulder lanes), vehicle types (e.g., car vs. truck), and number of detoured vehicles. We tested the performance of the revised algorithm in the Freeway-and-Arterial Combined subnetwork with two different traffic accidents at the same location: (i) a major traffic accident in the AM peak between 7AM and 8AM, and (ii) a minor traffic accident in the PM peak between 4PM and 5PM. Simulation results with 30% and 50% CAVs showed that the revised algorithm can achieve satisfactory performance with delay reduction above 3% for most of the scenarios. This demonstrates the potential of integrating CAVs into existing ICM systems to help mitigate traffic congestion. Especially, it reveals the benefits of sharing detour route information with road users, which is not limited to CAVs but should include those who can receive real-time traffic information, e.g., navigation app users. In the future, we are interested in improving the current framework with more complete features to handle multiple traffic incidents and detour routes. Also, we will use this framework to study policies and strategies of information sharing with navigation app users so as to manage traffic incidents more efficiently and effectively.

For the application of traffic light optimal speed advisory with CAVs, we have implemented the communications workflow that enables an RSU connected to a signalized intersection to broadcast real-time SPaT and MAP messages to nearby CAVs. CAVs will receive this information and use it as one of the inputs into their optimal speed advisory algorithm to generate advised speeds to follow. In this study, we implemented the Green Light Optimal Speed Advisory (GLOSA) application proposed in (Katsaros et al., 2011) with some minor revisions. Four RSUs were installed at four different intersections in the Arterial-Only subnetwork for demonstration purposes. We tested the performance of the revised GLOSA algorithm in the Arterial-Only subnetwork under different time periods, demand levels, and percentages of CAVs. Simulation results showed that the GLOSA algorithm generally provides better performance, but the improvement is minor with delay reduction below 1% for most of the scenarios. However, it is not surprising to see this low performance improvement in the Arterial-Only subnetwork for the following reasons: (i) traffic in the eastbound-westbound directions is uncoordinated, which makes it hard for CAVs

to cross the intersections without stopping; (ii) most of the left-turn movements at the four intersections equipped RSUs are permitted, which makes CAVs hard to make left turns due to conflicting traffic in the opposite direction; (iii) the GLOSA algorithm doesn't consider the existence of vehicle queues and lane blockages at the intersection, which may make the advised speed invalid as the predicted travel time to the intersection is no longer reliable. Therefore, in the future, we will devote efforts to addressing the aforementioned issues while developing new algorithms/methods to use CAVs to improve intersection performance. If methods in the first category "Driver guidance control systems based on signal and vehicle data" are not able to provide satisfactory outcomes, we will proceed to the next levels to develop methods in the second "Optimization of signal timings and phases based on data from CAVs" or third "Signal-vehicle coupled control (SVCC) systems with CAVs" categories.

This page left blank intentionally

5. Network-level impacts of Adaptive Cruise Control (ACC) and Cooperative Adaptive Cruise Control (CACC)

In Section 4, we have demonstrated how to use the integrated microsimulation platform in Aimsun to evaluate the performance of CAV applications in small networks. Three CAV applications, i.e., freeway speed harmonization with CAVs, route guidance with CAVs for traffic incident management, and traffic light optimal speed advisory with CAVs, have been implemented and tested in three different subnetworks, i.e., Freeway-Only, Arterial-Only, and Freeway-and-Arterial Combined subnetworks, under various traffic conditions and CAV percentages.

As a next step, it would be ideal if we could enable both ACC/CACC and V2X modules at the same time for simulations in large-scale networks, e.g., the I-210 network. However, we find that Aimsun becomes extremely slow (>1 week) and drains physical memories (>100 GB) quickly for each simulation replication in the I-210 network if the V2X module is enabled. Therefore, we only enable the ACC/CACC module in this section and focus on the evaluation of how ACC/CACC can help improve transportation network performance, e.g., reducing vehicle delay and improving vehicle travel speed.

In our scenario design, we consider the following factors that may impact simulation results:

(i) Road network geometry: The performance of ACC/CACC may be closely related to road geometries. For example, potential improvement on freeway networks may be different from that on arterial networks since they have significantly different road characteristics. Therefore, in this study, we generate three subnetworks from the original I-210 network to address this issue: Freeway-Only subnetwork, Arterial-Only subnetwork, Freeway-and-Arterial Combined subnetwork.

(ii) Vehicle routing/travel patterns: For a given network, bottlenecks can occur at different locations and times since vehicle routing/travel patterns change overtime. Especially for commute routes, we can see significant differences between AM and PM peak periods. When coupled with specific road geometries, these differences may also impact the performance of ACC/CACC. Therefore, in this study, we consider three different time periods: AM peak (7AM—9AM), PM peak (4PM—6PM), and Off peak (12PM—2PM).

(iii) Travel demand: Variations in travel demand may also impact the performance of ACC/CACC. For example, with lower travel demand, the existing bottlenecks may not occur. However, if travel demand is increased by a certain percentage, e.g., 10%, new bottlenecks may occur at other locations. Therefore, to better assess the performance of ACC/CACC, we consider scenarios with a 10% demand increase for the Freeway-Only and Arterial-Only subnetworks. We do not apply the 10% demand increase to the Freeway-and-Arterial combined subnetwork and the I-210 network since they are already very congested during peak periods.

(iv) Penetration rates of CAVs: When the penetration rate of CAVs is low, the improvement with ACC/CACC may not be that significant. As the penetration rate increases, we may be able to see significant delay reduction as well as speed improvement. However, there may also be the case that this improvement becomes minor after the penetration rate reaches a certain threshold. Therefore, in this study, we consider scenarios with different penetration rates of CAVs, e.g., 0%, 10%, 20%, …, 100%.

(v) Random seeds in microsimulation: Even for the same OD demand, different random seeds in microsimulation will yield different results as they will be used to determine the randomness in some internal processes, e.g., vehicle assignments. Therefore, we perform 10 replications for each scenario in the Freeway-Only and Arterial-Only subnetworks, and 5 replications for each scenario in the Freeway-and-Arterial Combined subnetwork and the I-210 network. Simulation results will then be averaged over these replications to reduce randomness caused by the random seeds.

Given the above scenario design, we have conducted a significant number of simulation scenarios to evaluate potential benefits that ACC/CACC can bring. Detailed results are provided in the following subsections.

5.1 Study networks and demand settings

5.1.1 Study networks

To evaluate the impact of ACC/CACC on transportation network performance, in this study we focus on the I-210 network, which is developed in Aimsun and well calibrated with 24-hrs traffic demand profiles on Weekday, Saturday, and Sunday. Furthermore, we generate three different subnetworks, e.g., Freeway-Only, Arterial-Only, and Freeway-and-Arterial Combined, from the original I-210 network to consider the performance difference related to road geometries.

5.1.1.1 The I-210 network

As shown in Figure 1, the I-210 network is located on the I-210 freeway in the San Gabriel Valley in Los Angeles County. It covers the freeway segment from the SR134/I-210 interchange to the I-605/I-210 interchange, with major arterial roads located in the cites of Pasadena, Arcadia, Monrovia, and Duarte. This study site is well instrumented with roadway sensors and the freeway is congested during morning and evening commute hours. This network has been built in the microsimulation software, Aimsun, and has been well calibrated using 24-hrs demand profiles on Weekday, Saturday, and Sunday. In addition, detour plans and signal timing plans have been developed to handle traffic incidents occurring at any place along the I-210 freeway segment.

5.1.1.2 Generation of subnetworks

To consider the performance difference related to road geometries, we further generate three different types of subnetworks for this study: (i) Freeway-Only subnetwork, (ii) Arterial-Only subnetwork, and (iii) Freeway-and-Arterial Combined subnetwork.

5.1.1.2.1 Freeway-Only subnetwork

As shown in Figure 20, the selected Freeway-Only subnetwork is a 5-mile-long freeway portion at the I-605/I-210 interchange. It consists of 274 sections/links and 182 nodes, with a total of 102 lane miles.

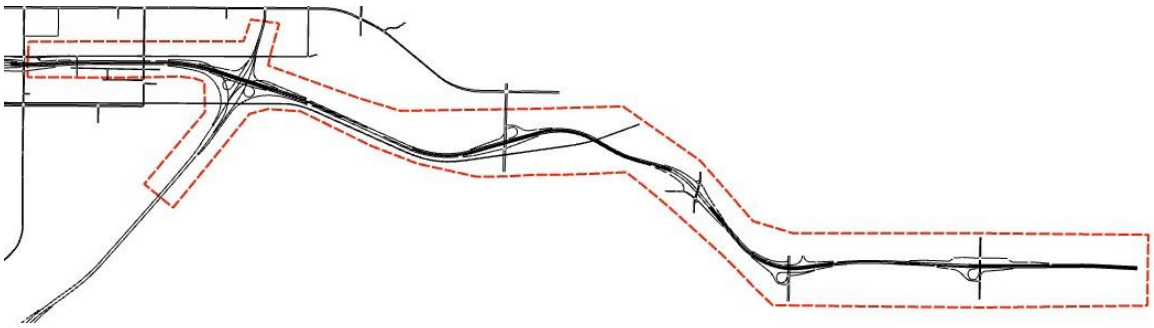

Figure 20. Freeway-Only subnetwork.

5.1.1.2.2 Arterial-Only subnetwork

As shown in Figure 21, the selected Arterial-Only subnetwork consists of 13 arterial intersections along Orange Grove Blvd, from Orange Grove@Raymond to Orange Grove@Martelo Ave with a total of 21 lane miles.

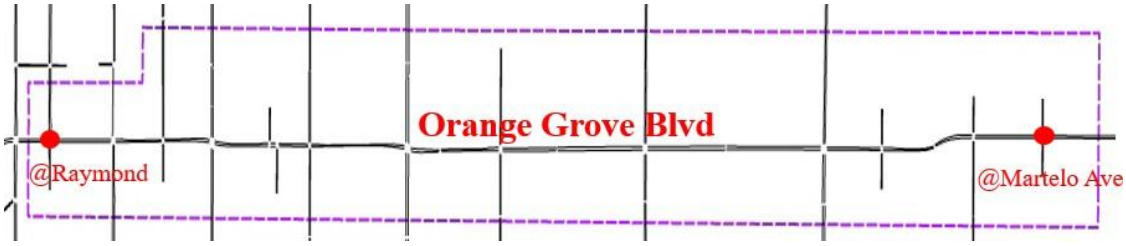

Figure 21. Arterial-Only subnetwork.

5.1.1.2.3 Freeway-and-Arterial Combined subnetwork

As shown in Figure 13, the selected Freeway-and-Arterial Combined subnetwork mainly consists of: (i) a freeway section starting from SR-134@Orange Grove Blvd to I-210@Rosemead Blvd; (ii) five major paralleled arterial streets, including Walnut St, Corson St, Maple St, Villa St, and Foothill Blvd. There are 725 sections and 333 nodes in this subnetwork, with a total of 182 lane miles. This subnetwork contains several bottlenecks on the I-210 freeway and is very congested during the AM and PM peak periods.

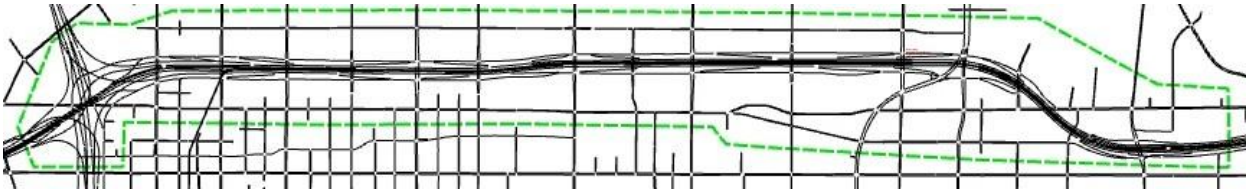

Figure 22. Freeway-and-Arterial Combined subnetwork.

5.1.2 Demand settings

In order to comprehensively evaluate the impact of CAVs on transportation network performance, we consider three different demand periods: AM peak, Off peak, and PM peak. A detailed list of selected time

periods for each network/subnetwork is provided in Table 10. Note that, for the Freeway-and-Arterial Combined subnetwork, the Off-peak period is different from those in other networks/subnetworks since the "Generate Dynamic Traversal" function provided in Aimsun repeatedly failed for the period 12PM – 2PM because of unknown issues. Also, we reduced the number of time periods in the I-210 network, e.g., excluding the PM peak, due to the constraint of long simulation time to finish one scenario replication.

Table 10. Selected time periods for the study networks.

Selected Networks	Selected Time Periods
Freeway-Only subnetwork	AM Peak 7:00AM-9:00AM
	PM Peak 4:00PM-6:00PM
	Off Peak 12:00PM-2:00PM
Arterial-Only subnetwork	AM Peak 7:00AM-9:00AM
	PM Peak 4:00PM-6:00PM
	Off Peak 12:00PM-2:00PM
Freeway-and-Arterial Combined subnetwork	AM Peak 7:00AM-9:00AM
	PM Peak 4:00PM-6:00PM
	Off Peak 1:00PM-3:00PM
The I-210 network	AM Peak 7:00AM-9:00AM
	Off Peak 12:00PM-2:00PM

In this study, we generate OD demand profiles for four targeted vehicle types: Car, Car HOV, Truck Medium, and Truck Heavy. In order to use both the ACC/CACC and V2X modules at the same time during simulation, the solution is to create a new type with 100% CAVs for each vehicle type, e.g., "Car CAV" for "Car". Therefore, in a mixed traffic environment, e.g., with 10% Car CAVs and 90% Cars, we need to adjust the OD demand profiles for both.

For example, let's assume the original demand matrix for the vehicle type "Car" is $\Theta^{100\%}_{dtcar}$. For the case of $xx\%$ CAVs, we need to split $\Theta^{100\%}_{dtcar}$ into two: $\Theta^{(100-xx)\%}_{dtcar}$ (i.e., $(1-\frac{xx}{100})*\Theta^{100\%}_{dtcar}$) for $(100-xx)\%$ vehicles of "Car", and $\Theta^{xx\%}_{dtcar\,dtcav}$ (i.e., $\frac{xx}{100}*\Theta^{100\%}_{dtcar}$) for the other $xx\%$ vehicles of "Car CAV". This applies to any percentage of CAVs as well as other vehicle types, e.g., Car HOV, Truck Medium, and Truck Heavy. In Figure 23, we provide an example of adjusted OD demand profile for a traffic simulation with 10% CAVs.

In order to explore the impact of CAVs from 0% to 100%, we expect to create many adjusted OD demand matrices for the targeted vehicle types. In our simulations, our evaluation interval of CAV percentage is 10%, which means we only consider the following 11 CAV percentages: 0%, 10%, 20%, …, 100%.

Figure 23. Example of adjusted OD demand profile for a traffic simulation with 10% CAVs.

5.2 Simulation results

In this subsection, we conducted various simulation scenarios in different sizes of networks/subnetworks under different time periods, e.g., AM peak, PM peak, and Off peak, and different demand levels, e.g., 100% vs. 110%. Detailed simulation results are provided below.

5.2.1 Results in the Freeway-Only subnetwork

In Figure 24, we provide a snapshot of AM peak speed heatmap in the Freeway-Only subnetwork at 7:20 AM. As shown in the figure, both cases show the same bottleneck at the merging junction between I-210EB and I-605NB, which is caused by the ramp meter. For other locations, we do see the differences in congestion levels. Especially along the I-210WB, traffic is less congested when 50% of vehicles are CAVs.

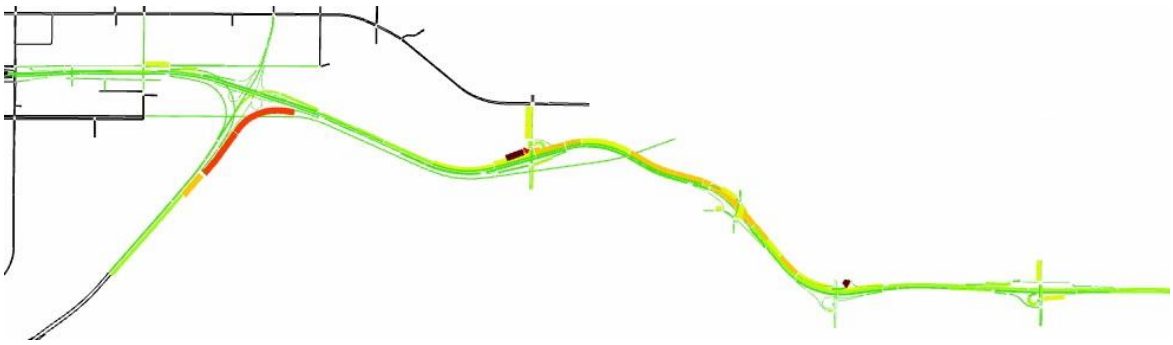

(a) At 7:20AM with 0% CAVs and 100% demand level

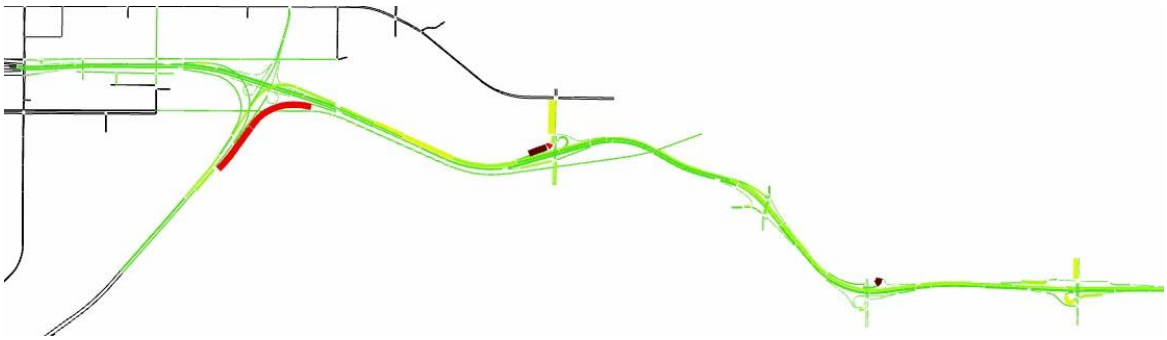

(b) At 7:20AM with 50% CAVs and 100% demand level

Figure 24. Snapshot of AM peak speed heatmap in the Freeway-Only subnetwork.

We further conducted many simulation scenarios to investigate the performance improvement under different penetration rates (percentages) of CAVs in the AM peak period with 100% demand level. As shown in Figure 25, we can achieve a delay reduction of 38.7% for all vehicles with 100% CAVs. The drop is significant as the percentage of CAVs increases to about 50%. After that, the gain is very minor. We even see the delay slightly increases as the percentage of CAVs increases to 100%. This phenomenon may be caused by more conservative parameter settings in the ACC/CACC module. Besides the significant delay reduction, as shown in Figure 26, the speed improvement is also significant, which is 22.3% when all vehicles are CAVs.

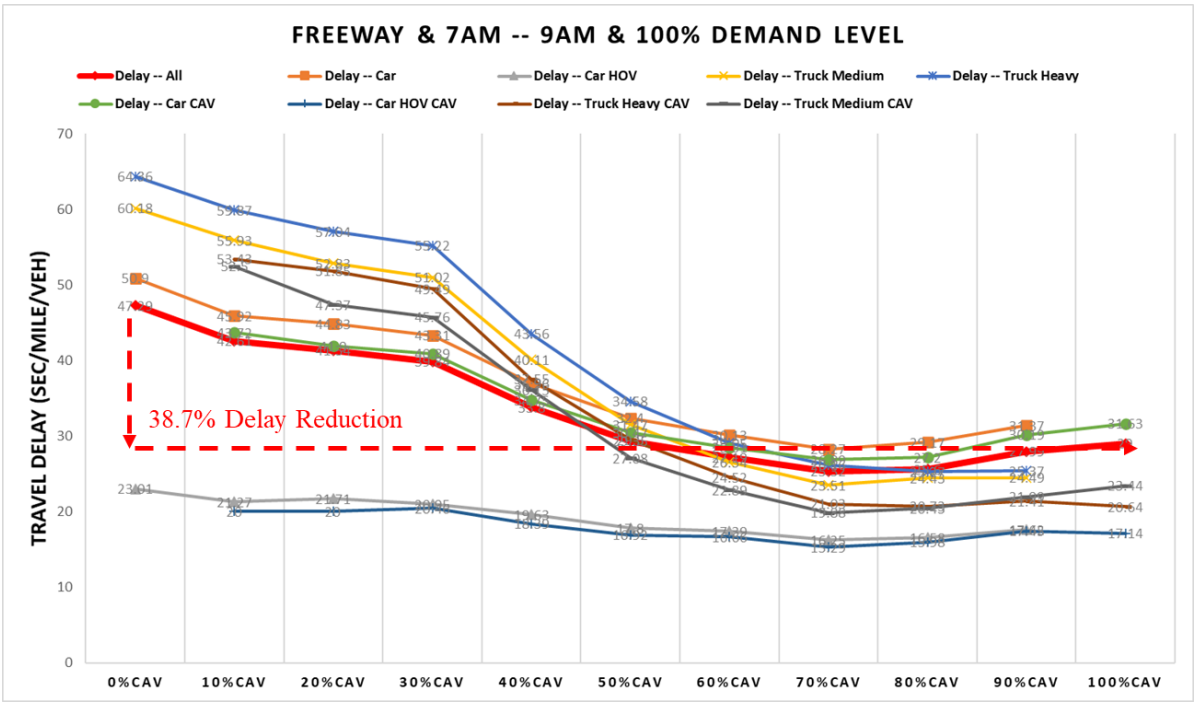

Figure 25. Example of delay reduction with different CAV percentages in the Freeway-Only subnetwork.

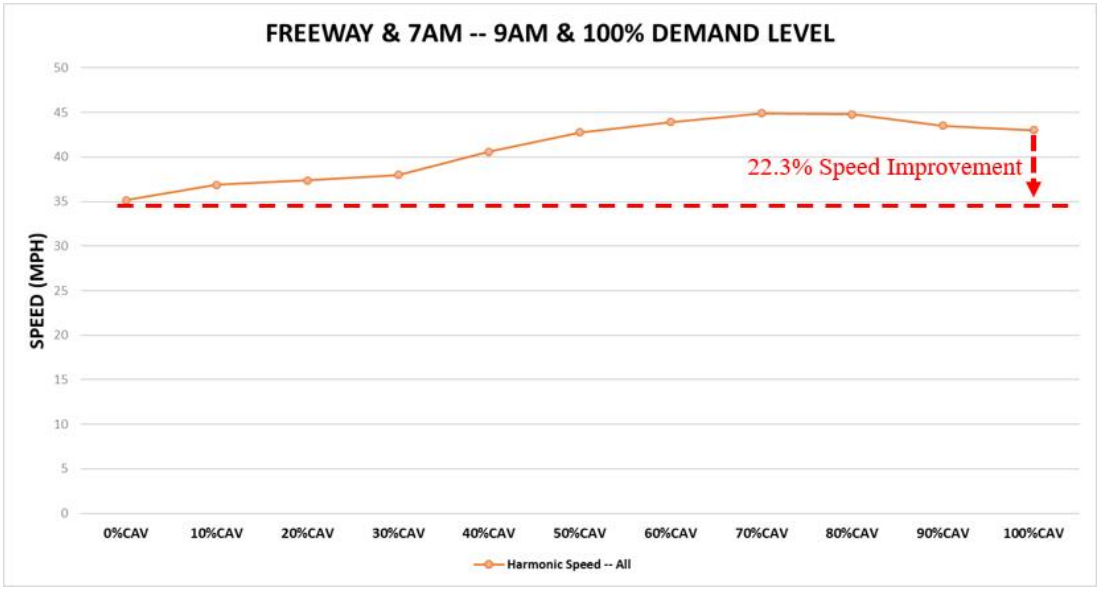

Figure 26. Example of speed improvement with different CAV percentages in the Freeway-Only subnetwork.

In addition, we conducted extra simulation scenarios under different traffic conditions, e.g., AM peak, PM peak, and Off peak. We also tried simulations with increased demand levels, e.g., 110%, to have more

congested traffic in the network. These simulation results are summarized in Table 11. As shown in the table, delay reduction and speed improvement vary under different traffic conditions. On average, the delay reduction is about 40% and the speed improvement is about 22% in the Freeway-Only subnetwork.

Table 11. Summary of delay reduction and speed improvement under different time periods and demand levels in the Freeway-Only subnetwork.

Time Period	Demand Level	Delay Reduction With 100% CAV	Speed Improvement With 100% CAV
7AM—9AM	100%	38.7%	22.3%
7AM—9AM	110%	40.5%	28.8%
12PM—2PM	100%	35.0%	14.2%
12PM—2PM	110%	25.9%	12.9%
4PM—6PM	100%	52.4%	25.1%
4PM—6PM	110%	46.0%	28.7%
	Average	39.75%	22%

5.2.2 Results in the Arterial-Only subnetwork

In Figure 27, we provide a snapshot of PM peak speed heatmap in the Arterial-Only subnetwork at 4:45PM. As shown in the figure, the Arterial-Only subnetwork is not very congested in the baseline scenario with 0% CAVs and 100% demand level. Therefore, no significant improvement is observed when there are 50% CAVs assigned in the network.

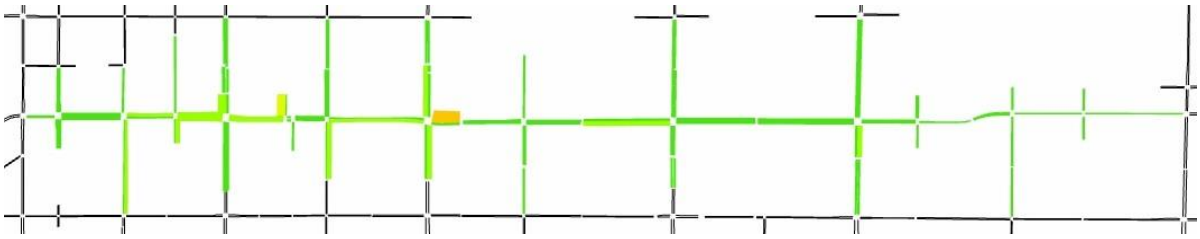

(a) At 4:45PM with 0% CAVs and 100% demand level

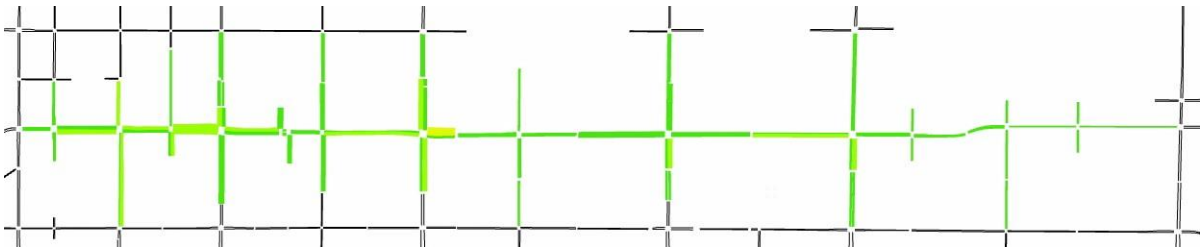

(b) At 4:45PM with 50% CAVs and 100% demand level

Figure 27. Snapshot of PM peak speed heatmap in the Arterial-Only subnetwork.

We further conducted many simulation scenarios with different penetration rates (percentages) of CAVs and 110% PM peak demand in the Arterial-Only subnetwork. As shown in Figure 28, delay reduces as the percentage of CAVs increases. However, compared to the Freeway-Only subnetwork, the delay reduction

is much less, which is only 16.4% with 100% CAVs. Similarly, as shown in Figure 29, the corresponding speed improvement is lower than that in the Freeway-Only subnetwork, which is only 7.2% with 100% CAVs.

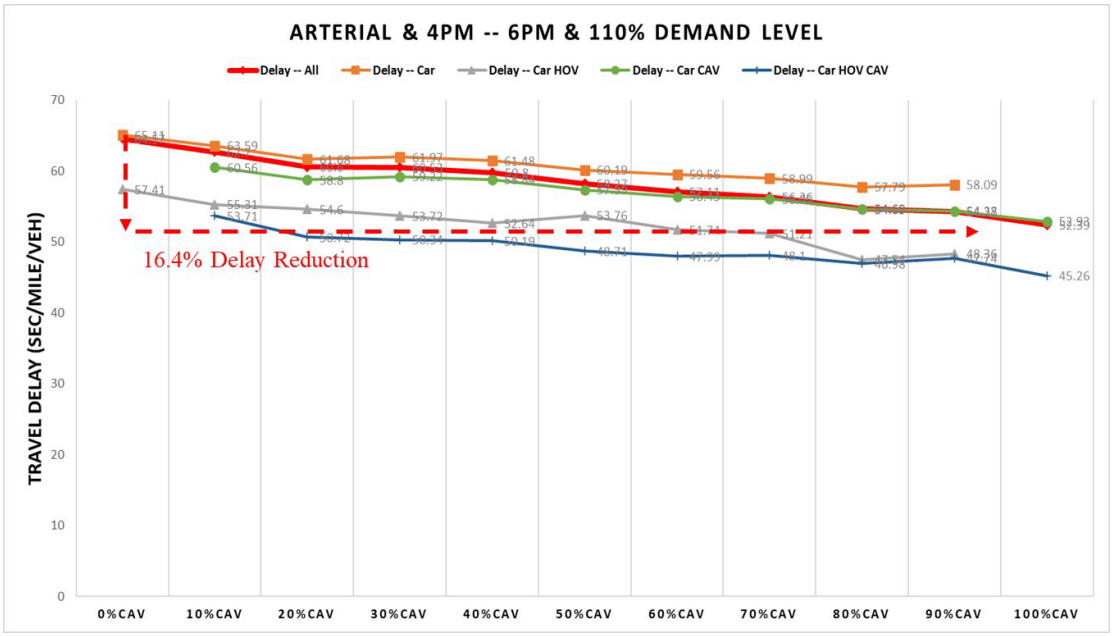

Figure 28. Example of delay reduction with different CAV percentages in the Arterial-Only subnetwork.

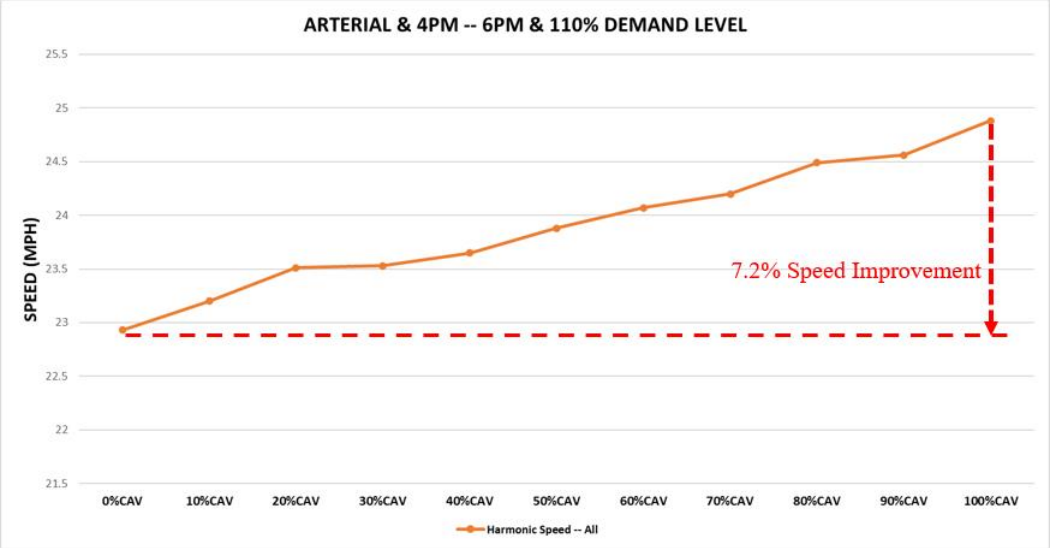

Figure 29. Example of speed improvement with different CAV percentages in the Arterial-Only subnetwork.

Similar to the Freeway-Only network, we conducted extensive simulation scenarios under different traffic conditions, e.g., AM peak, PM peak, and Off peak, and different demand levels, e.g., 100% and 110%. Simulation results are summarized in Table 12. According to Table 12, we find that:

(i) On average, the delay reduction is 15% and the speed improvement is 6.25% with 100% CAVs in the Arterial-Only subnetwork. This improvement is much lower than that in the Freeway-Only subnetwork. That is as expected because arterial signals play an important role in vehicle delay. Without V2I/I2V communications with intersection controllers, it is very difficult to further reduce vehicle delay even with 100% CAVs.

(ii) The improvement is more significant when traffic is more congested, which is true for the case of 110% demand level in the Arterial-Only subnetwork. This is probably related to the fact that traffic is not very congested with the original demand level (100%). Therefore, with a 10% increase in travel demand, traffic gets more congested and thus the improvement is more obvious.

Table 12. Summary of delay reduction and speed improvement under different time periods and demand levels in the Arterial-Only subnetwork.

Time Period	Demand Level	Delay Reduction With 100% CAV	Speed Improvement With 100% CAV
7AM—9AM	100%	14.3%	5.9%
7AM—9AM	110%	19.1%	8.5%
12PM—2PM	100%	12.5%	4.7%
12PM—2PM	110%	13.9%	5.4%
4PM—6PM	100%	13.8%	5.8%
4PM—6PM	110%	16.4%	7.2%
	Average	15%	6.25%

5.2.3 Results in the Freeway-and-Arterial Combined subnetwork

In Figure 30, we provide a snapshot of PM peak speed heatmap in the Freeway-and-Arterial Combined subnetwork at 4:20PM. From the figure, it is clear to see that traffic is much less congested when 50% of the vehicles are CAVs. This improvement is network-wide, on both freeway and arterial road links.

We further conducted various simulation scenarios with different penetration rates of CAVs in the PM peak period with 100% demand level. As shown in Figure 31, the delay reduction is significant, which is 26.9% when the penetration rate is 100%. The corresponding speed improvement is also significant, which is 16% with 100% CAVs in Figure 32. Though this improvement is less than that in the Freeway-Only subnetwork, it is still much higher than that in the Arterial-Only subnetwork.

In addition, we conducted extra simulation scenarios under different traffic conditions, e.g., AM peak, PM peak, and Off peak. Due to the size of the network and a small simulation time step (0.1s) to enable ACC/CACC, the simulation time is very long for each scenario replication. Therefore, we only simulate the scenarios with 100% demand level. Simulation results are summarized in Table 13. On average, the delay reduction is about 26.6% and the speed improvement is about 15.7% with 100% CAVs. As we can see, this improvement is not as high as in the Freeway-Only subnetwork but is much higher than that in the Arterial-Only subnetwork. Because the study network consists of both freeway and arterial road links, it is expected to see the improvement is between those in the Freeway-Only and Arterial-Only subnetworks.

(a) At 4:20PM with 0% CAVs and 100% demand level

(b) At 4:20PM with 50% CAVs and 100% demand level

Figure 30. Snapshot of PM peak speed heatmap in the Freeway-and-Arterial Combined subnetwork.

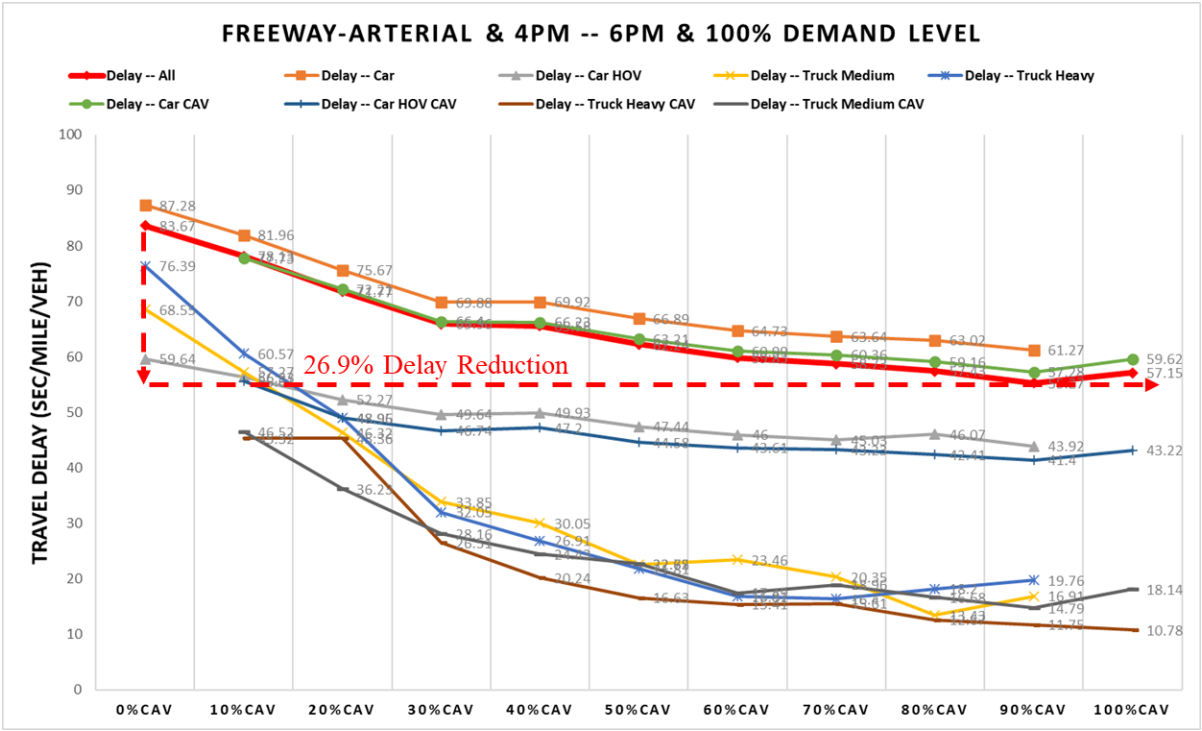

Figure 31. Example of delay reduction with different CAV percentages in the Freeway-and-Arterial Combined subnetwork.

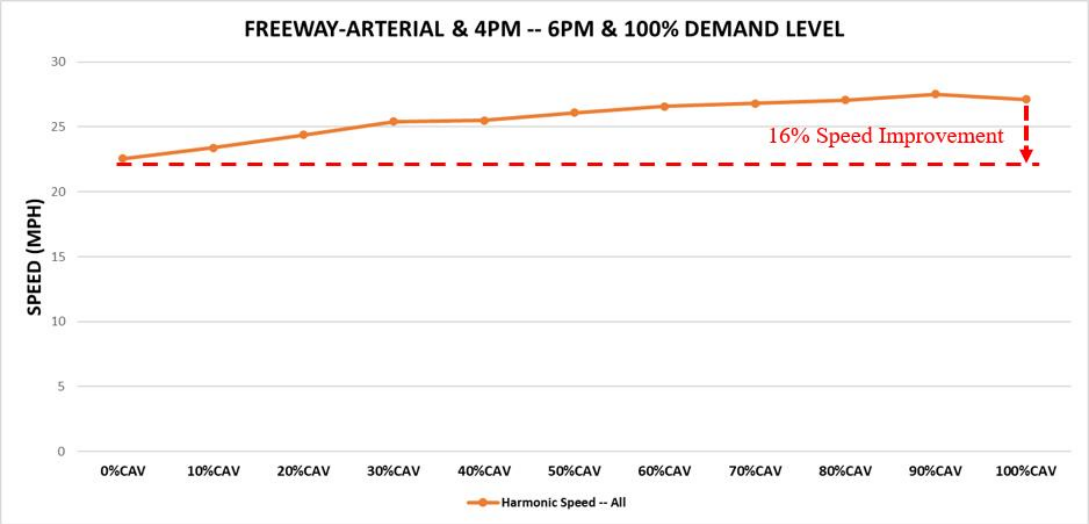

Figure 32. Example of speed improvement with different CAV percentages in the Freeway-and-Arterial Combined subnetwork.

Table 13. Summary of delay reduction and speed improvement under different time periods in the Freeway-and-Arterial Combined subnetwork.

Time Period	Demand Level	Delay Reduction With 100% CAV	Speed Improvement With 100% CAV
7AM—9AM	100%	28.4%	18.0%
1PM—3PM	100%	24.5%	13.0%
4PM—6PM	100%	26.9%	16.0%
	Average	26.6%	15.7%

5.2.4 Results in the I-210 network

In Figure 33, we provide a snapshot of AM peak speed heatmap in the I-210 network at 7:55AM. As shown in the figure, traffic performance is significantly improved with 50% CAVs in the network. This improvement is network-wide with fewer congested spots on both freeway and arterial road links.

We further conducted many simulations with different penetration rates of CAVs in the I-210 network during the AM period. As shown in Figure 34 and Figure 35, the delay reduction is 15.3% and the speed improvement is 9.4% when the penetration rate of CAVs reaches 100%. Compared with the three subnetworks, this level of improvement is as expected. As demonstrated in the Arterial-Only subnetwork, the overall improvement is relatively low even with 100% CAVs. Since there is a significant portion of arterial road links in the I-210 network, the overall improvement should be lower than that in the Freeway-and-Arterial Combined subnetwork.

The simulation time for each scenario replication is very long in the I-210 network when ACC/CACC is enabled. Therefore, we only ran simulations for two selected time periods: AM peak and Off peak. Simulation results are provided in Table 14. Overall, the averaged delay reduction is 14.6% and the averaged speed improvement is 8.3% with 100% CAVs. These results are consistent with those in the above three subnetworks.

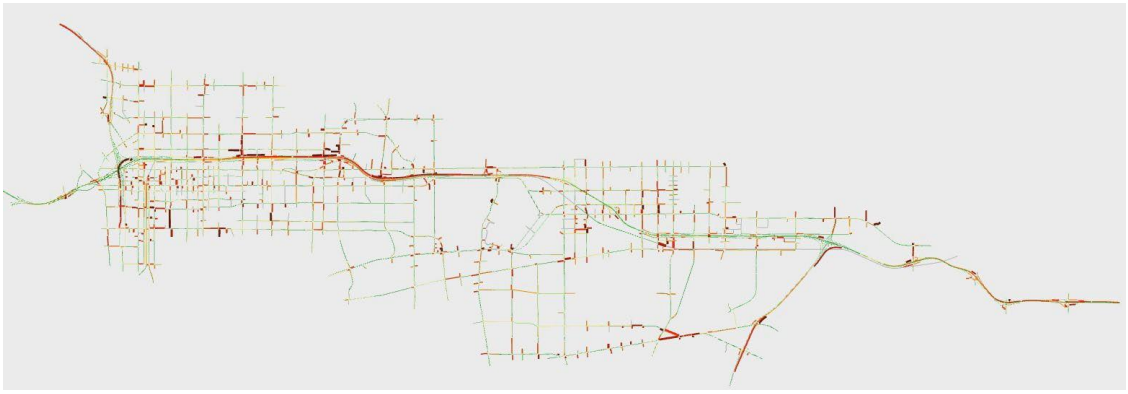

(a) At 7:55AM with 0% CAVs and 100% demand level

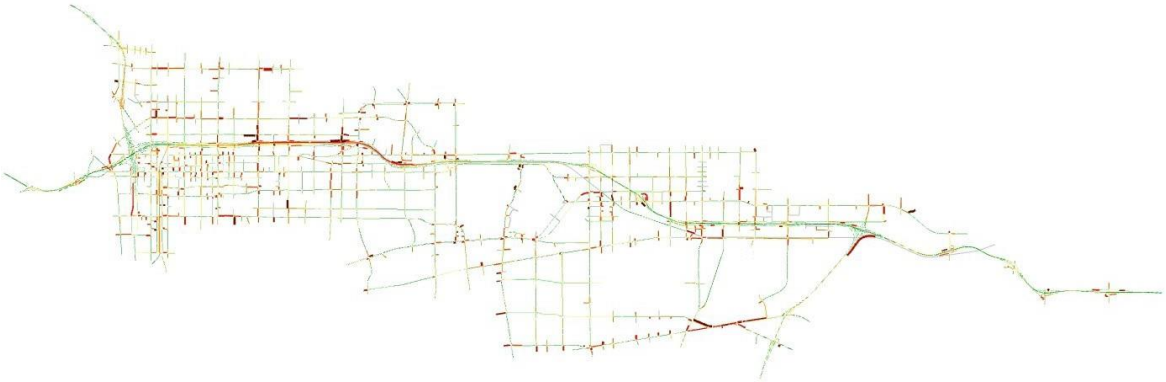

(b) At 7:55AM with 50% CAVs and 100% demand level

Figure 33. Snapshot of AM peak speed heatmap in the I-210 network.

Table 14. Summary of delay reduction and speed improvement under different time periods in the I-210 network.

Time Period	Demand Level	Delay Reduction With 100% CAV	Speed Improvement With 100% CAV
7AM—9AM	100%	15.3%	9.4%
12PM—2PM	100%	13.9%	7.2%
	Average	14.6%	8.3%

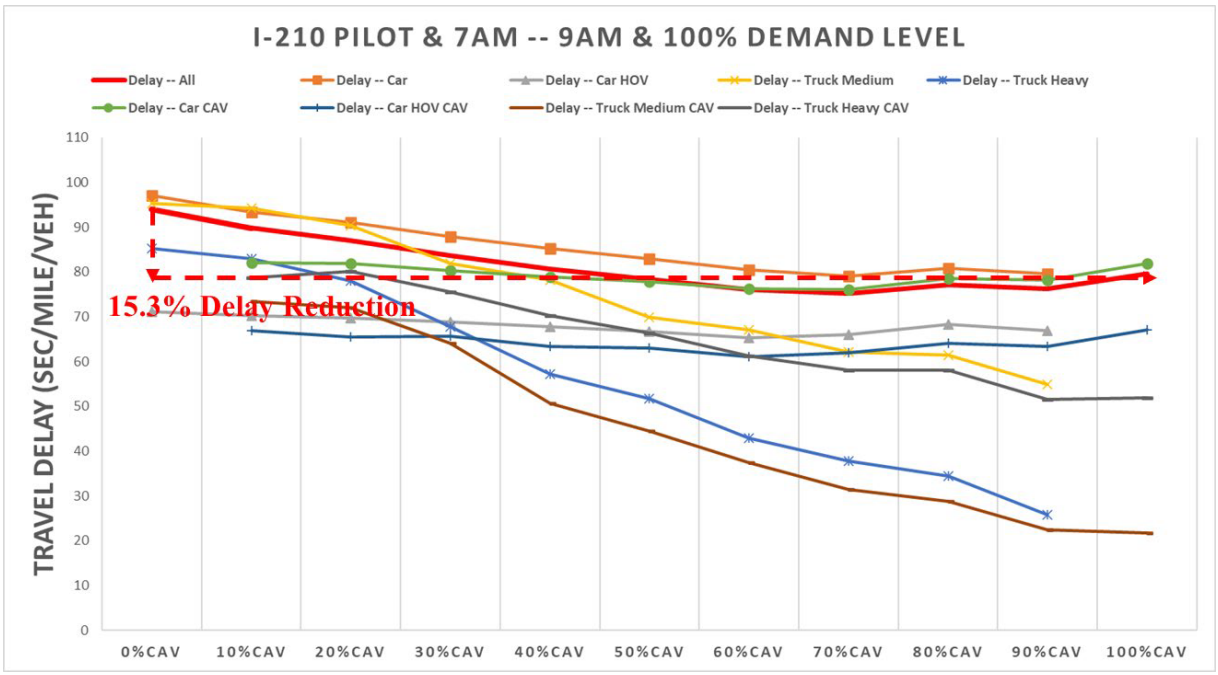

Figure 34. Example of delay reduction with different CAV percentages in the I-210 network.

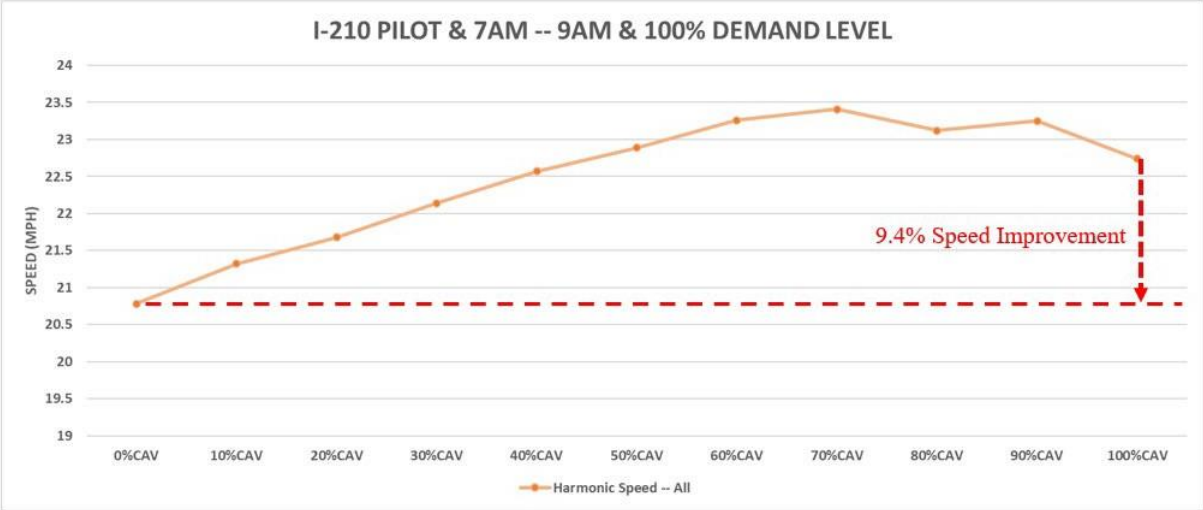

Figure 35. Example of speed improvement with different CAV percentages in the I-210 network.

5.2.5 Summary

The above simulation results demonstrate that ACC/CACC has great potential to improve transportation network performance. When ACC/CACC is enabled, it is interesting to find that significant improvement can be achieved when the penetration rate of CAVs reaches 50%. However, after that threshold, the

improvement is minor even when the penetration rate keeps on increasing up to 100%. This is true for all simulation scenarios in the I-210 network and its subnetworks.

Meanwhile, we find that due to the presence of signal control, improvement on arterials is generally lower than on freeways for the same penetration rates of CAVs. With 100% CAVs, the overall delay reduction is:

- 40% in the Freeway-Only subnetwork;
- 15% in the Arterial-Only subnetwork;
- 27% in the Freeway-and-Arterial Combined subnetwork;
- 15% in the I-210 network.

This finding demonstrates the need of V2I/I2V communications on arterial road links if we want to further reduce vehicle delay. With real-time signal phase information from a downstream intersection, CAVs can decide whether to stop like other regular automobiles or speed up to cross the intersection, which in return will reduce travel delay caused by the signal control.

In addition, we would like to emphasize that the parameter settings in the ACC/CACC module seem to be more conservative than the ones in Aimsun's default car-following model. Therefore, sometimes we do see delay slightly increasing as the penetration rate of CAVs increases from 50% to 100%. We believe better performance can be achieved if we have more aggressive settings in the ACC/CACC module.

5.3 Discussion

In this section, we focused on the evaluation of network-level impacts of ACC/CACC. We first introduced our study networks as well as our scenario design. To consider potential impacts of road geometry on the performance of ACC/CACC, we generated three different subnetworks from the original I-210 network, i.e., Freeway-Only subnetwork, Arterial-Only subnetwork, and Freeway-and-Arterial Combined subnetwork. Furthermore, we generated OD demand profiles for AM peak, PM peak, and Off peak periods to consider potential impacts of vehicle routes. Meanwhile, we created scenarios with traffic demand increased by 10% for the Freeway-Only and Arterial-Only subnetworks to consider potential impacts of travel demand when coupled with specific road geometries. In addition, we sampled the CAV penetration rate from 0% to 100% with an interval of 10% to assess the relationship between penetration rate of CAVs and the corresponding performance improvement. To reduce noise generated by the random seeds in microsimulation, we performed 10 replications for each scenario in the Freeway-Only and Arterial-Only subnetworks and 5 replications for each scenario in the Freeway-and-Arterial Combined subnetwork and the I-210 network. Based on the simulation results, we find that:

(i) The implementation of ACC/CACC can improve network performance. However, this performance improvement varies in different networks. The most significant improvement occurred in the Freeway-Only subnetwork, in which vehicle delay can be reduced by 40% and vehicle speed can be improved by 22% with 100% CAVs. The Arterial-Only subnetwork achieved the lowest performance improvement, with 15% delay reduction and 6.25% speed improvement for 100% CAVs. This difference makes sense since vehicle delay in arterial networks is mostly caused by traffic signals. Without V2I/I2V communications between signalized intersections and CAVs, it is hard to further reduce vehicle's travel delay.

(ii) There exists a threshold of CAV penetration rates, above which performance improvement is marginal. In our case, it seems this threshold is about 50%. When the penetration rate is between 0% and 50%, we do see significant performance improvement. However, when the penetration rate is above this value, the performance improvement is not obvious.

Meanwhile, we find that our parameter settings in the ACC/CACC module tend to be more conservative than those in the default car-following model in Aimsun. For some simulation scenarios, we do see delay slightly increases when the penetration rate of CAVs increases from 50% to 100%. Therefore, the performance of ACC/CACC may be more significant when we have more aggressive parameter settings in the ACC/CACC module.

In the future, with potential improvement in the software design of the V2X module in Aimsun, we are interested in evaluating the performance improvement with the implementation of both ACC/CACC and V2X in large-scale networks, e.g., the I-210 network. Also, it is worth analyzing potential impacts of parameter settings in the ACC/CACC module on model stability as well as network performance.

This page left blank intentionally

6. Future research plans

In this project, we have developed an integrated microsimulation platform in Aimsun for mixed traffic with CAVs. This platform consists of two levels of functionalities. At the vehicle control level, it uses the ACC/CACC module to control the longitudinal movements of AVs/CAVs. At the communications level, it uses the V2X module to enable communications among ITS elements, for example, RSUs, CVs/CAVs with OBUs, and TMCs. To demonstrate how to apply this integrated platform to study network-level impacts of CAV applications, we have implemented the following three applications and tested their performance in different subnetworks generated from the original I-210 network: (i) freeway speed harmonization with CAVs, (ii) route guidance with CAVs for traffic incident management, and (iii) traffic light optimal speed advisory with CAVs. Furthermore, we have activated the ACC/CACC module in the I-210 network and evaluated its network-level impacts under various settings of road geometries, vehicle routes, demand levels, and percentages of CAVs.

In the future, we would like to apply this integrated microsimulation platform to the following studies:

- **Guidance on RSU placement in the network.**
  In the application of freeway speed harmonization with CAVs, we do find it is critical to address the following question: where should we install RSUs in the network so as to achieve desired performance while staying within the budget? This is not a simple question since the performance of a CAV application may be impacted by various factors which include but are not limited to: road geometries, traffic demand, vehicle routes, existing sensing and control settings, RSU settings, and parameter settings in the CAV application.

  Fortunately, we can address this question with the help of the integrated microsimulation platform and the well-calibrated I-210 network. On the one hand, we can implement required workflows as well as algorithms in the integrated microsimulation platform for the CAV applications of particular interest. We also can have different settings in the communications channels to take into account some practical issues like package latency and loss caused by channel congestion and attenuation effect caused by buildings. On the other hand, the I-210 network is comprehensive enough that enables us to generate various subnetworks with different road geometries, traffic demand patterns, and control settings. We can test different strategies on the placement of RSUs, e.g., at traffic bottlenecks or evenly in the network, to see which one achieves the best performance across selected subnetworks and CAV applications. Eventually, all these efforts can lead to a guidance document on how to place RSUs in the transportation network to help future deployment of CAVs.
- **Applications to the California CV Testbed.**
  In the California CV Testbed (https://caconnectedvehicletestbed.org/index.php/about.php), currently 16 intersections are equipped with RSUs to broadcast real-time SPaT and MAP messages. This testbed recently has been used to demonstrate two CV applications in the Multi-Modal Intelligent Traffic Signal System (MMITSS): (i) CV-based traffic signal control and signal priority for transit, freight, and pedestrians, and (ii) Environmentally-Friendly Driving.

The integrated microsimulation platform developed in this project perfectly meets the needs of the California CV Testbed for future enhancement and development as it can create a mixed traffic environment similar to the real-world case. We can create and calibrate a microsimulation model in Aimsun for the testbed. We also can install RSUs at the same intersections in the testbed and adjust the parameters (e.g., latency, maximum range, and package loss rate) accordingly. Then we can connect to the MMITSS to evaluate the performance of available CV applications under different settings of traffic demands and penetration rates of CVs. Furthermore, it can be used as a testing platform before field deployment if new applications are developed in the MMITSS.

- **Extension to more V2X applications for multi-modal traffic.**
  In the V2X module in Aimsun, we can assign OBUs to various transportation modes, such as car, bus, truck, train, pedestrian, taxi, and cyclist. Therefore, we can further improve the current integrated microsimulation platform with communications capabilities for the aforementioned transportation modes and create a more realistic multi-modal traffic environment for analysis. Once such an environment is created, we can develop and evaluate more V2X applications for multi-modal traffic, for example, those listed in (5G Automotive Association, 2019; 5G Automotive Association, 2020).
- **Information sharing policies and strategies with navigation app users for traffic incident management.**
  As shown in the application of route guidance with CAVs for traffic incident management, significant improvement can be achieved if timely detour route information is shared with CAVs in the upstream of the incident location. However, this information sharing should not be limited to the CAVs but should include road users who have capabilities to receive real-time traffic information, e.g., navigation app users.

  Since more and more drivers are using navigation apps for their daily travels, their uncoordinated responses when traffic incidents occur may significantly degrade the effectiveness of the detour routes recommended by the TMCs. Therefore, it is of great importance to study how to share this detour route information with navigation app users so as to manage traffic incidents more effectively and efficiently.
- **Development of optimal signal control strategies with CAVs.**
  As shown in the application of traffic light optimal speed advisory with CAVs, even though the GLOSA algorithm generally performs better than the baseline model, the delay improvement is very minor, which is less than 1% for most of the scenarios. This low performance improvement may be caused by various factors, for example, traffic coordination settings, permitted left turn settings, and existence of vehicle queues and lane blockages at the intersection approach.

  Therefore, more efforts are needed to evaluate existing or even develop new optimal signal control strategies with data from CAVs. In the I-210 network, we are able to generate different Arterial-Only subnetworks with various signal phase and coordination settings, which are perfect to be used as test networks. According to (Guo et al., 2019), we will first implement and evaluate existing driver guidance control systems based on signal and CAV data. If they cannot offer satisfactory performance, we will proceed to implement and evaluate existing methods/algorithms that optimize signal timings and phases based on data from CAVs or even signal-vehicle coupled control (SVCC) systems with CAVs.

This page left blank intentionally

7. Conclusion

In this project, we successfully developed an integrated microsimulation platform for real-world mixed traffic using the ACC/CACC and V2X modules in Aimsun. We first provided a literature review on recent development of CAVs. In particular, we focused on the review of the following topics related to cooperative traffic efficiency: (i) co-operative adaptive cruise control and platooning, (ii) freeway speed harmonization, (iii) traffic light optimal speed advisory, and (iv) route guidance. Besides that, we also reviewed the car-following model implemented in Aimsun to help better understand how it controls the longitudinal movements of regular vehicles.

Next, we listed the available control modes in the ACC/CACC module and explained the decision chart on how these modes switch between each other. We also introduced the key elements and their properties in the V2X module. Given the fact that the ACC/CACC and the V2X modules were developed separately, we resolved this issue by introducing a new CAV type equipped with 100% CACC and 100% OBUs for each vehicle type, e.g., "CAV Car" for "Car", and adjusting the demand matrix according to the penetration rate of the new CAV type.

To demonstrate how to apply this integrated microsimulation platform to evaluate network-level impacts of CAV applications, we implemented the following three applications in this project: (i) freeway speed harmonization with CAVs, (ii) route guidance with CAVs for traffic incident management, and (iii) traffic light optimal speed advisory with CAVs. To test their network-level performance, we generated three subnetworks from the original I-210 network: (i) a Freeway-Only subnetwork, (ii) an Arterial-Only subnetwork, and (iii) a Freeway-and-Arterial Combined subnetwork.

For the application of freeway speed harmonization with CAVs, we implemented the required workflow to enable V2I/I2V communications between RSUs and CAVs and V2V communications between CAVs. We also implemented three different speed harmonization algorithms, which are the rule-based algorithm in (Talebpour et al., 2013), the VSL-VSA algorithm in (Lu et al., 2015; Hale et al., 2016), and the C-VSLS in (Grumert et al., 2015). We tested their performance in a Freeway-Only subnetwork under various traffic demands and percentages of CAVs. Simulation results showed that the these speed harmonization algorithms have very different performance. The rule-based algorithm and the VSL-VSA algorithm tend to have better performance when the percentage of CAVs is high, e.g., 80% or higher, while the C-VSLS tends to have better performance with a relatively low percentage of CAVs, e.g., about 40%, and under light traffic congestion. In terms of the level of improvement, the rule-based algorithm and the C-VSLS can only achieve a relatively small delay reduction between 1% and 2%, while the VSL-VSA algorithm can achieve a relatively large delay reduction between 2% and 6%. However, we do find that many factors can impact the performance of the speed harmonization algorithms with CAVs. These factors include, but are not limited to, road geometries, existing detector placement and control settings, traffic demand and OD patterns, settings of the speed harmonization zones, settings in the RSUs and the V2I/I2V communications, and parameter settings in the speed harmonization algorithms.

For the application of route guidance with CAVs for traffic incident management, we implemented two separate workflows. The first is the incident management workflow which mimics the incident management process in the ICM system. The second is the communications workflow which enables the I2V communications between RSUs and CAVs and the V2V communications between CAVs to share the

detour route information from the TMCs. We further revised the algorithm in (Samimi Abianeh et al., 2020) to mimic CAV's route choice decisions with considerations of potential impacts from lane index (e.g., inner lanes vs. shoulder lanes), vehicle types (e.g., car vs. truck), and number of detoured vehicles. We tested the performance of this application in the Freeway-and-Arterial Combined subnetwork under the settings of two different traffic accidents occurring at the same location but with different levels of severity. Simulation results with 30% and 50% CAVs showed that this application can achieve satisfactory performance with a delay reduction above 3% in the test network. This demonstrates that with timely information sharing with CAVs, we can better utilize the proposed detour routes and thus manage traffic accidents more efficiently. However, we want to emphasize that this information sharing should not be limited to CAVs but should include road users who have the capability to receive real-time traffic information, e.g., navigation app users. It is important to consider navigation app users in the decision making process in the ICM system since uncoordinated decisions of navigation app users may significantly degrade the response plans recommended by the TMCs and even make them invalid.

For the application of traffic light optimal speed advisory with CAVs, we have implemented the communications workflow to enable I2V communications between RSUs and CAVs so that RSUs can broadcast real-time SPaT and MAP messages to the CAVs. For demonstration purposes, we also implemented the Green Light Optimal Speed Advisory (GLOSA) application proposed in (Katsaros et al., 2011) with some minor revisions. We tested the performance of the revised GLOSA algorithm in the Arterial-Only subnetwork under different time periods, demand levels, and percentages of CAVs. Simulation results showed that the GLOSA algorithm generally performs better than the baseline model. However, the improvement is minor, with delay reduction less than 1% for most of the scenarios. This is not surprising since many factors can impact the performance of the revised GLOSA algorithm. These factors include, but are not limited to: coordination settings among the signalized intersections, permitted left turn settings at individual intersections, and existence of vehicle queues and lane blockages at individual intersection approaches.

When we wanted to enable the V2X module in the I-210 network, we found that Aimsun becomes extremely slow and drains physical memory very quickly. Therefore, we only activated the ACC/CACC module in the I-210 network and focused on the impact of ACC/CACC on corridor networks. We conducted various simulation scenarios under different network sizes, time periods, demand levels, and percentages of CAVs. Simulation results showed that ACC/CACC can significantly reduce network vehicle delay and improve network vehicle speed when the percentage of CAVs is over 50%. This improvement is more obvious in freeway networks with delay reduction over 40% and speed improvement over 22% for 100% CAVs. However, compared to that in freeway networks, the improvement in arterial networks is much lower, with only 15% delay reduction and 6.25% speed improvement for 100% CAVs. This is not surprising since vehicle delay in arterial networks is mostly caused by traffic signals. Without I2V/V2I communications between signalized intersections/RSUs and CAVs, it is hard to further reduce vehicle's travel delay. Meanwhile, we do notice that there exists an optimal threshold of CAV percentages, above which the performance improvement is marginal. According to our simulation results, it seems this threshold is about 50% in our study networks.

With the integrated microsimulation platform developed in this project and the well-calibrated I-210 corridor network, in the future we would like to devote our efforts in the following directions:

(i) A guidance document on RSU placement for future deployment of CAVs. In this topic, we would like to utilize the integrated microsimulation platform as well as the I-210 network to develop a general guideline on how to install RSUs in the network so as to achieve desired performance for CAV applications of particular interest while staying within the budget.

(ii) Applications to the California CV Testbed. In this topic, we would like to create a microsimulation network in Aimsun for the California CV Testbed and install RSUs to the same intersections in the field. Then we can connect the integrated microsimulation platform to the Multi-Modal Intelligent Traffic Signal System (MMITSS) in the testbed so as to test the performance of various CV applications.

(iii) Extension to more V2X applications for multi-modal traffic. In this topic, we would like to enhance the features in the integrated microsimulation platform with additional communications capabilities for other transportation modes, such as bus, train, pedestrian, taxi, and cyclist. With this improved microsimulation environment, we can implement more V2X applications for multi-modal traffic, e.g., those listed in (5G Automotive Association,2019; 5G Automotive Association, 2020), and evaluate their performance.

(iv) Information sharing policies and strategies with navigation app users. As demonstrated in the application of route guidance with CAVs for traffic incident management, traffic congestion can be significantly reduced if timely detour route information is shared with CAVs. However, this information sharing should not be limited to CAVs but should include other road users who have the capability to receive real-time traffic information. As navigation apps become more and more popular for daily travels, it is important to study potential policies and strategies to share detour route information with navigation app users so as to have better utilization of detour routes when traffic incidents occur.

(v) Optimal signal control strategies with CAVs. As demonstrated in the application of traffic light optimal speed advisory with CAVs, it is hard to reduce vehicle's travel delay by solely adjusting CAV's approaching speeds at signalized intersections. Many factors which include traffic coordination settings, permitted left turn settings, and existence of vehicle queues and lane blockages at the intersection approach need to be considered when we develop optimal signal control strategies with CAVs. Therefore, in the future, we would like to use the integrated microsimulation platform to evaluate existing or even develop new optimal signal control strategies with data from CAVs.

This page left blank intentionally

References

Aiello, M., Agarwal, P., Hilfinger, S., Grigorian, C., & Kantaros, D. (2017) 2017 Connected Cars & Autonomous Vehicles Survey. https://www.foley.com/en/insights/publications/2017/10/2017-connected-cars--autonomous-vehicles-survey

Aimsun Next (2020a). Available at: qthelp://aimsun.com.aimsun.20.0/doc/UsersManual/MicrosimulationModellingVehicleMovement.html#car_following_model.d

Aimsun Next (2020b). Modeling interaction with driverless vehicles. https://www.aimsun.com/articles/modeling-software/ (Last visited: 2021-12-26)

Aimsun Next (2020c). ACC/CACC car following models. qthelp://aimsun.com.aimsun.20.0/doc/UsersManual/MicrosimulationModellingVehicleMovement.html#acc_cacc_car_following

Aimsun Next (2020d). Aimsun Next 20 V2X Software Development Kit: qthelp://aimsun.com.aimsun.20.0/doc/UsersManual/V2X.html

Aimsun Next (2020e). Aimsun Next 20 SDK Programming: qthelp://aimsun.com.aimsun.20.0/doc/UsersManual/ApiV2X.html

Alfaseeh, L., Djavadian, S., & Farooq, B. (2018). Impact of distributed routing of intelligent vehicles on urban traffic. In 2018 IEEE International Smart Cities Conference (ISC2) (pp. 1-7). IEEE.

Allaby, P., Hellinga, B., & Bullock, M. (2007). Variable speed limits: Safety and operational impacts of a candidate control strategy for freeway applications. IEEE Transactions on Intelligent Transportation Systems, 8(4), 671-680.

Altan, O. D., Wu, G., Barth, M. J., Boriboonsomsin, K., & Stark, J. A. (2017). GlidePath: Eco-friendly automated approach and departure at signalized intersections. IEEE Transactions on Intelligent Vehicles, 2(4), 266-277.

Bansal, P., & Kockelman, K. M. (2017). Forecasting Americans' long-term adoption of connected and autonomous vehicle technologies. Transportation Research Part A: Policy and Practice, 95, 49-63.

Bodenheimer, R., Brauer, A., Eckhoff, D., & German, R. (2014). Enabling GLOSA for adaptive traffic lights. In 2014 IEEE Vehicular Networking Conference (VNC) (pp. 167-174). IEEE.

Boyd, S., Parikh, N., & Chu, E. (2011). Distributed optimization and statistical learning via the alternating direction method of multipliers. Now Publishers Inc.

Brackstone, M., & McDonald, M. (1999). Car-following: a historical review. Transportation Research Part F: Traffic Psychology and Behaviour, 2(4), 181-196.

Chandler, R. E., Herman, R., & Montroll, E. W. (1958). Traffic dynamics: studies in car following. Operations research, 6(2), 165-184.

Chu, K. F., Lam, A. Y., & Li, V. O. (2017). Dynamic lane reversal routing and scheduling for connected autonomous vehicles. In 2017 International Smart Cities Conference (ISC2) (pp. 1-6). IEEE.

Chu, K. F., Lam, A. Y., & Li, V. O. (2019). Dynamic lane reversal routing and scheduling for connected and autonomous vehicles: Formulation and distributed algorithm. IEEE Transactions on Intelligent Transportation Systems, 21(6), 2557-2570.

Cruise (2020). Cruise 75 Minutes of Autonomous Driving with Kyle Vogt and Sam Altman. https://www.youtube.com/watch?v=sliYTyRpRB8 (Last visited: 2021-12-26)

Davis, L. C. (2017). Dynamic origin-to-destination routing of wirelessly connected, autonomous vehicles on a congested network. Physica A: Statistical Mechanics and its Applications, 478, 93-102.

Djavadian, S., & Farooq, B. (2018). Distributed dynamic routing using network of intelligent intersections. ITS Canada ACGM, 2018, 22.

Ekram, A. A., & Rahman, M. S. (2018). Effects of connected and autonomous vehicles on contraflow operations for emergency evacuation: a microsimulation study (No. 18-06791).

Elliott, D., Keen, W., & Miao, L. (2019). Recent advances in connected and automated vehicles. Journal of Traffic and Transportation Engineering (English Edition).

ETSI, T. (2009). Intelligent transport systems (ITS); vehicular communications; basic set of applications; definitions. Tech. Rep. ETSI TR 102 6382009.

ETSI, T. (2010). Intelligent transport systems (its); vehicular communications; basic set of applications; part 1: Functional requirements. ETSI TS, 102, 637-1.

Fritzsche, H. T. (1994). A model for traffic simulation. Traffic Engineering & Control, 35(5), 317-21.

Gipps, P. G. (1981). A behavioural car-following model for computer simulation. Transportation Research Part B: Methodological, 15(2), 105-111.

Gazis, D. C., Herman, R., & Rothery, R. W. (1961). Nonlinear follow-the-leader models of traffic flow. Operations research, 9(4), 545-567.

Grumert, E., Ma, X., & Tapani, A. (2015). Analysis of a cooperative variable speed limit system using microscopic traffic simulation. Transportation research part C: emerging technologies, 52, 173-186.

Guo, Q., Li, L., & Ban, X. J. (2019). Urban traffic signal control with connected and automated vehicles: A survey. Transportation research part C: emerging technologies, 101, 313-334.

Hale, D., Phillips, T., Raboy, K., Ma, J., Su, P., Lu, X. Y., & Dailey, D. J. (2016). Introduction of cooperative vehicle-to-infrastructure systems to improve speed harmonization (No. FHWA-HRT-16-023). United States. Federal Highway Administration. Office of Operations Research and Development.

Hao, P., Wu, G., Boriboonsomsin, K., & Barth, M. J. (2015). Developing a framework of eco-approach and departure application for actuated signal control. In 2015 IEEE Intelligent Vehicles Symposium (IV) (pp. 796-801). IEEE.

Hao, P., Wu, G., Boriboonsomsin, K., & Barth, M. J. (2018). Eco-approach and departure (EAD) application for actuated signals in real-world traffic. IEEE Transactions on Intelligent Transportation Systems, 20(1), 30-40.

He, D. (2018). Dynamic routing and information sharing for connected and autonomous vehicles. Master thesis, The University of Texas at Austin, URI: http://hdl.handle.net/2152/68046

Houshmand, A., Wollenstein-Betech, S., & Cassandras, C. G. (2019). The penetration rate effect of connected and automated vehicles in mixed traffic routing. In 2019 IEEE Intelligent Transportation Systems Conference (ITSC) (pp. 1755-1760). IEEE.

Huawei (2021). The REAL L4 Autonomous Driving brought by Chinese tech giant Huawei, demonstrated in Shanghai. https://www.youtube.com/watch?v=8BoE21o8rfw&t=31s (Last visited: 2021-12-26)

Katsaros, K., Kernchen, R., Dianati, M., & Rieck, D. (2011). Performance study of a Green Light Optimized Speed Advisory (GLOSA) application using an integrated cooperative ITS simulation platform. In 2011 7th International Wireless Communications and Mobile Computing Conference (pp. 918-923). IEEE.

Kesting, A., Treiber, M., & Helbing, D. (2010). Enhanced intelligent driver model to access the impact of driving strategies on traffic capacity. Philosophical Transactions of the Royal Society of London A: Mathematical, Physical and Engineering Sciences, 368(1928), 4585-4605.

Learn, S., Ma, J., Raboy, K., Zhou, F., & Guo, Y. (2017). Freeway speed harmonisation experiment using connected and automated vehicles. IET Intelligent Transport Systems, 12(5), 319-326.

Li, X., & Khattak, A. J. (2018). Large-scale incident-induced congestion: en-route diversions of commercial and non-commercial traffic under connected and automated vehicles. In 2018 Winter Simulation Conference (WSC) (pp. 1132-1143). IEEE.

Litman, T. (2020). Autonomous vehicle implementation predictions: Implications for transport planning. Victoria Transport Policy Institute.

Liu, H., Kan, X., Shladover, S. E., Lu, X. Y., & Ferlis, R. E. (2018a). Impact of cooperative adaptive cruise control on multilane freeway merge capacity. Journal of Intelligent Transportation Systems, 22(3), 263-275.

Liu, H., Kan, X. D., Shladover, S. E., Lu, X. Y., & Ferlis, R. E. (2018b). Modeling impacts of cooperative adaptive cruise control on mixed traffic flow in multi-lane freeway facilities. Transportation Research Part C: Emerging Technologies, 95, 261-279.

Liu, H., Lu, X. Y., & Shladover, S. E. (2019). Traffic signal control by leveraging Cooperative Adaptive Cruise Control (CACC) vehicle platooning capabilities. Transportation research part C: emerging technologies, 104, 390-407.

Lu, X. Y., Kan, X., Shladover, S. E., Wei, D., & Ferlis, R. A. (2017). An enhanced microscopic traffic simulation model for application to connected automated vehicles. In 96th Annual Meeting of the Transportation Research Board, Washington, DC.

Lu, X. Y., Shladover, S. E., Jawad, I., Jagannathan, R., & Phillips, T. (2015). Novel algorithm for variable speed limits and advisories for a freeway corridor with multiple bottlenecks. Transportation Research Record, 2489(1), 86-96.

Ma, J., Li, X., Shladover, S., Rakha, H. A., Lu, X. Y., Jagannathan, R., & Dailey, D. J. (2016). Freeway speed harmonization. IEEE Transactions on Intelligent Vehicles, 1(1), 78-89.

Milanés, V., & Shladover, S. E. (2014). Modeling cooperative and autonomous adaptive cruise control dynamic responses using experimental data. Transportation Research Part C: Emerging Technologies, 48, 285-300.

Milanés, V., Shladover, S. E., Spring, J., Nowakowski, C., Kawazoe, H., & Nakamura, M. (2013). Cooperative adaptive cruise control in real traffic situations. IEEE Transactions on intelligent transportation systems, 15(1), 296-305.

Nowakowski, C., O'Connell, J., Shladover, S. E., & Cody, D. (2010). Cooperative adaptive cruise control: Driver acceptance of following gap settings less than one second. In Proceedings of the Human Factors and Ergonomics Society Annual Meeting (Vol. 54, No. 24, pp. 2033-2037). Sage CA: Los Angeles, CA: SAGE Publications.

Olstam, J. J., & Tapani, A. (2004). Comparison of Car-following models (Vol. 960). Linköping: Swedish National Road and Transport Research Institute.

Panwai, S., & Dia, H. (2005). Comparative evaluation of microscopic car-following behavior. IEEE Transactions on Intelligent Transportation Systems, 6(3), 314-325.

Perkins Coie LLP and AUVSI (2019). 2019 Autonomous Vehicles Survey Report. Available online: https://www.perkinscoie.com/images/content/2/1/v3/216738/2019-Autonomous-Vehicles-Survey-Report-v.3.pdf.

PTV Vissim (2017). Connected Autonomous Vehicles. http://www.sfbayite.org/wp-content/uploads/2017/04/1%20VISSIM_CAV_SFITE_April2017.pdf (Last visited: 2021-12-26)

PTV Vissim (2021), Autonomous Vehicles and New Mobility. https://www.ptvgroup.com/en/solutions/products/ptv-vissim/areas-of-application/autonomous-vehicles-and-new-mobility/ (Last visited: 2021-12-26)

Samimi Abianeh, A., Burris, M., Talebpour, A., & Sinha, K. (2020). The impacts of connected vehicle technology on network-wide traffic operation and fuel consumption under various incident scenarios. Transportation Planning and Technology, 43(3), 293-312.

Schakel, W. J., Van Arem, B., & Netten, B. D. (2010). Effects of cooperative adaptive cruise control on traffic flow stability. In Intelligent Transportation Systems (ITSC), 2010 13th International IEEE Conference on (pp. 759-764). IEEE.

Shladover, S., Su, D., & Lu, X. Y. (2012). Impacts of cooperative adaptive cruise control on freeway traffic flow. Transportation Research Record: Journal of the Transportation Research Board, (2324), 63-70.

Smith, Stanley W., Yeojun Kim, Jacopo Guanetti, Ruolin Li, Roya Firoozi, Bruce Wootton, Alexander A. Kurzhanskiy, Francesco Borrelli, Roberto Horowitz, and Murat Arcak. (2020) Improving Urban Traffic Throughput with Vehicle Platooning: Theory and Experiments. arXiv preprint arXiv:2006.10272 .

Sun, J., Yang, Y., & Li, K. (2016). Integrated coupling of road traffic and network simulation for realistic emulation of connected vehicle applications. Simulation, 92(5), 447-457.

Talebpour, A., & Mahmassani, H. S. (2016). Influence of connected and autonomous vehicles on traffic flow stability and throughput. Transportation Research Part C: Emerging Technologies, 71, 143-163.

Talebpour, A., Mahmassani, H. S., & Hamdar, S. H. (2013). Speed harmonization: Evaluation of effectiveness under congested conditions. Transportation research record, 2391(1), 69-79.

Tesla (2019). Tesla Full Self-Driving. https://www.youtube.com/watch?v=tlThdr3O5Qo (Last visited: 2021-12-26)

TransModeler (2021). New Features in TransModeler 6.0. https://www.caliper.com/transmodeler/new-features-transmodeler-6.htm (Last visited: 2021-12-26)

Treiber, M., Hennecke, A., & Helbing, D. (2000). Congested traffic states in empirical observations and microscopic simulations. Physical Review E, 62(2), 1805.

US Bureau of Public Roads. Office of Planning. Urban Planning Division. (1964). Traffic Assignment Manual for Application with a Large, High Speed Computer. US Department of Commerce.

USDOT (2019). Ensuring American Leadership in Automated Vehicle Technologies: Automated Vehicle 4.0. Available online: https://www.transportation.gov/policy-initiatives/automated-vehicles/av-40

van Arem, B., Driever, H., Feenstra, P., Ploeg, J., Klunder, G., Wilmink, I., Zoutendijk, A., Papp, Z. (2007), “Design and evaluation of an Integrated Full-Range Speed Assistant”, TNO Report 2007-DR0280/B.

Van Arem, B., Van Driel, C. J., & Visser, R. (2006). The impact of cooperative adaptive cruise control on traffic-flow characteristics. Intelligent Transportation Systems, IEEE Transactions on, 7(4), 429-436.

van Toorenburg, J.A.C., de Kok, M.L., 1999. Automatic Incident Detection in the Motorway Control System mtm. Technical Report, Bureau Transpute, Gouda, Holland.

Waymo (2018). Waymo 360° Experience: A Fully Autonomous Driving Journey. https://www.youtube.com/watch?v=B8R148hFxPw (Last visited: 2021-12-26)

Wiedemann, R. (1974). Simulation des Straßenverkehrsflusses. Schriftenreihe Heft 8. Institute for Transportation Science, University of Karlsruhe, Germany.

Wiedemann, R., & Reiter, U. (1992). Microscopic traffic simulation: the simulation system MISSION, background and actual state. Project ICARUS (V1052) Final Report, 2, 1-53.

Wu, G., Boriboonsomsin, K., Xia, H., & Barth, M. (2014). Supplementary benefits from partial vehicle automation in an ecoapproach and departure application at signalized intersections. Transportation Research Record, 2424(1), 66-75.

Xia, H., Boriboonsomsin, K., & Barth, M. (2013). Dynamic eco-driving for signalized arterial corridors and its indirect network-wide energy/emissions benefits. Journal of Intelligent Transportation Systems, 17(1), 31-41.

Zheng, Z., Ahn, S., Chen, D., & Laval, J. (2011). Applications of wavelet transform for analysis of freeway traffic: Bottlenecks, transient traffic, and traffic oscillations. Transportation Research Part B: Methodological, 45(2), 372-384.

5G Automotive Association. (2019). C-V2X use cases methodology, examples and service level requirements. Whitepaper, Jun.

5GAA Automotive Association. (2020). C-V2X use cases volume II: Examples and service level requirements. Technical Report.